Mechanisms Regulating Type I Interferon Signaling in Human Keratinocytes Triggered by Exogenous DNA

by

Ranjitha Uppala

A dissertation submitted in partial fulfillment
of the requirements for the degree of
Doctor of Philosophy
(Immunology)
in the University of Michigan
2023

Doctoral Committee:

Professor Johann E. Gudjonsson, Chair
Associate Professor Ulus Atasoy
Associate Professor Michelle J. Kahlenberg
Associate Professor Kanakadurga Singer
Assistant Professor Lam C. Tsoi

Ranjitha Uppala

uranjith@med.umich.edu

ORCID iD: 0000-0001-9865-2100

Dedication

To my incredible family, who have been my rock and source of unwavering support, I am eternally grateful.

Acknowledgements

I am humbled to acknowledge that completing this dissertation would not have been possible without the unwavering support, mentorship, and love of numerous individuals who have played a significant role in my journey as a graduate student. It is with a heart brimming with joy that I attempt to express my appreciation, though I know my words will inevitably fall short. First and foremost, I want to express my deepest gratitude to my esteemed research mentor, Dr. Johann E. Gudjonsson. Your belief in me and your decision to guide and mentor me have been life changing. I cannot express enough gratitude for the supportive and encouraging environment you have created, which has facilitated my professional development and fostered my personal growth.

In addition to being a mentor, you have been a remarkable role model to me. Your passion and dedication in the clinic and the lab have been a constant source of inspiration. I am in awe of your profound expertise and the constructive feedback you have provided me with. Your guidance has propelled me forward, motivating me to surpass my expectations and strive for excellence. I am genuinely grateful for your exceptional guidance and mentorship, which have played an instrumental role in shaping my scientific journey.

I would like to express my heartful gratitude to my dissertation committee members: Drs. Michelle J. Kahlenberg, Ulus Atasoy, Kanakadurga Singer, and Lam C. Tsoi. Their invaluable insight, guidance, and unwavering encouragement have played a pivotal role in advancing my research projects and fostering my professional development. I am truly grateful for their time, dedication, kindness, and contributions to shaping the quality and significance of my dissertation.

I am deeply thankful for the incredible individuals of the Gudjonsson lab who have enriched my journey. The current and past lab members whose camaraderie and shared pursuit of knowledge have created an environment of collaboration and inspiration; I am grateful for each of them. Mrinal, thanks for guiding me in the intricacies of generating CRISPR knockouts. Xianying, I am immensely grateful for your instructions on staining techniques. Olesya, your guidance in imaging has been invaluable. Allison, your troubleshooting expertise has been a true lifesaver. Chang, I am deeply grateful for your tips on western blotting and navigating graduate school life. Kelly, thanks for teaching me IP/pull-down assays. Enze, thanks for being a fellow graduate student in the lab and sharing experiences, both joyful and challenging. To my dear lab mate Joey, you have been more than just a colleague; you have been like a little brother to me. I cherish the memories we have made together and appreciate your constant support and friendship. Marisa, thanks for your support in managing the lab supplies and making sure we have the necessary materials in the lab. To all the remaining lab members: Nazy, Craig, Austin, and Anthony, thank you for offering help when needed and celebrating achievements together. To all my lab mates, thank you for being there to cheer me on during rough days, contributing to my growth, and making my time in the lab such a rewarding and memorable experience.

I am grateful to the nurturing and supportive community within the Graduate Program in Immunology at the University of Michigan. I want to sincerely thank Dr. Malini Raghavan for your dedication to the program. I am grateful for how have encouraged me to participate in the Immunology short course and retreat planning activities. Your support has empowered me to embrace new opportunities and expand my horizons; I am truly thankful for that. To Drs. Beth Moore and Kanakadurga Singer for their past leadership and contributions to the program. To my teachers, Drs. Venkat Keshamouni, Michal Olszewski, Cheong-Hee Chang, and Gary Huffnagle,

I want to express my heartfelt thanks for being a source of inspiration and having played a vital role in shaping my academic journey. To the Immunology program administrators, Catrice Evans, Molly Bannow, and Zarinah Aquil, for your efforts and support in creating a learning environment for all the students.

I am honored also to have been a part of the Dermatology community at the University of Michigan. Thanks to all the faculty of Dermatology for fostering a sense of community and collaboration. To the administrators, Diane Fiolek, Katie Hayes, and Carmel McKeon, thanks for all the support and service to the department.

Graduate school has truly been a blessing, and one of the greatest gifts it has bestowed upon me is friendship. Amnah and Francisco, from day one, you both have been there for me, offering support, laughter, and comfort. The memories we have created, sharing good food, dancing, and shedding tears together, are treasures I will cherish forever. Judy, thanks for being my constant. From hosting the fun-filled game nights to the delightful potlucks, our shared enthusiasm for plants has brought us closer together. Qingyang, thanks for bringing laughter and writing thesis with me. Alex, Luis, and Mack, your friendship has enriched my graduate school experience, thank you for navigating the highs and lows of this journey.

To my grandparents, parents, sister, brother in-law, in-laws and extended family, whose unwavering love and encouragement have been my anchor throughout, I offer my heartfelt appreciation. Above all, I am forever grateful to my mom and dad for all their hard work in planting roots so deep and strong in a foreign land. They faced countless challenges, leaving behind everything they knew in search of better opportunities for our family. Words cannot adequately express the depth of my appreciation for everything they have done for us. Lastly, I want to extend my heartfelt gratitude to my husband, who has been by my side through every twist and turn of

life. I deeply appreciate the sacrifices you have made for us, always putting our relationship and well-being above all else. I love you more than words can express.

Table of Contents

List of Figures

List of Abbreviations

APOBEC	Apolipoprotein B mRNA-editing enzyme, catalytic polypeptide
CGAMP	Cyclic GMP-AMP
CLE	Cutaneous Lupus Erythematosus
CRISPR	Clustered Regularly Interspaced Short Palindromic Repeats
DEG	Differentially expressed genes
DNA	Deoxyribose Nucleic Acid
DNMT	DNA methyltransferases
FB	Fibroblasts
FDR	False Discovery Rate
GFP	Green Fluorescent Protein
GO	Gene Ontology
HEK	Human Embryonic Kidney
HERC	HECT And RLD Domain Containing
HPV	Human papillomavirus
IFN	Interferon
IFNAR	Interferon Alpha Receptor
IFNB	Interferon Beta
IFNK	Interferon Kappa
INDEL	Insertions or Deletions
IRF	Interferon Response Factor
ISG	Interferon Stimulated Gene
ISGF	Interferon Stimulated Gene Factor
ISRE	Interferon-Sensitive Response Element
JAK	Janus Activated Kinase

KC	Keratinocytes
KO	Knockout
LATS	Large tumor suppressor kinase
MAVS	Mitochondrial antiviral-signaling
MOI	Multiplicity of Infection
MX	Myxovirus resistance gene
NHK	Normal Human Keratinocytes
NT	Not treated
OAS1	Oligoadenylate Synthetase 1
PBMC	peripheral blood mononuclear cells
PCR	Polymerase Chain Reaction
RNA	Ribonucleic Acid
RPLP0	Ribosomal protein lateral stalk subunit P0
STAT	Signal Transducer and Activator of Transcription
TBK1	Tank Binding Kinase-1
TEAD	TEA domain transcription factor
TLR	Toll-like Receptor
TMEM173	transmembrane protein 173
VGLL3	Vestigial-like family member 3
YAP	Yes-associated Protein

Abstract

Activation of STING DNA sensing pathway triggers the production of type I interferons (IFNs) in keratinocytes. In lupus keratinocytes, this pathway becomes overactive, leading to sustained, STING dependent type I IFN production through an autocrine loop, skewed towards females. Thus, strategies to inhibit STING and its downstream events including type I IFN signaling are an active research area to identify therapies for lupus. While a pathogenic role for type I IFNs and STING signaling in autoimmune skin diseases is well established, the key regulators of IFN signaling, the interplay between STING and type I IFN signaling pathways, and the mechanisms underlying the female bias in IFN activity remain to be fully understood.

Here we show that HERC6, an IFN-induced E3 ubiquitin ligase is induced in human keratinocytes through the epidermal type I IFN; IFN-κ. Knockdown of HERC6 in human keratinocytes led to increased activation of interferon-stimulated genes (ISGs) when treated with a double-stranded (ds)DNA STING activator cGAMP, but not in response to the RNA-sensing TLR3 agonist. In the absence of HERC6, keratinocytes display sustained STING signaling following cGAMP stimulation due to changes in the activity of LATS2, a key kinase involved in Hippo signaling, resulting in more robust IFN responses, particularly in female keratinocytes. This enhanced female-biased immune responses with loss of HERC6 is dependent on VGLL3, a sex-biased autoimmune regulator. These findings highlight HERC6 as a novel negative regulator of ISG expression specific to dsDNA sensing and establish it as a regulator of female-biased immune responses through modulation of Hippo signaling pathway.

In contrast to an autoimmune response, IFNs and STING activity in keratinocytes provide defense responses upon sensing exogenous DNA. This is evident by the fact that keratinocytes have poor DNA transfection efficiency, hindering CRISPR-Cas9 mediated genetic knockouts (KO) generation. The mechanism involving transfection resistance in keratinocytes is not well characterized. We show that CRISPR plasmid transfection activates STING, resulting in production of type I IFN through induction of IFNκ, ISG expression, and the cytidine deaminase, APOBEC3G, to decrease the plasmid stability. KOs generated in keratinocytes show persistent IFNκ suppression and DNMT3B-mediated hypermethylation in the IFNK gene promoter. Inhibiting type I IFN signaling using baricitinib before transfection resulted in increased transfection efficiency, normal IFNκ activity, and ISG expression without hypermethylation in the *IFNK* promoter region. This data suggests that CRISPR-based gene editing modifies antiviral IFN responses, which can be prevented by blocking the IFN signaling. This study has implications for gene therapy in treating inherited skin disorders using CRISPR technology.

Together, these data identify the complex immune signaling regulation in keratinocytes upon sensing exogenous DNA. Our investigation into the cross-regulation of STING-Hippo signaling has broadened our understanding of the downstream IFN signaling, identified a novel role for HERC6, and elucidated a way to generate genetic KOs in keratinocytes.

Chapter 1 Introduction

1.1 Chapter Summary

Interferons (IFNs) are a group of pleiotropic cytokines secreted by host cells in response to infections. Most cells in the body that are infected with bacteria or virus release IFNs to signal the nearby cells to turn on their antiviral responses. IFNs comprise three family members: type I, II, and III. Studies demonstrate a pathogenic role for type I IFNs in autoimmune skin diseases like cutaneous lupus erythematosus (CLE) and Sjogren's syndrome. Interestingly, IFN-kappa (IFNκ) is the only type I interferon secreted by human basal epidermal keratinocytes at baseline prior to any stimulation. Through an autocrine signaling loop that is unique to keratinocytes, IFNκ maintains basal IFN responses in keratinocytes that are heightened in autoimmune diseases. Currently the key molecules or pathways involved in autocrine type I IFN signaling remain unknown, which can be crucial to understanding their biology and finding novel drug targets for autoimmune skin diseases. In this chapter, we review the IFN types, type I IFN signaling pathway and their characteristics pertaining to keratinocytes among healthy and autoimmune skin diseases. In this chapter we also review STING dependency of IFNκ activity, sex bias in IFN activity, and the complex crosstalk between STING-IFN-Hippo signaling pathways in keratinocytes.

1.2 Interferons

Interferons (IFNs) are the first discovered distinct class of pleiotropic cytokines that are secreted by the host cells and play a significant role in triggering defense responses during

infections and cancer. Initially known for their antiviral properties, IFNs regulate the production of proinflammatory cytokines, inhibiting viral replication in infected cells (1). IFNs are crucial in defending the host during acute infections, and various viruses have developed mechanisms to inhibit IFN signaling, highlighting the importance of the pathway (2, 3). Different factors regulate IFN secretion in response to various microbial stimuli, an active area of ongoing research (4). IFNs can function in autocrine or paracrine fashion to signal the same cell or a nearby cell (5). In addition to their role in viral infections, IFNs have immunomodulatory properties and can affect cellular differentiation of epithelial, immune, and stem cells (6-8), augmentation of cytotoxic activity (9) and activation of the adaptive arm of the immune system leading to a memory response against invading pathogens (10-12).

The human epidermis is the outermost skin layer that serves as a barrier between the host and the external environment. It is predominantly composed of keratinocytes, which are the primary cell population within the epidermis. Previous research has shown that only keratinocytes, not endothelial cells, or fibroblasts, maintain a baseline expression of IFNκ - a type I IFN, and IFN stimulated gene (ISG) expression in human primary keratinocytes (Figure 1.1) (13, 14). This unique characteristic of keratinocytes may be attributed to their role as a critical barrier against infections, particularly viral. Recent research has uncovered a novel mechanistic model within keratinocytes, whereby the initial induction of IFNκ in reaction to Polyinosinic: polycytidylic acid (Poly(I:C)) and Ultraviolet B (UVB) is reliant upon IFNβ1. This suggests that robust IFNκ production in response to Poly(I:C) or UVB is dependent on an initial upregulation of IFNβ1 (15). In autoimmune and inflammatory skin diseases, an increased IFN response occurs due to excessive autocrine IFNκ signaling, leading to disease flares and pathogenesis (13, 16). However, the specific mediators responsible for this heightened IFN signaling in disease development remain

largely unexplored. Identification of the molecules and pathways involved in autocrine IFN signaling regulation would significantly contribute to our understanding of the role of IFNs in skin biology and the field of autoimmune skin diseases. Furthermore, such identification could lead to the discovery of novel drug targets for autoimmune skin diseases which are female-biased (17), thereby improving the quality of life for affected individuals and the proportion of resources going into the medical care.

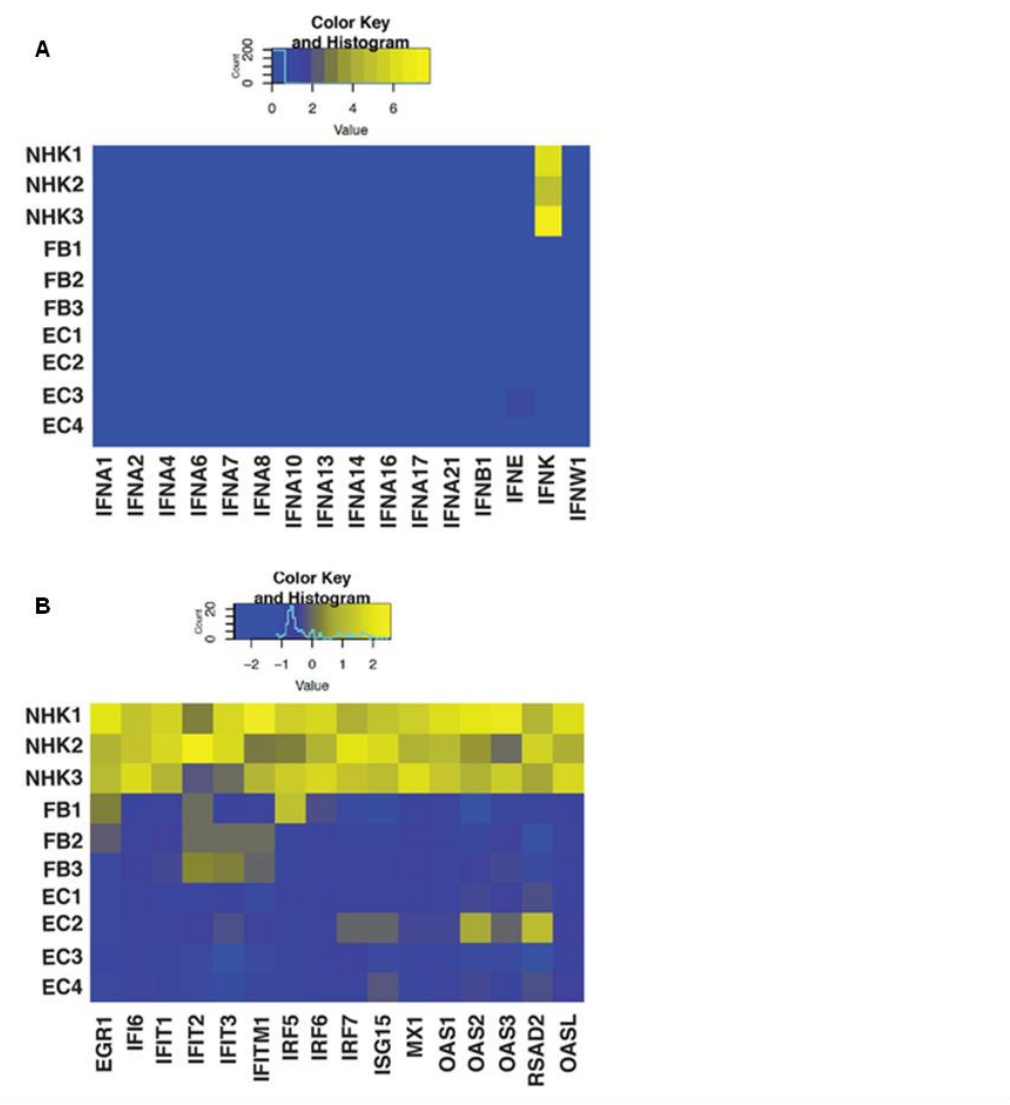

Figure 1.1: Baseline IFNK and ISG expression in keratinocytes.

A. RNA-sequencing analysis of type I IFN genes in normal human keratinocytes (NHK), dermal fibroblasts (FB), and dermal endothelial cells (EC). B. ISG expression in unstimulated NHKs, FBs, and ECs. (n=3) for each experiment. ***Adapted from MK Sarkar et al., 2018 (13, 14)***.

1.3 Types of Interferons

The IFN family comprises three groups of cytokines - type I, II, and III. Type I IFN include IFNα, IFNβ, IFNε, IFNκ and IFNω (18). While plasmacytoid dendritic cells (pDCs) are predominant producers, various cells in the human body produce type I IFNs upon pattern recognition receptors (PRRs) sensing microbes or their components (19). The cells producing type I IFNs in the skin are pDCs, monocytes, fibroblasts, and Langerhans cells (20). Keratinocytes express several PRRs, including Stimulator of Interferon Genes (STING) and Toll-like receptors (TLRs) that sense dsDNA (21, 22), retinoic acid-inducible gene-like receptors (RLRs) that sense RNA (23), nucleotide oligomerization domain-like receptors (NLRs) that sense microbes and cellular stress (24) and c-type lectin-like receptors (CLRs) that sense glycans on microbes (25). These receptors trigger the production of type I IFNs in keratinocytes as an initial host response. Hence, keratinocytes can act as immune sentinels.

IFNγ is the only type II IFN family member primarily produced by natural killer cells and T cells during infections (26, 27). IFNγ is a proinflammatory cytokine and human keratinocytes express its high-affinity receptor (IFNγR) abundantly (28). Stimulation of keratinocytes with recombinant IFNγ leads to the production of other cytokines, a characteristic observed in patients with atopic dermatitis (AD), an inflammatory skin disease with patients being hyperresponsive to IFNγ (29). Furthermore, in cases of allergic contact dermatitis, keratinocytes respond to antigen challenge by producing IFNγ. This production of IFNγ serves to activate antigen-specific T cells (30).

Type III IFNs, consisting of IFNλ1, IFNλ2, IFNλ3, and IFNλ4 (a pseudogene) form a newer group of cytokines (31). These IFNs are produced predominantly by epithelial cells, endothelial cells, macrophages, neutrophils, and a subset of dendritic cells (32, 33). B cells have been demonstrated to react to IFNL, although T cell responses remain uncertain (34). In the epidermis, keratinocytes and melanocytes are the main cell types expressing the IFNλ1 receptor which shows strong responsiveness to recombinant IFNλ stimulation. In addition to their involvement in chronic viral infections, studies have shown the therapeutic potential of the type III IFNs in treating skin cancers (35).

1.4 Type I Interferon signaling

All members of the IFN family rely on their specific receptors to initiate downstream signaling and activate the transcription of target genes. Type I IFNs utilize shared receptors - IFNαR1 and IFNαR2, which form a dimer and activate Janus kinase (JAK1) and tyrosine kinase (TYK2). This triggers a signaling cascade that involves phosphorylation, activating the signal transducer and activator of transcription (STATs-1/2) (36). The activated STATs recruit IFN response factor (IRF9) and form a complex called IFN-Stimulated gene factor 3 (ISGF3) (37). The ISGF complex translocate to the nucleus and binds to IFN-stimulated response elements (ISREs) in the promoter regions, initiating the transcription of numerous IFN-responsive genes, including MX1, which encode proteins with antiviral properties (Figure 1.2) (38). The induction of type I IFN responses is tightly regulated by a family of transcription factors called IRFs, and previous studies have demonstrated the positive feedback regulation of type I IFN induction during infections.

Type II IFN, or IFNγ, signals through its receptor, IFNγR, which engages and activates JAK1 and JAK2 kinases (37). This activation leads to homodimerization and phosphorylation of

STAT1, which then binds to IFNγ activated sites (GASs) in the nucleus, initiating the transcription of effector genes (39). Type III IFNs, like type I IFNs, utilize a similar signaling mechanism. However, they employ a different set of receptors, IFNλR1 and IL10RB, to bind their ligands and initiate downstream signaling (40).

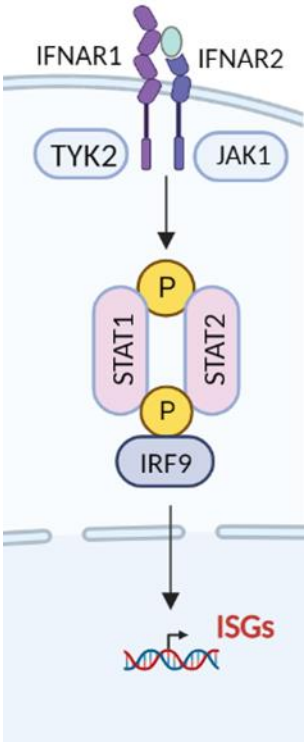

Figure 1.2: Type I IFN signaling pathway.

Interferon binding to its cognate receptors, IFNAR1 and IFNAR2, results in the formation of receptor dimers with JAK1 and TYK2 kinases. This complex activates the transcription factors, STAT1 and STAT2, leading to their phosphorylation and subsequent translocation to the nucleus. Together with IRF9, they form a complex that initiates the expression of a wide range of interferon-stimulated genes (ISGs). These ISGs are crucial in antiviral and immune responses (Image created in BioRender).

1.5 Type I Interferons in healthy skin

The skin acts as a natural barrier against microbial entry, playing a crucial role in host defense against infections. IFNκ is the sole type I IFN expressed in healthy epidermal keratinocytes without external stimulation. Viruses like the human papillomavirus (HPV) and herpes simplex

virus-1 (HSV-1) specifically target and transcriptionally repress IFNκ in keratinocytes as a strategy to evade the antiviral effects of induced IFNs (41, 42). IFNκ in keratinocytes plays a crucial role in wound repair after an injury. However, in diabetic conditions, IFNκ expression was reduced in wound keratinocytes, leading to impaired wound healing (43). Additional studies have revealed that type I IFNs exhibit anti-proliferative and anti-angiogenesis effects on cultured human keratinocytes, indicating their anti-tumor functions in cutaneous squamous and basal cell carcinoma (44, 45). Thus, research indicates the role of defense responses of type I IFNs in healthy skin to various stimuli.

1.6 Autocrine type I Interferon signaling in autoimmune and inflammatory skin diseases

Cutaneous lupus erythematosus

Systemic lupus erythematosus (SLE) is a heterogeneous autoimmune disease that affects multiple organ systems. One of the manifestations of SLE is sensitivity to UV light, leading to the development of skin lesions known as cutaneous lupus erythematosus (CLE) (46). These lesions in CLE exhibit increased cell death of keratinocytes, infiltration of immune cells, and elevated levels of inflammatory cytokines (47-49). IFN-regulated genes are expressed at a significantly higher rate in both lesional and non-lesional skin from adults with lupus. Genetic risk factors, such as polymorphisms in loci encompassing genes like *STAT4*, *IRF5*, *TREX1*, *TYK2*, and *IFNK*, contribute to amplified type I IFN responses in keratinocytes, playing a role in the pathogenesis of CLE (50-53). Environmental factors, such as UV radiation, can trigger the apoptosis of keratinocytes and the presentation of self-antigens, a characteristic feature of CLE. Standard treatment options for CLE involve topical corticosteroids followed by immunosuppressants for more severe cases.

Photosensitivity can trigger robust type I IFN and inflammatory responses in CLE patients (13). Human keratinocytes exposed to UVB radiation or TLR agonists produced higher levels of IL-6, a proinflammatory cytokine involved in the pathogenesis of SLE and CLE and regulated by autocrine IFNκ (48). Moreover, inhibition of IFNκ has been shown to prevent UVB-induced apoptosis in keratinocytes. Thus, research is focused on targeting IFNκ as a potential therapy for CLE.

Psoriasis

Psoriasis is a complex chronic inflammatory skin disease characterized by hyperproliferation and aberrant differentiation of keratinocytes. As a result, the skin lesions are dry, itchy, and scaly. Pathogenesis of psoriasis involves impaired immune responses in genetically susceptible individuals resulting in robust activation of the T helper cells (Th17) (39). The activated T cells trigger hyperproliferation of keratinocytes (54). Psoriasis is induced by applying a topical cream called imiquimod, a TLR7 agonist used to treat warts and basal cell carcinoma (55). Imiquimod is shown to initiate psoriasiform inflammation in transgenic mice that overexpress IFNκ in the epidermis with upregulated type I IFN responses(56). Although the mechanism of action of IFNκ is largely unknown in psoriasis, studies demonstrate correlated IFN responses with psoriasis-associated genes and identify type I IFN signaling as a potential therapeutic target. However, a phase I clinical trial using a monoclonal antibody against IFNα did not show clinical benefits among patients with chronic plaque psoriasis (57).

Sjogren's syndrome

Sjogren's syndrome (SS) is a systemic autoimmune disease characterized by impaired lacrimal and salivary gland function, leading to symptoms of dry eyes and dry mouth (58). While the primary target organs are the glands, skin involvement is observed in 16% to 50% of SS

patients, often presenting as painful skin rashes (59). The pathogenesis of SS is not fully understood. Still, studies have shown increased expression of both type I and type II IFNs in peripheral blood and lesional skin of SS patients and in animal models of the disease (60). Hydroxychloroquine, which inhibits the activation of stimulator of IFN genes (STING), has been described in some studies (61). Hydroxychloroquine has been shown to impact type I IFN induction, resulting in the resolution of skin rashes and inhibition of lesion development in SS patients (62). This suggests the role of type I IFNs in disease pathogenesis.

1.7 STING-dependent autocrine type I Interferon activity in basal keratinocytes

STING is a universal adaptor molecule that is activated upon sensing cytosolic dsDNA by Cyclic GMP-AMP Synthase (cGAS) to mount innate immune responses via induction of type I IFN genes. cGAS binds cytosolic DNA leading to the production of 2’3’ cGAMP that serves as a potent agonist for endoplasmic reticulum (ER) resident STING (63). STING induces phosphorylation of TANK-binding kinase 1 (TBK1) and Interferon Regulatory Factor 3 (IRF3) to produce type I IFNs, induce ISG expression, and transcription of pro-inflammatory genes (64). Aberrant activation of STING and type I IFN signaling by keratinocytes has been implicated in autoimmune diseases like lupus (65). Basal level expression of IFNK, a predominant type I IFN expressed by keratinocytes, is STING-driven and drives a unique and sustained IFN activity that can be alleviated by suppressing baseline IFNK (Figure 1.3) (63). Hence, regulation of STING signaling that positively feeds into IFN signaling occurs at multiple levels, including post-translational modifications such as ubiquitination, sumoylation, phosphorylation, methylation, and acetylation of STING or other key molecules involved in the pathway (66-71). Several studies suggest ISGs in keratinocytes have a role in regulating the IFN signaling. However, studies on

whether ISGs regulate IFN signaling by modulating STING pathway which are dysregulated in skin autoimmune diseases are limited.

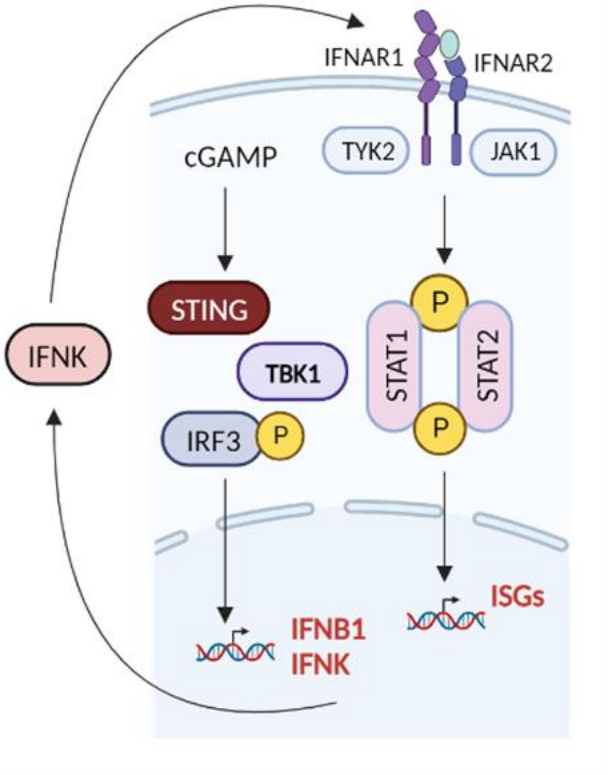

Figure 1.3: STING signaling pathway.

Cytosolic DNA sensing by cGAS catalyzes the production of cGAMP. cGAMP acts as a second messenger and binds to STING on the endoplasmic reticulum membrane. The binding of cGAMP to STING causes a conformational change, leading to the recruitment and activation of TBK1 kinase. Activated TBK1 phosphorylates IRF3 resulting in its dimerization and nuclear translocation. IRF3 induces the expression of type I interferons and other pro-inflammatory cytokines in the nucleus. Secreted IFNs signal through the JAK-STAT pathway (Figure 1.2) (Image created in BioRender).

1.8 Sexual dimorphism in Interferon activity

Emerging evidence suggests a sex bias in IFN production and activity (72). Studies have shown differences in IFN production between males and females in response to viral infections and autoimmune diseases. Females mount a stronger immune response against viral pathogens as

they produce higher levels of type I IFNs than males (73). Sex hormones may influence this difference, as estrogen has been shown to enhance IFN production (74).

Autoimmune skin diseases, which often involve dysregulated IFN responses, also exhibit sex bias in their prevalence (17). SLE and SS are more common in females and are characterized by increased IFN activity. The most prominent risk factor contributing to the development of SLE is being female, with a female to male ratio of 9:1 (75). Sjögren's disease demonstrates a higher occurrence rate in women, with certain studies indicating a gender ratio as substantial as 16:1, for females to male (76). Recent findings have shown variations in the female to male ratio for Sjögren's disease, ranging from 6 females to 1 male in smaller US studies (77) to 14 females to 1 male in larger global studies involving adults (78). The prevalence of psoriasis shows no sex-specific differences, but women tend to bear a greater disease burden and are more frequently affected by polyarthritis (79).

The underlying mechanisms for this sex bias in IFN responses in autoimmune diseases are not fully understood. Studies have shown that the X-linked TLR7 gene is preferentially active in females escaping X chromosome inactivation. TLR7 is associated with enhanced type I IFN production and significantly contributes to SLE pathogenesis (80). Recent investigations on VGLL3, a transcriptional coactivator of the Hippo pathway, have identified its relevance to psoriasis and SLE pathogenesis. Overexpression of *VGLL3* in the epidermis of mice led to inflammatory skin disease with features resembling CLE and a systemic autoimmune response resembling SLE (81). VGLL3 overexpression in mouse models has been shown to promote epidermal hyperplasia and inflammatory responses. Furthermore, the involvement of VGLL3 in promoting the IFN response via the Hippo pathway in inflammatory autoimmune conditions like

rheumatoid arthritis suggests a potential mechanism by which VGLL3 may contribute to autoimmune pathogenesis (82).

The sex bias in IFN responses highlights the complex interplay between sex hormones, genetics, and the immune system. Additional research is necessary to gain a better understanding of the underlying mechanisms and implications of these sex differences in IFN responses, which may have important implications for the development of personalized therapies for viral infections and autoimmune diseases.

1.9 Hippo pathway

The highly conserved Hippo signaling pathway, very well known to regulate cell proliferation and tissue homeostasis has recently gained attention in virus-induced diseases and cancer. MST1/2 are serine/threonine kinases activated in response to various upstream signals, such as cell-cell contact, mechanical cues, and extracellular signaling molecules (83). Activated MST1/2 phosphorylate to activate LATS1/2 kinases (84). LATS1/2, in turn, phosphorylate downstream targets. YAP and TAZ are transcriptional coactivators that are the main effectors of the Hippo pathway (85). When the Hippo pathway is active, YAP/TAZ are phosphorylated by LATS1/2, leading to their cytoplasmic retention and proteasomal degradation. Conversely, when the Hippo pathway is suppressed, YAP/TAZ translocate to the nucleus and interact with transcription factors to activate gene expression related to cell proliferation, survival, and organ growth (83). YAP/TAZ interact with TEAD (1-4) transcription factors in the nucleus to promote the expression of target genes. Although new evidence points to a role for VGLL3, a component of the Hippo pathway, in promoting IFN activity, further research is needed to fully understand the underlying mechanism by which VGLL3 regulates type I IFN signaling and the specific conditions under which this regulation occurs (Figure 1.4) (82, 86).

Upstream of the IFN signaling, the Hippo pathway is further modulated through STING signaling activation. TBK1, a critical component of the STING pathway, was shown to inhibit YAP1 activity during infections (87). In the context of fibrosis, TBK1 has been shown to regulate YAP1 by modulating its phosphorylation and promoting its nuclear translocation (88). These findings suggest further investigations on TBK1-YAP1 regulation during STING activation and the mechanism behind this regulation, particularly in the skin where the research is limited.

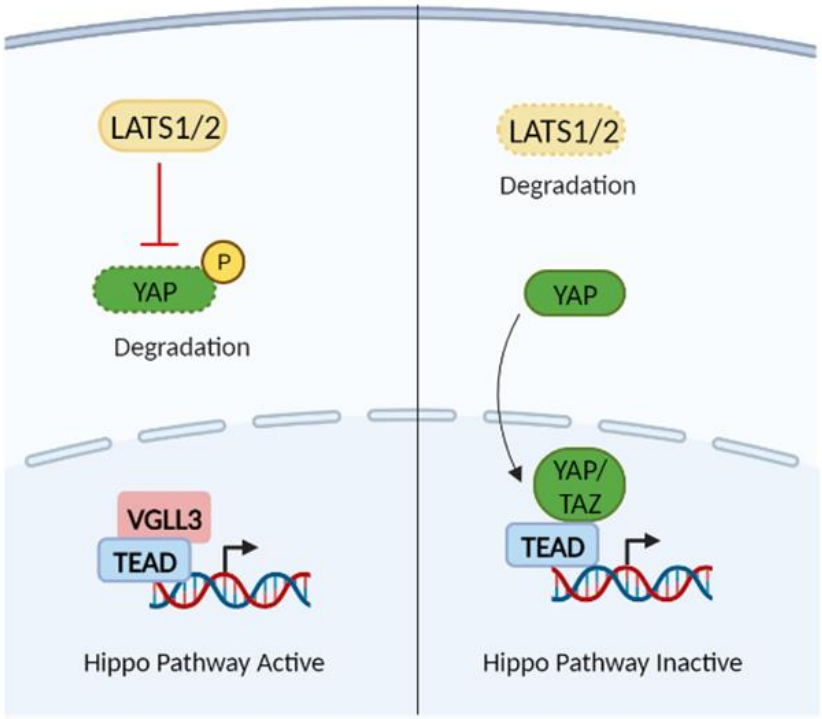

Figure 1.4: Hippo signaling pathway.

Hippo kinase, MST activates the downstream kinase Lats1/2. Active Lats1/2 then phosphorylates and inhibits the transcriptional co-activators YAP and TAZ. When YAP/TAZ are phosphorylated, they are sequestered in the cytoplasm, preventing their translocation in the nucleus, and suppressing the transcriptional activity of YAP/TAZ target gene expression. VGLL3, a transcription cofactor for TEADs, promoted Hippo signaling activation to drive sex differences in downstream signaling, such as type I IFN signaling. Conversely, when the Hippo pathway is inactive, such as when Lats1/2 is quickly degraded, YAP/TAZ become dephosphorylated. Dephosphorylated YAP/TAZ translocate into the nucleus, where they bind to transcription factors such as TEAD, activating target genes involved in cell proliferation (Image created in BioRender).

1.10 Summary and conclusions

Type I IFNs are an immunomodulatory group of proteins that mediate antiviral and antibacterial responses and activate immune responses upon stimulus or when needed in the skin. Mutations in genes involved in the type I IFN signaling in humans and mice resulted in their increased susceptibility to bacterial and viral infections. A balanced secretion of type I IFNs is crucial for healthy skin; tipping off the balance can lead to autoimmune and inflammatory skin diseases. The role of IFNK as the only type I IFN expressed in basal epidermal keratinocytes is well established which can further induce activation of type I IFNs through an autocrine signaling loop (Figure 1). Further research into identifying the key molecules and pathways involved in this autocrine signaling in keratinocytes helps understand IFN biology in normal skin and identify novel drug targets for autoimmune skin diseases.

The STING and the Hippo signaling pathways are two distinct cellular pathways that have been studied extensively and independently. Emerging research suggests potential links and cross-regulation between the STING, IFN, and Hippo signaling pathways, particularly in immune responses and inflammation. YAP/Taz activity can influence the expression of immune-related and inflammatory genes. The Hippo pathway may intersect with the STING to regulate IFN production. STING activation can activate and modulate YAP/TAZ transcriptional activity. This suggests that inflammatory cues may impact the Hippo pathway and its downstream regulation of IFN signaling.

While the precise molecular mechanisms underlying the interplay between the STING, IFN, and Hippo pathways remain to be fully elucidated, it is an intriguing area of ongoing research. Further studies are needed to identify the potential crosstalk and reciprocal regulation between

these pathways and to determine their implications for immune responses, inflammation, and autoimmune disease processes.

1.11 Scope of the dissertation

This dissertation aimed to enhance our comprehension of the molecular mechanisms underlying the regulation of the type I interferon (IFN) pathway in keratinocytes when exposed to double-stranded DNA (dsDNA) agonists. The primary objective was to investigate the crucial molecules and post-translational modifications associated with the regulation of IFN signaling, with a specific emphasis on elucidating the alterations in their activities during autoimmune conditions or in response to the detection of foreign DNA. The findings from this study will contribute to a better understanding of IFN signaling regulation in keratinocytes and facilitate the development of novel therapeutic approaches for autoimmune and infectious skin disorders.

Chapter 2 – The E3 ubiquitin ligase HERC6 regulates STING-TBK1 activity in a sex-biased manner through modulation of LATS2/VGLL3 Hippo signaling.

This chapter is focused on the function of HERC6 in keratinocytes. Our findings revealed that HERC6 is a negative regulator of type I IFN signaling in response to dsDNA agonists. The knockout of HERC6 enhanced IFN signaling, suggesting its inhibitory role in this context. Additionally, we uncovered the mechanism by which HERC6 modulates IFN signaling, implicating its involvement in upstream signaling events. These findings significantly contribute to our understanding of the regulatory mechanisms governing type I IFN signaling in keratinocytes and provide potential insights into the pathogenesis and treatment of autoimmune and infectious skin disorders. Our approach, supporting data, and conclusions are outlined in chapter 2.

Chapter 3 – STING-IFN-κ-APOBEC3G axis mediates resistance to CRISPR DNA in keratinocytes.

This chapter is focused on investigating the mechanisms underlying the poor transfection efficacy of CRISPR DNA in keratinocytes. Post-translational modifications in keratinocytes hinder DNA entry, attributed to the role of keratinocytes as immune sentinels. DNA methyltransferases induce a type I interferon response triggered by exogenous CRISPR DNA. Successful generation of CRISPR knockout keratinocytes was achieved by inhibiting type I interferon signaling. Chapter 3 provides a detailed account of the approach, supporting data, and conclusions.

Chapter 2 – The E3 Ubiquitin Ligase HERC6 Regulates STING-TBK1 Activity in a Sex-Biased Manner Through Modulation of LATS2/VGLL3 Hippo Signaling

Portions of this chapter have been submitted for publication:

Ranjitha Uppala, Mrinal K. Sarkar, Kelly Z. Young, Feiyang Ma, Pritika Vemulapalli, Rachael Wasikowski, Olesya Plazyo, William R. Swindell, Emanual Maverakis, Mehrnaz Gharaee-Kermani, Allison C. Billi, Lam C. Tsoi, Michelle J. Kahlenberg, Johann E. Gudjonsson.

2.1 Chapter Summary

Aberrant Interferon (IFN) signaling is a hallmark of systemic lupus erythematosus (SLE), a female-biased disease. We show that HERC6, an IFN-induced E3 ubiquitin ligase, is induced in human keratinocytes through the epidermal type I IFN; IFN-κ. HERC6 knockdown in human keratinocytes results in enhanced induction of interferon-stimulated genes (ISGs) upon treatment with a double-stranded (ds)DNA STING activator cGAMP, but not in response to the RNA-sensing TLR3 agonist. Keratinocytes lacking HERC6 exhibit sustained STING-TBK1 signaling following cGAMP stimulation through modulation of LATS2 and TBK1 activity, unmasking more robust responses in female cells. This enhanced female-biased immune response with loss of HERC6 is dependent on VGLL3, a sex-biased autoimmune regulator. In conclusion, we show that HERC6 is a novel negative regulator of ISG expression specific to dsDNA sensing and establish it as a regulator of female-biased immune responses through modulation of STING signaling.

2.2 Introduction

Systemic lupus erythematosus (SLE) is characterized by prominent activation of type I interferon (IFN) responses, resulting in dysregulated innate and adaptive immune activation that often precedes the clinical presentation of the disease (89). SLE predominantly affects women, with female-to-male prevalence ratio of 9:1, yet the etiology of this sex disparity cannot be fully explained by environmental factors or sex hormones. Despite the observed association between heightened type I IFN activity and sex bias in various autoimmune diseases, the mechanistic relationship between these factors remains elusive (17).

The significance of the skin in the pathogenesis of SLE has been well established. Skin manifestations are frequently observed in SLE (90), and the skin exposure to UV irradiation is known to trigger SLE flares (48). We have recently demonstrated a close association between photosensitivity in SLE and interferon kappa (IFN-κ), a type I IFN produced by keratinocytes (13). The cyclic GMP-AMP synthase (cGAS) –STING pathway, which serves as a sensor of foreign DNA (91) plays a critical role in regulating IFN-κ expression in keratinocytes (63). It has been shown that lupus keratinocytes can sense cytosolic DNA through STING (92). Activation of this pathway leads to the phosphorylation of TANK-binding kinase 1 (TBK1) and Interferon Regulatory Factor 3 (IRF3) (64), ultimately resulting in the induction of interferon-stimulated genes (ISGs). This upregulation of ISGs is particularly prominent in lupus keratinocytes and correlated with disease severity (93). Many of these ISGs encode proteins with antiviral properties (1, 94), some of which can further enhance the responses of STING (66). The specific molecules involved in this process vary depending on the mechanism but are believed to include positive feedback regulation through STAT1 promoter binding (66), ubiquitination (67), sumoylation (68), phosphorylation (69), methylation (71), or acetylation (70), of cGAS or STING itself.

HERC represents an evolutionarily conserved family of E3 ubiquitin ligases that comprises six family members, HERC1-6. The varied expression patterns of these HERC family members in different tissues likely signify their diverse functional roles (95). Through strong and recurrent adaptive evolution in mammals, HERC6 has been implicated in potential immune responses to viral pathogens (95). This notion is supported by reports of HERC6 induction in tissues infected with COVID-19 (96) and its identification as a biomarker for SLE (97). It is worth noting that HERC6 functions differ between humans and mice. Thus, mouse Herc6 exhibits functional similarities to human HERC5, and there is no identified homolog for human HERC6 in mice, limiting the scope of functional testing of HERC6 to human cells and tissues (98).

Several studies have provided evidence that women exhibit stronger Type I IFN responses than men, which confer protective effects against viral infections. However, most of these studies have primarily focused on plasmacytoid dendritic cells, which are a significant source of IFN alpha (IFN-α) (99), and in the context of TLR7 (100, 101). The involvement of STING signaling in sex-biased immune responses has not been previously reported.

This study investigated the interplay between STING, IFN signaling, and HERC6 in epithelial keratinocytes, a major source of the type I IFN-κ. Our findings revealed that HERC6 is an ISG and exerts its effects by ubiquitinating LATS2, a regulator of the Hippo signaling pathway. This ubiquitination process modulates the activation of STING. Interestingly, we observed a sex bias in this modulation of STING activation, which is dependent on VGLL3. These results establish HERC6 as a suppressor of female-biased immune responses induced by STING activation.

2.3 Materials and Methods

2.3.1 Human Subjects

SLE patients and healthy controls were recruited from the Taubman Institute Innovative Research Program Personalized Medicine through Integration of Immune Phenotypes in Autoimmune Skin Disease (TIIP-PerMIPA cohort) as described in a previous study (102). Skin biopsies were collected from volunteer patients in accordance with the University of Michigan institutional review board-approved protocols and with the subjects' informed consent. As per the principles of the Declaration of Helsinki, all patients and healthy controls gave written, informed consent before inclusion in the study.

2.3.2 Human primary cell culture

Human keratinocytes were obtained from SLE patients and healthy adults by following the procedure described in a previous study (103). The cultures were maintained using serum-free medium (Medium 154, Invitrogen/Cascade Biologics) and were used for experimentation at passage 2 or 3 with a calcium concentration of 0.1 mM. Primary human dermal fibroblasts were isolated from human skin described in a previous study (104).

2.3.3 Cell culture and stimulations

N/TERT human immortalized keratinocyte cell line was obtained from Dr. James G. Rheinwald and was used for performing gene knockdowns or knockout (KO) experiments (105). These cells have demonstrated typical differentiation traits in both monolayer and organotypic skin models. N/TERTs or KOs were cultured in Keratinocyte Serum Free Medium (KSFM, ThermoFisher #17005-042), which was enriched with 30 μg/ml bovine pituitary extract, 0.2 ng/ml epidermal growth factor, and 0.3 mM calcium chloride (106). Cells were used for various experiments following the attainment of the appropriate confluency. Cells were deprived of growth factors for

24 hours before being exposed to recombinant human IFN-α (PBI assay, 11100-1). Complete growth media was used for cGAMP (Invivogen, tlrl-nacga23) or TLR3 agonist (Invivogen, tlrl-pic) stimulations. Total RNA or protein was isolated after indicated time points of stimulations or transfections.

2.3.4 Accell siRNA-based knockdown

Keratinocytes were seeded into 48-well plates and incubated overnight at 37°C with 5% CO2. A 100μM siRNA stock (HERC6: E-005175, TMEM173: E-024333, and LATS2: E-003865) was prepared using siRNA buffer (Dharmacon# B-002000-UB-100), diluted to 1μM siRNA using Accell siRNA delivery media, and added to each well (Dharmacon #B-005000). A non-targeting control siRNA (Dharmacon # D-001910-01-05) was used for negative control. Total RNA was isolated after 48 hours of siRNA incubation. cGAMP or TLR3 agonist stimulations were performed after 48 hours of incubation with siRNA.

2.3.5 Knockout keratinocyte generation using CRISPR/Cas9

CRISPR KO keratinocytes were generated as previously described [5]. Briefly, the target single-guide RNA (sgRNA) was designed using a web interface specifically developed for CRISPR design by the BROAD institute (https://portals.broadinstitute.org/gpp/public/analysis-tools/sgrna-design). The target sequences for synthetic sgRNA were integrated into a cloning backbone known as pSpCas9 (BB)_2A-GFP (Addgene plasmid # 48138). Integrated sgRNA sequences into the plasmids were transformed using the competent E. coli (ThermoFisher # C737303). Verified plasmid DNA by Sanger sequencing was used to transfect the N/TERT cells using TransfeX (ATCC# ACS4005). GFP-expressing cells were clonally expanded and sequenced to investigate the INDELs. *IFNK*, *TYK2*, *IFNB1*, and *STING* KO keratinocytes were generated as previously described [5, 6]. *HERC6* KO keratinocytes were generated by annealing the following

oligonucleotides: HERC6E1SG2F1: 5'-CACCGATTGTTGATCTCGTGAGCTG-3' and HERC6E1SG2R1: 5'-AAACCAGCTCACGAGATCAACAATC-3'. Genotyping for HERC6 clones was performed using specific primers for HERC6: HERC6PCRF4: AAAGTGCTGTCTTAAACTTGTGT and HERC6PCRR4: TTGAATAAATGAAGGAGTGGGTTGA.

2.3.6 Stable MX1 reporter line generation

A 2nd generation promoterless lentiviral vector carrying a puromycin selection marker was purchased from abm which contains a multiple cloning site (MCS) upstream of GFP (Cat# ABM-LV059). The MX1 promoter region of 991bps upstream of the transcription start site was cloned into MCS using the EcoRI and XbaI restriction sites. Agarose gels and sanger sequencing confirmed MX1 cloning into the lentiviral backbone vector. HEK293T cells were used to package and generate viral particles. Viral particles generated were collected after 48hrs of transfection and immediately used to transduce the keratinocytes at a multiplicity of infection (MOI) of 1. The transduced keratinocytes were expanded in a selection medium containing 10ug/ml puromycin for 5 days or until all the un-transduced cells were dead. Puromycin concentration of 10ug/ml was determined after performing a drug kill curve in keratinocytes. CMV promoter-driven GFP (Cat# ABM-LV011-a) or promoterless empty vectors were used as controls. Single cell sorted transduced keratinocytes were expanded, and validation experiments were performed to choose an optimum clone.

2.3.7 Western blot analysis

Total protein was extracted from the cells using Pierce RIPA buffer (89900, ThermoFisher) supplemented with protease and phosphatase inhibitor cocktail (36978, Sigma). 20ug of total protein samples were then subjected to electrophoresis on pre-cast TRIS-Glycine gels (456-1094S,

Bio-Rad). After blocking with 5% BSA, the membrane was probed with primary antibodies, including STAT1 (CST #9172S), P-STAT1 (CST #9167S), STAT2 (CST #72604S), P-STAT2 (CST #4441S), IRF3 (CST #4302S), P-IRF3 (CST #37829S), TBK1 (CST #38066S), P-TBK1 (CST #5483S), STING (Invitrogen #PA5-26751), P-STING (Invitrogen #PA5-105674), LATS1/2 (Invitrogen #BS-4081R), P-LATS1/2 (Invitrogen #PA5-64591), YAP1 (CST #8418S), P-YAP1 (CST #913008S), and ACTIN (CST #8457S) followed by secondary antibodies (CST #58802S & 93702S). Membranes were washed three times and were imaged on iBright using the ECL substrate. All experiments were performed at least three times with similar results.

2.3.8 Gene expression analysis

Total RNA was harvested from cells using Qiagen RNeasy plus kit (Cat#74136). qRT-PCR was performed on a 7900HT Fast Real-time PCR system (AppliedBiosystems) using TaqMan Universal PCR Master Mix (ThermoFisher Scientific) and *RPLP0* was used as endogenous control.

2.3.9 Flow cytometry

Single cell suspension was prepared from untransduced, CMVGFP and MX1GFP transduced keratinocytes. Live cells were first gated manually to exclude dead cells or debris, and GFP expressing cells were gating based on CMVGFP transduced cells which constitutively expressed stable GFP on a BD LSR II (BD Biosciences). Data was analyzed using FlowJo software.

2.3.10 Bulk RNA sequencing

Bulk RNAseq for control or HERC6 KD primary human keratinocytes with or without GAMP stimulation were performed (n=3 each group and 3 male and 3 female keratinocytes were included per group). 50bp single-ended reads were generated. The reads were adapter trimmed and aligned to the human genome hg19, with only the uniquely mapped reads being used for expression level

quantification. DESeq2 was used to perform read normalization and differential expression analyses. The data are available on GEO (Accession # pending)

2.3.11 Single-cell RNA-sequencing of human skin

We used single-cell data from SLE skin that we had previously generated. Samples were processed as described [51] with >80% viability were run on the Single Cell Immune Profiling product from 10X Genomics. Single-cell libraries were generated using the 10X Genomics V2 protocols as described by the manufacturer, and sequencing was done using the Illumina NovaSeq6000 platform. We used the Cell Ranger software, supported by 10X Genomics, to conduct alignment, barcode, and unique molecular identifier read counting for analysis. We clustered cell sub-populations and used SCDE, a statistical package for analyzing scRNA-sequencing data, for differential expression analysis and ENRICHR tool for pathway analysis.

2.3.12 Transient transfections

Cells were transfected using Lipofectamine transfection reagent in Opti-MEM (GIBCO #31985–070). Plasmid DNA (2 μg per 6-well dish or 1μg per 24-well dish) was diluted in Opti-MEM, lipofectamine, and p3000 reagent was separately diluted in Opti-MEM. After 5 min, the DNA was added to the p3000 mix and incubated at room temperature for 15 min. The mixed solution was pipetted dropwise into the medium, covering the adherent cells. Cells were transfected for 48hr before harvesting for downstream analysis.

2.3.13 HERC6 over-expressing keratinocytes

HERC6 over-expressing keratinocytes were generated by lentiviral transduction like previously described [6]. Briefly, human HERC6 (RC218907, Origene) ORF-containing mammalian vector were packaged using the packaging plasmids (TR30037, Origene) and turbofectin (TF8100, Origene) in HEK293T cells. A day before transduction, keratinocytes were plated in serum-free

media and transduced with the virus with 8µg/ml of polybrene (TR-1003-G, Sigma Aldrich). After drug selection, surviving clones were obtained by limited dilution, and the OE clones were verified by western blotting.

2.3.14 Immunoprecipitation assay

HEK 293 cells were grown in Dulbecco's modified Eagle's medium (Invitrogen) with 10% fetal bovine serum. Cells were transfected using Lipofectamine 3000 (ThermoFisher) with the DYK-HERC6 (Genscript, SC1626) or Myc-LATS2 (Addgene, 66852) or both tagged cDNA constructs and harvested after 48 hours. 500µg total protein was incubated overnight with mono or polyubiquitin conjugates antibody on a shaker at 4°C. Pierce Protein Magnetic Protein A/G (ThermoFisher #88803) beads were used to pull down immune complexes, which were then analyzed by western blotting.

2.3.15 Immunohistochemistry and Immunofluorescence staining

For in vitro studies, immunofluorescence staining was performed on cells plated on 8-well chamber slides. Cells were initially washed in ice-cold PBS, fixed in 4% PFA, blocked in BSA, and incubated with primary antibodies (HERC6 (#PA5-57426), STING (#PA5-26751), LATS2 (#17H14L2) overnight at 4°C. The following day, cells were incubated for 1 hr in fluorochrome-conjugated secondary antibodies (#A-11008 & #A8_2340767). Chamber slides were washed and prepared in mounting media with DAPI. Images were acquired using an inverted Zeiss microscope. Immunohistochemistry was performed on FFPE tissue slides from healthy or lupus individuals. Slides were heated at 60°C for 30 minutes, rehydrated, and epitope retrieved with tris-EDTA (pH 6). Slides were blocked in secondary antibody source serum for 1 hr and incubated with primary antibodies overnight at 4°C. Slides were incubated with biotinylated secondary antibodies (biotinylated goat anti-rabbit IgG antibody, BA1000, Vector Laboratories; biotinylated horse anti-

mouse IgG antibody, BA2000, Vector Laboratories) and then incubated with fluorochrome-conjugated streptavidin. Slides were prepared in mounting medium with 4′,6-diamidino-2-phenylindole (DAPI) (VECTASHIELD Antifade Mounting Medium with DAPI, H-1200, VECTOR). Images were acquired using an inverted Zeiss microscope. Images presented are representative of at least three biological replicates.

2.3.16 Statistical Analysis

Statistical testing was performed on data obtained from at least three independent experiments using GraphPad Prism version 9. Statistical significance was determined using Student's unpaired t-test or analysis of variance (ANOVA) as indicated in the legend (*P < 0.05, **P < 0.01, ***P < 0.001, ****P <0.0001). After two-way ANOVA, Tukey's multiple comparison posthoc test was used with a 95% family-wise confidence level. Flow cytometry data were analyzed using FlowJo v10. The number of sampled units, n, is indicated in the figure legends and as data points on the bar plots. For microarray and bulk RNA-sequencing, a false discovery rate (FDR) of 0.05 was used to adjust and control for multiple testing.

2.4 Results

2.4.1 HERC6 is rapidly induced by type I IFNs in keratinocytes

We analyzed RNA-sequencing data of IFNα-stimulated primary human keratinocytes. We found that HERC6 expression was rapidly up-regulated (FDR <0.05) by IFNα and positively correlated with type I ISGs in primary human keratinocytes, including *MX1*, *IFNK*, and *ISG15* (Fig 2.4.1A). Notably, HERC6 was one of the top 5 genes that correlated with MX1, a well-known ISG (107), with a correlation coefficient of r=0.97 (Fig. 2.4.1B, C). HERC6 induction occurred rapidly and within 6 hours of IFNα-stimulation (Fig. 2.4.1D). These data demonstrate that HERC6 is an ISG in keratinocytes.

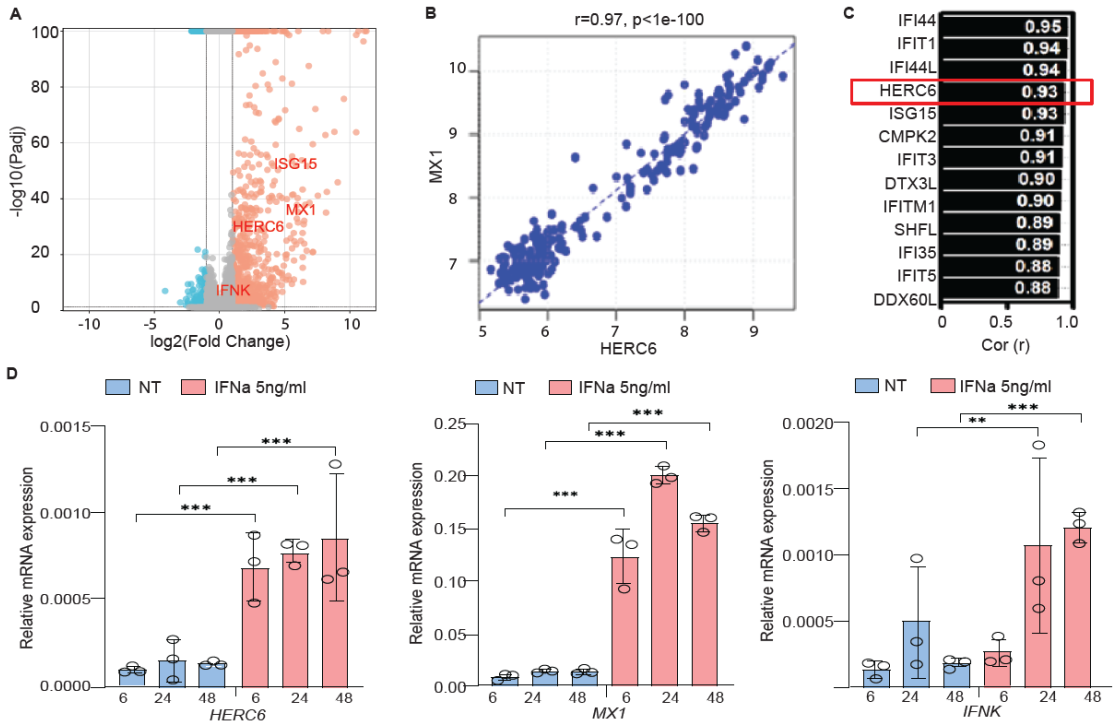

Figure 2.4.1: HERC6 is an interferon stimulated gene.

A) Volcano plot showing 1582 up-regulated, and 585 down-regulated genes with IFN-α stimulation in primary human keratinocytes (FDR<0.05). B) HERC6 expression correlation analysis with *MX1* from primary human keratinocytes. C) MX1 correlated genes in primary human keratinocytes upon IFN-α stimulation. D) Gene expression analysis of IFN-α stimulated N/TERT keratinocytes at indicated time points (Mean +/- SD, P<0.001 = ***, P<0.01 = **, P<0.05 = *, ns = not significant, Student's t-test, n=3). Assume that NT = no treatment group.

2.4.2 HERC6 negatively regulates IFN response to dsDNA, but not to dsRNA, stimuli

To determine if HERC6 plays a role in the activation of type I IFN responses, we stimulated control or *HERC6* knockdown (KD) primary keratinocytes with or without the STING agonist, cyclic GMP-AMP (cGAMP), or the TLR3 agonist Polyinosinic: polycytidylic acid (Poly(I:C)). Both STING and TLR3 activation resulted in the expression of ISGs, including *HERC6*, in control cells (Fig. 2.4.2A). However, siRNA targeting of HERC6 (>85% KD efficiency as shown in Fig. 2.4.2A), resulted in increased ISG responses to cGAMP but not to Poly(I:C) (Fig. 2.4.2A). Notably, no significant changes were observed in ISG expression following cGAMP stimulation with HERC6 in primary human fibroblasts which do not express *IFNK* (Fig. 2.4.2B). This suggests that *HERC6* KD regulation is specific to keratinocytes sensing dsDNA mimic. To confirm the regulatory effects of HERC6 on ISGs, we employed a stable MX1 reporter line in keratinocytes, where MX1 transcriptional activity is reported by GFP expression with IFNα-stimulation (Fig. 2.4.2C). As expected, GFP expression in the MX1-GFP reporter was higher in *HERC6* KD compared to the control cells (Fig. 2.4.2D).

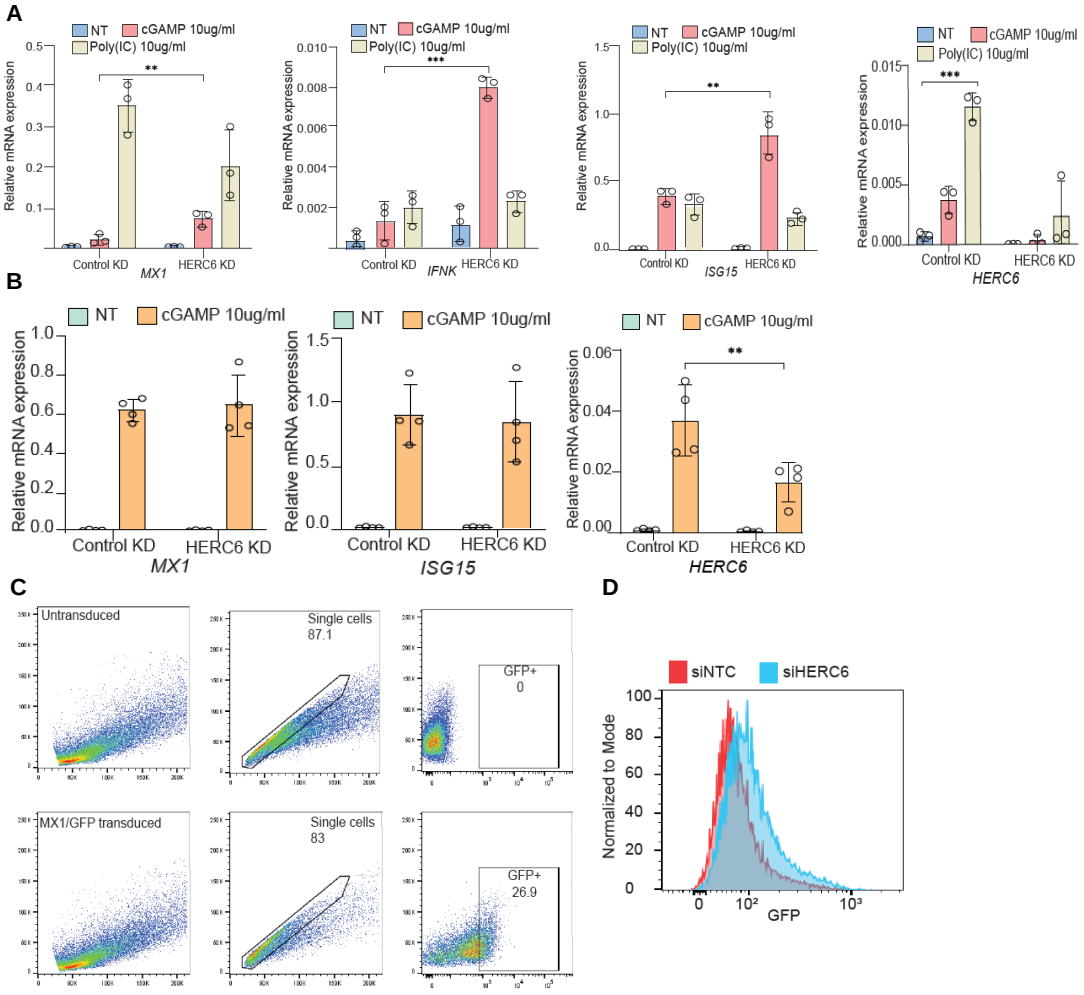

Figure 2.4.2: HERC6 negatively regulates type I IFN activity in cGAMP-stimulated keratinocytes.

A) Gene expression analysis of cGAMP or Poly(I:C) stimulated control or *HERC6* knockdown primary human keratinocytes (Mean +/- SD, P<0.001 = ***, P<0.01 = **, P<0.05 = *, ns = not significant, Student's t-test, n=3). Assume that NT = no treatment group. B) Gene expression analysis of cGAMP stimulated control or *HERC6* knockdown primary human fibroblasts (Mean +/- SD, P<0.001 = ***, P<0.01 = **, P<0.05 = *, ns = not significant, Student's t-test, n=4). Assume that NT = no treatment group. C) Gating strategy to sort GFP expressing single cells (GFP+) after IFN-α stimulation for 24 hrs in untransduced or MX1/GFP transduced keratinocytes. D) Histogram representing GFP expression in MX1/GFP reporter with control (siNTC) or HERC6 (siHERC6) knockdown.

2.4.3 HERC6 expression and activity is dependent on autocrine STING/IFNK expression

To determine whether HERC6 is dependent on IFN or STING activity in keratinocytes, we assessed HERC6 levels and ISG expression for *TYK2*, *IFNK*, *TMEM173*, and *IFNB1* knockout (KO) keratinocytes. HERC6 was absent in *IFNB1*, *TYK2*, *STING*, and *IFNK* KO keratinocytes (Fig. 2.4.3A) and decreased at transcript level (Fig. 2.4.3B). Interestingly cGAMP responses were suppressed in *TYK2*, *IFNB1*, and *IFNK* KO lines and absent in *TMEM173* (STING protein) KO keratinocytes (Fig. 2.4.3C), demonstrating the dependency of HERC6 on autocrine type I IFN activity, which is absent in fibroblasts, and STING activation. Together, these findings indicate that HERC6 requires STING-dependent IFN-k activity for its expression and function.

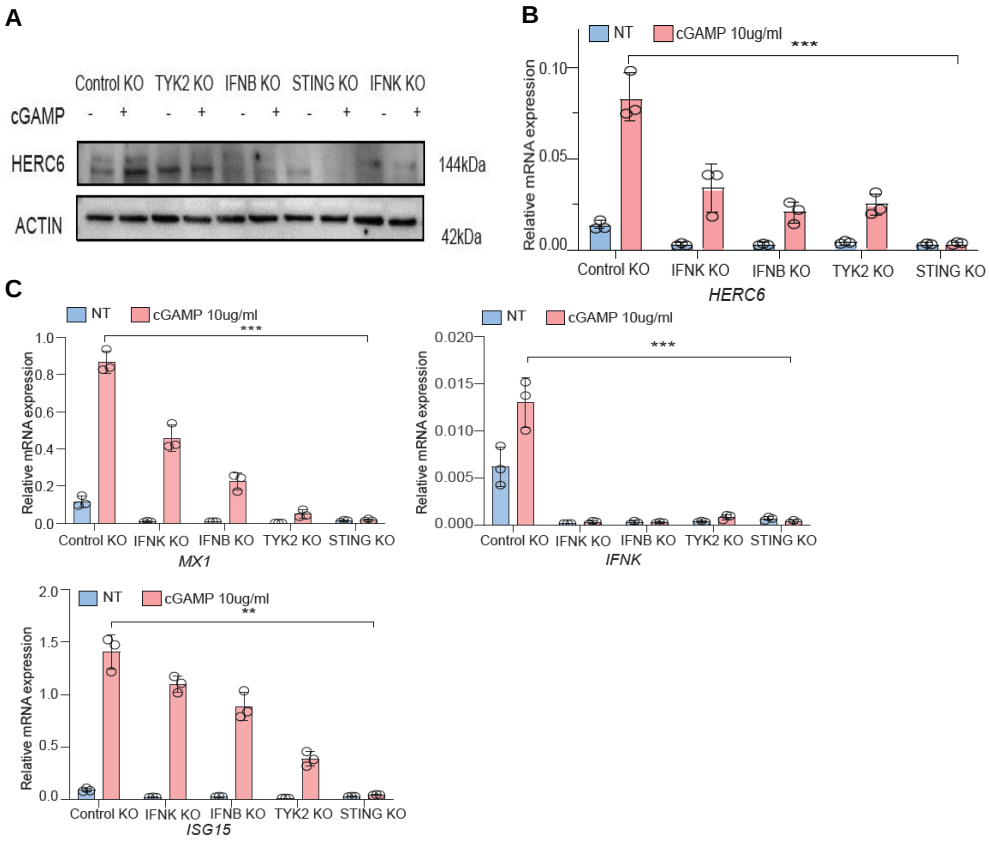

Figure 2.4.3: HERC6 expression in keratinocytes in STING/IFNK-dependent.

A) Western blot analysis of HERC6 in indicated knockout keratinocytes. B) *HERC6* gene expression in indicated knockout keratinocytes (Mean +/- SD, P<0.001 = ***, P<0.01 = **, P<0.05 = *, ns = not significant, Two-way ANOVA, n=3). NT = no treatment group. C) Gene expression analysis of cGAMP stimulated indicated knockout keratinocytes (Mean +/- SD, P<0.001 = ***, P<0.01 = **, P<0.05 = *, ns = not significant, Student's t-test, n=4). Assume that NT = no treatment group.

2.4.4 HERC6 knockout amplifies IFN signaling in keratinocytes

To address the role of HERC6 in keratinocytes, we generated *HERC6 KO* using CRISPR/Cas9 in N/TERT cells as previously described (13). A 23 bp deletion in HERC6 exon1 region was confirmed by Sanger sequencing, western blotting, and QRT-PCR analysis (Fig. 2.4.4A). Consistent with the findings from siHERC6 (Fig. 2.4.2A), *HERC6* KO resulted in amplified expression of *IFNK* and other ISGs upon cGAMP stimulation (Fig. 2.4.4B). In addition, we observed a persistent elevation in type I IFN signaling in cGAMP-stimulated *HERC6* KO keratinocytes, as evidenced by the upregulation of STAT1, phosphor (p)-STAT1, STAT2, and p-STAT2 (Fig. 2.4.4C).

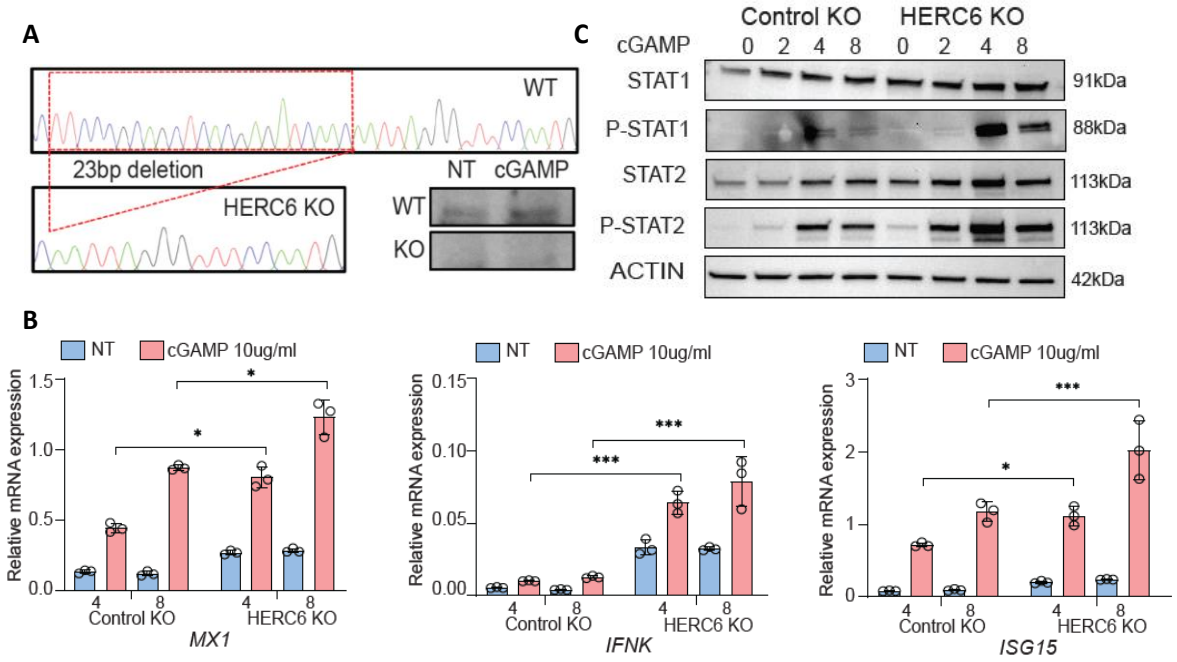

Figure 2.4.4: HERC6 knockout keratinocytes have amplified type I IFN signaling.

A) Sanger sequencing of exon1 and western blot analysis of *HERC6* knockout keratinocytes generated using CRISPR/Cas9 in N/TERT cells. B) Gene expression analysis for ISGs in cGAMP stimulated control or HERC6 knockout keratinocytes at indicated time points (Mean +/- SD, P<0.001 = ***, P<0.01 = **, P<0.05 = *, ns = not significant, Two-way ANOVA, n=3). Assume that NT = no treatment group. C) Western blot analysis of type I interferon-related genes in cGAMP stimulated control or *HERC6* knockout keratinocytes at indicated time points in hours.

2.4.5 Amplification of IFN responses secondary to loss of HERC6 is due to increased STING-TBK1 activity

Consistent with increased activity of STING/TBK1 activity in *HERC6* KO keratinocytes, we observed increased levels of p-STING, p-IRF3, and p-TBK1 with cGAMP stimulation in *HERC6* KO compared to control KO keratinocytes (Fig. 2.4.5A). The effect on STAT1/STAT2 signaling was seen as early as 2hrs following after cGAMP treatment as shown by increased P-STAT1 and P-STAT2 in *HERC6* KO keratinocytes and after 4 and 8 hrs cGAMP treatment on STING-TBK1 signaling (Fig. 2.4.4C & Fig. 2.4.5A), suggesting that the increased ISG response

is secondary to STING activation. In line with these findings, *HERC6* KO keratinocytes demonstrated increased expression of *IFNB1* and *IL6* by QRT-PCR (Fig. 2.4.5B). Thus, *HERC6* KOs exhibited a difference in IFN and STING signaling compared to control, with higher levels of p-STAT2 and p-TBK1, even without stimulation. Consistent with these responses being primarily STING-driven, we examined the effects of STING knockdown by siRNA (TMEM173). We observed that knockdown of STING attenuated the elevated expression of *IFNB1* and *IL6* in *HERC6* KO keratinocytes (Fig. 2.4.5C).

To determine the broader effect of HERC6 on STING activation, we performed bulkRNA-sequencing of non-targeting control (siNTC) or *HERC6* KD (siHERC6) primary human keratinocytes with or without cGAMP stimulation. Using a threshold of false-discovery rate (FDR) <0.05, we assessed the number of differentially expressed genes (DEGs). *HERC6* KD in keratinocytes had an increased number of DEGs compared to control with 80 DEGs in common (Fig. 2.4.5D). Gene ontology (GO) terms for the 80 shared DEGs were enriched for targets of transcription factors, including IRF3, STAT1, TEAD1, RELA, and molecular functions related to innate immune response, including DNA and RNA binding, CXCR3 chemokine receptor binding and ubiquitin-protein transferase activity (Fig. 2.4.5D). Several ISGs, including *OAS1*, *STAT2*, *XAF1*, and *IFIT3* were upregulated in cGAMP-stimulated *HERC6* KD keratinocytes compared to cGAMP-stimulated control (Fig. 2.4.5E), with *HERC6* KD having an overall broader and stronger impact compared to control KD keratinocytes (Fig. 2.4.5F). In summary, these data demonstrate that HERC6 negatively regulates type I IFN activity through modulation of STING-TBK1 signaling.

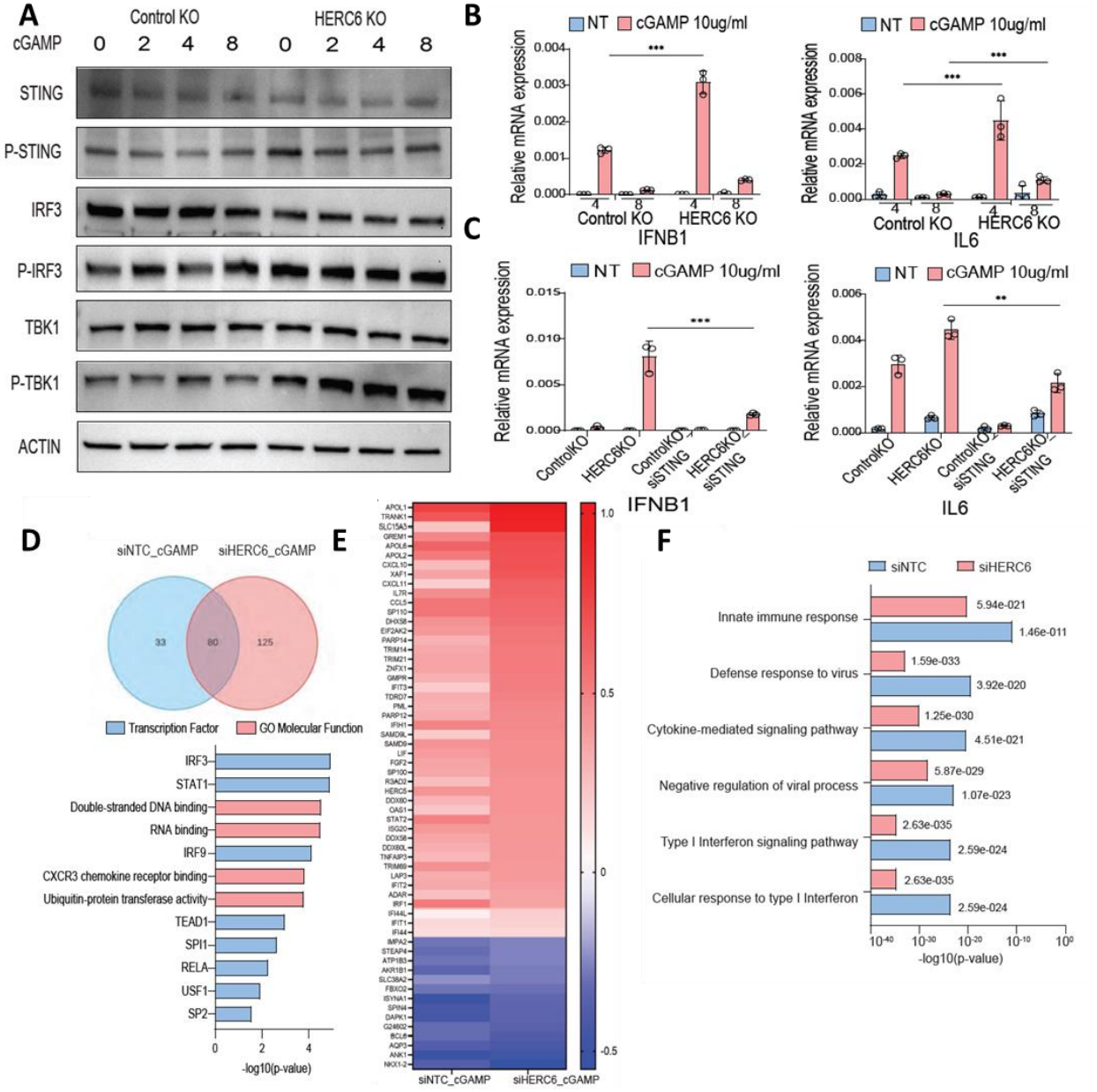

Figure 2.4.5: Amplified type I IFN signaling in HERC6 knockout keratinocytes is due to sustained STING-TBK1 activity.

A) Western blot analysis of STING pathway-related genes in cGAMP stimulated control or *HERC6* knockout keratinocytes at indicated time points in hours. B) Gene expression analysis for STING-induced genes in control or *HERC6* knockout keratinocytes (Mean +/- SD, P<0.001 = ***, P<0.01 = **, P<0.05 = *, ns = not significant, Two-way ANOVA, n=3). Assume that NT = no treatment group. C) Gene expression analysis for STING-induced genes with or without STING knockdown in control or *HERC6* knockout keratinocytes (Mean +/- SD, P<0.001 = ***, P<0.01 = **, P<0.05 = *, ns = not significant, Two-way ANOVA, n=3). Assume that NT = no treatment group. D) (Top) Venn diagram showing the total number of genes differentially regulated in non-targeting control (siNTC) or *HERC6* (siHERC6) knockdown keratinocytes with cGAMP

stimulation (FDR < 0.05, n=3 males and 3 females; (Bottom) GO terms of 80 DEGs that overlap between control and *HERC6* knockdown keratinocytes for transcription factors in blue and molecular function in coral. E) Heatmap representing dysregulated genes in log2 fold change in control or *HERC6* knockdown primary human keratinocytes with cGAMP stimulation (n=6). F) GO terms biological processes for control knockdown (siNTC) and *HERC6* knockdown (siHERC6) primary human keratinocytes showing significance with cGAMP stimulation (FDR-adjusted p-value of 0.05, n=3 males & 3 females).

2.4.6 HERC6 over expression attenuated the increased IFN activity to basal levels

We generated HERC6 over-expressing keratinocytes using a lentiviral system to investigate if this would alter ISG responses. Conversely, HERC6 over-expressing (OE) keratinocytes attenuated ISG responses to cGAMP stimulation (Fig. 2.4.6 A & B).

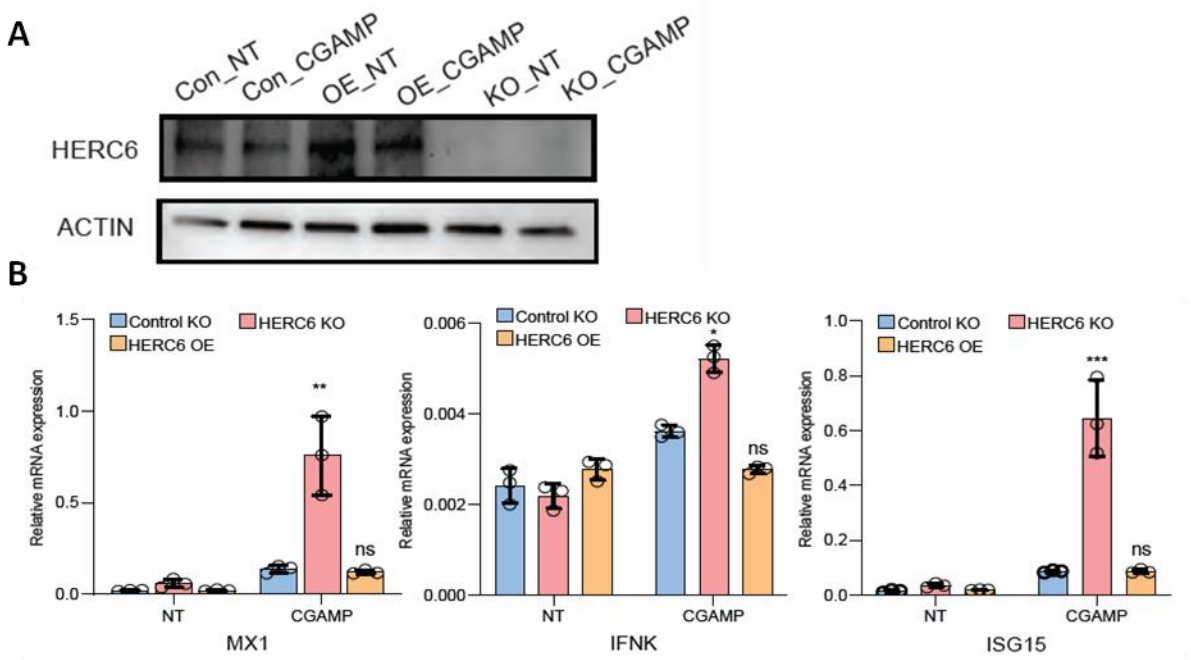

Figure 2.4.6: ISG responses are attenuated in HERC6 over-expressing keratinocytes.

A) Western blot analysis of control (Con), *HERC6* OE (OE), or *HERC6* KO (KO) keratinocytes. B) Gene expression analysis of ISGs in un-treated (NT) or CGAMP-treated control KO, *HERC6* KO, and *HERC6* OE keratinocytes (Mean +/- SD, P<0.001 = ***, P<0.01 = **, P<0.05 = *, ns = not significant, Student's t-test, n=3).

2.4.7 cGAMP stimulation resulted in enhanced LATS2 activity in *HERC6* KO keratinocytes

HERC6 has been reported to bind to LATS2 (108), a serine/threonine protein kinase that regulates the Hippo signaling pathway through phosphorylation of YAP1 for cytosolic sequestration (109). Intriguingly, TEAD1, a transcription factor downstream of Hippo signaling (110), is significantly affected by *HERC6* KD (Fig. 2.4.5D). To assess the relationship between HERC6 and LATS2 function, we first determined *LATS2* mRNA expression by QRT-PCR in control or *HERC6* KO keratinocytes with or without cGAMP. We observed increased *LATS2* mRNA expression in cGAMP-stimulated *HERC6* KO keratinocytes compared to the control (Fig. 2.4.7A), which was also validated in our bulk RNA-seq data from *HERC6* KD primary human keratinocytes (Fig. 2.4.7C). These findings were validated on the protein level by western blotting. In addition, increased and sustained total and p-LATS1/2 levels were observed in *HERC6* KO with cGAMP stimulation (Fig. 2.4.7B).

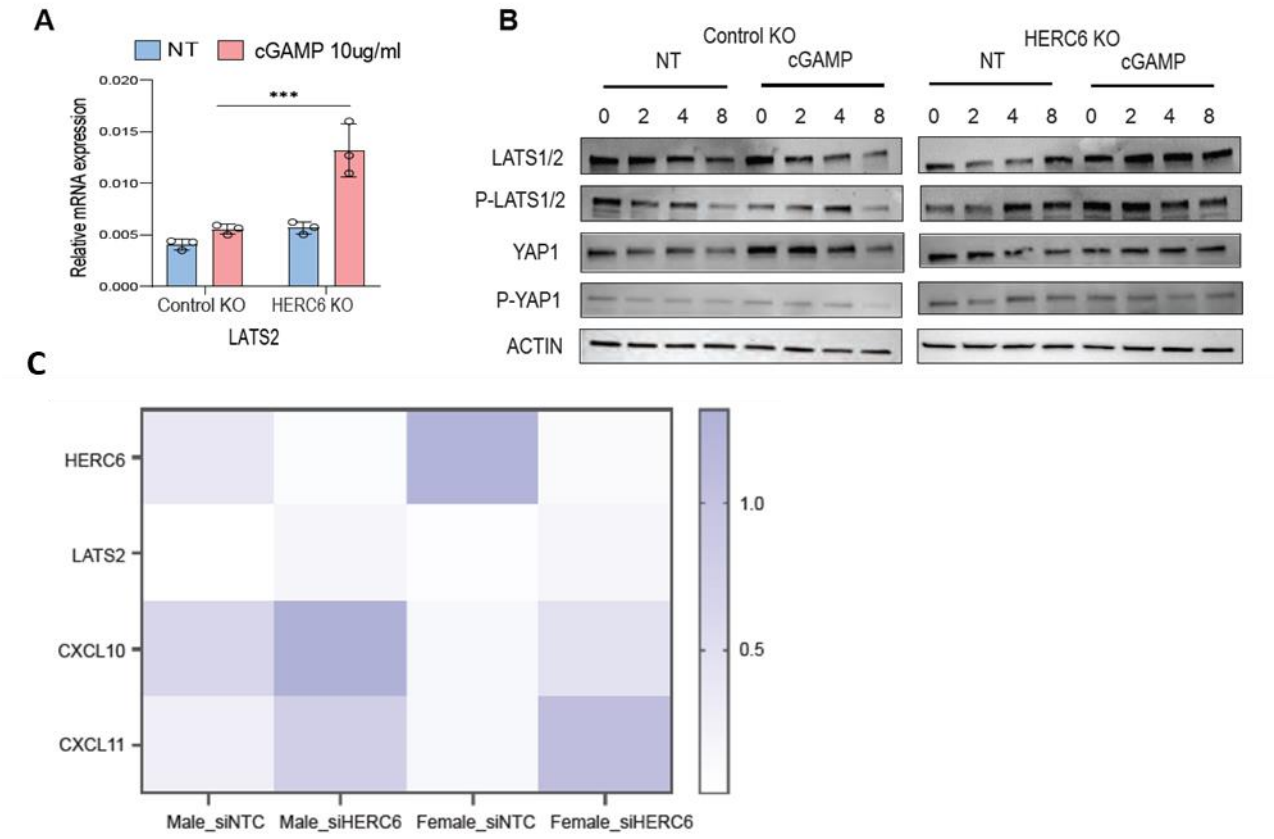

Figure 2.4.7: Increased LATS2 expression in HERC6 knockout keratinocytes.

A) *LATS2* gene expression in control or *HERC6* knockout keratinocytes after cGAMP stimulation (Mean +/- SD, P<0.001 = ***, P<0.01 = **, P<0.05 = *, ns = not significant, Student's t-test, n=3). Assume that NT = no treatment group. B) Western blot analysis of LATS2 and YAP1 in cGAMP stimulated control or in *HERC6* knockout keratinocytes at indicated time points in hours. Assume that NT = no treatment group. C) Heat-map representing Log2 fold change of HERC6, LATS2, CXCL10, and CXCL11 in non-treated versus cGAMP stimulated control or HERC6 knockdown human primary keratinocytes through bulk RNA-sequencing.

2.4.8 The increased STING/TKB1 activity with loss of HERC6 is LATS2 dependent

To determine the role of LATS2 in modulating the increased STING/TBK1 activity observed with the loss of HERC6, we used siRNA targeting *LATS2* (KD efficiency >75%), which attenuated ISG responses in *HERC6* KOs (Fig. 2.4.8A). To assess the levels of YAP1, we performed fractioned western blot analyses of the cytosolic and nuclear fractions of both control

and *HERC6* KO with or without cGAMP stimulation. This demonstrated reduced cytosolic and nuclear YAP1 levels in *HERC6* KO keratinocytes (Fig. 2.4.8B). The observed reduction in cytosolic YAP1 levels led us to hypothesize that YAP1 undergoes increased degradation. To examine this, we inhibited total proteasomal degradation using the proteasomal inhibitor MG132 (111). MG132, alone or with cGAMP treatment, increased YAP1 levels in *HERC6* KO, suggesting that the decrease in YAP1 levels is due to increased YAP1 proteasomal degradation (Fig. 2.4.8C). To determine how this relates to LATS2, we used TRULI, a small molecule inhibitor of LATS2 kinase activity (112). Inhibition of LATS2 activity resulted in decreased expression of ISGs, consistent with what we observed in *HERC6* KO keratinocytes (Figure 2.4.8E). Consistent with the role of YAP1 acting as an inhibitor of TBK1/STING activation, increased TBK1 expression was observed in *HERC6* KO with cGAMP activation (Fig. 2.4.8D) and pTKB1 (Fig. 2.4.8F), which was suppressed with the LAST2 inhibitor in cGAMP-stimulated *HERC6* KO (Fig. 2.4.8F).

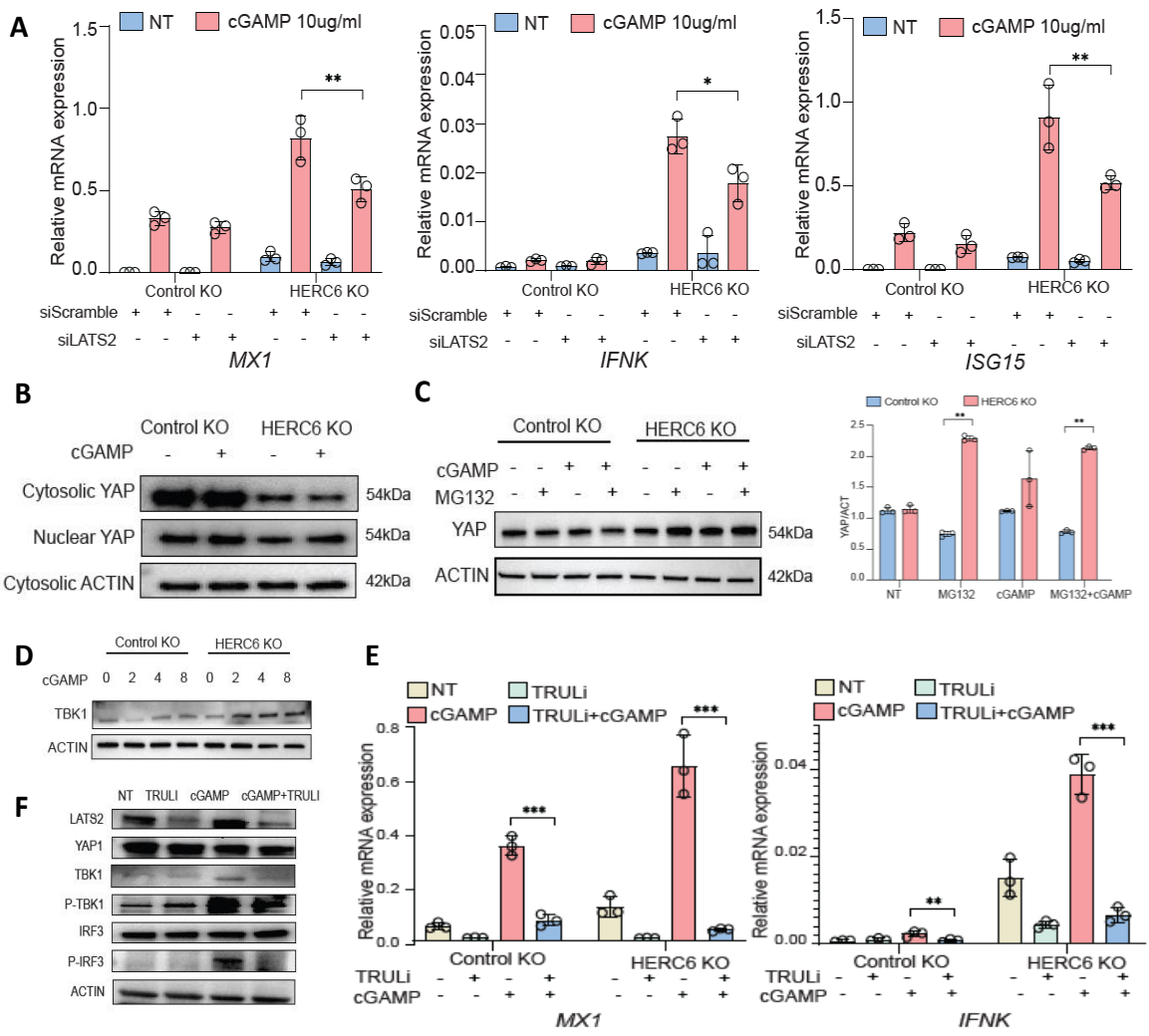

Figure 2.4.8: Increased LATS2 in HERC6 knockout keratinocytes promotes increased YAP1 degradation and heightened TBK1 activity.

A) Gene expression analysis of ISGs in cGAMP stimulated control or HERC6 knockout keratinocytes with or without LATS2 knockdown (Mean +/- SD, P<0.001 = ***, P<0.01 = **, P<0.05 = *, ns = not significant, Two-way ANOVA, n=3). Assume that NT = no treatment group. B) Western blot analysis of cytosolic and nuclear YAP1 in control or HERC6 knockout keratinocytes. C) Western blot analysis of YAP1 (on the left) and relative quantification (on the right) in cGAMP stimulated control or HERC6 knockout keratinocytes and with or without proteasomal inhibitor, MG132. D) Western blot analysis of TBK1 in cGAMP stimulated control or HERC6 knockout keratinocytes. E) LATS2 inhibition using TRULI in cGAMP stimulated control or HERC6 KO keratinocytes (Mean +/- SD, P<0.001 = ***, P<0.01 = **, P<0.05 = *, ns = not significant, Two-way ANOVA, n=3). F) Western blot analysis of LATS2, YAP1, and TBK1 in cGAMP stimulated HERC6 knockouts with TRULI treatment.

2.4.9 HERC6 ubiquitinates LATS2 in cGAMP stimulated keratinocytes

HERC6 belongs to a family of E3 ubiquitin ligases (103). We, therefore, examined whether HERC6 regulated LATS2 through ubiquitination. We performed ubiquitin conjugates immunoprecipitation followed by a pull-down of LATS2 in empty (PCMV6) or HERC6-transfected HEK293 cells. LATS2 was ubiquitinated at a higher level in HERC6-transfected cells than empty vector-transfected cells (Fig. 2.4.9A). Furthermore, HERC6 and LATS2 colocalized in the cytoplasm upon cGAMP treatment (Fig. 2.4.9B). No evidence was found for HERC6-mediated ubiquitination of STING. These results indicate that HERC6 regulates STING activation through the ubiquitination of LATS2, which, in turn, inhibits TBK1 through increased YAP1, thereby suppressing downstream responses from STING (Fig. 2.4.9C).

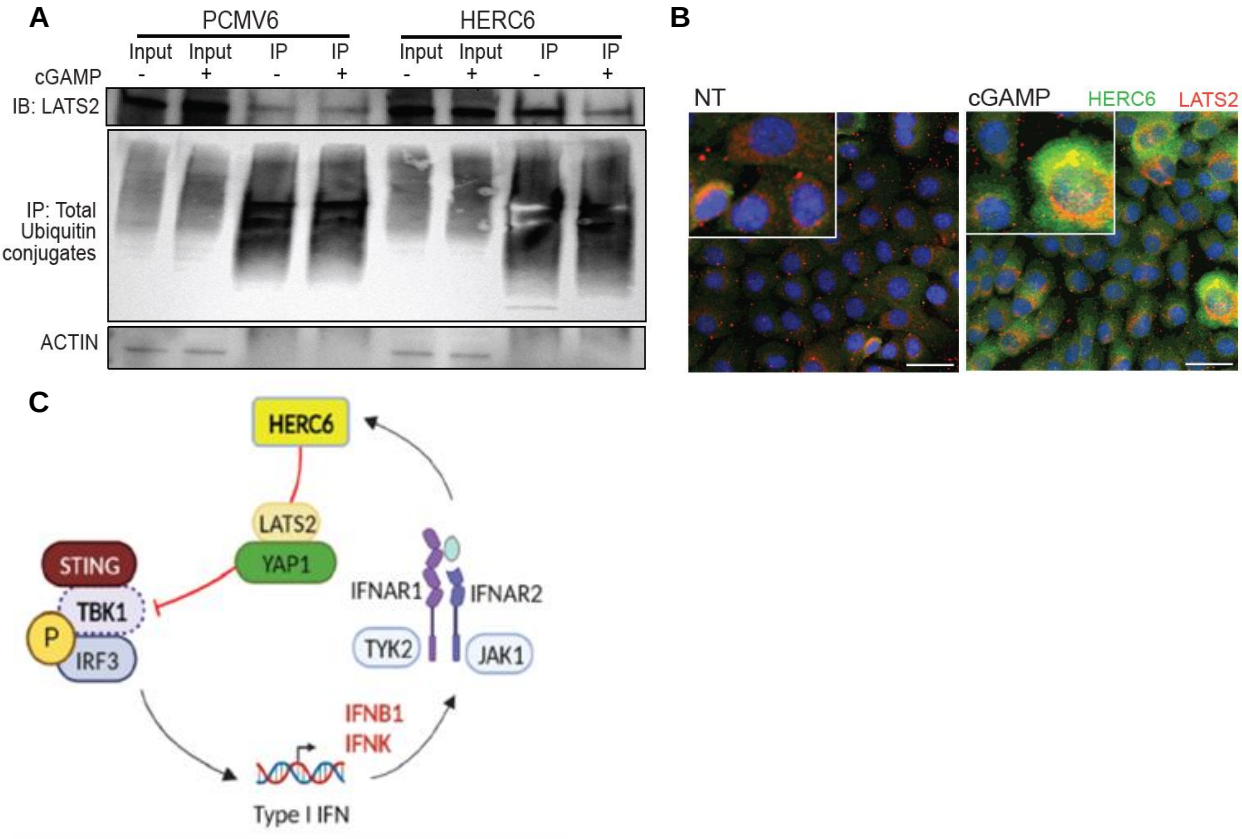

Figure 2.4.9: HERC6 functions by ubiquitinating LATS2 in cGAMP-stimulated keratinocytes.

A) Western blot analysis of ubiquitin conjugates immunoprecipitation pull-down of empty (PCVM6) or HERC6 transfected HEK293 cells. B) Confocal image analysis of control knockouts with or without cGAMP (HERC6 in green, LATS2 in red, and DAPI nuclear staining in blue). C) Schematic illustrating ubiquitination of LATS2 by HERC6, resulting in decreased YAP1 and increased TBK1/ISG activity in keratinocytes. Created in BioRender.

2.4.10 HERC6 suppressed female-biased STING responses

While there was no difference in *HERC6* mRNA expression between primary keratinocytes from healthy males and females, we observed greater *HERC6* mRNA induction upon cGAMP stimulation in female SLE keratinocytes compared to healthy male or female keratinocytes (Fig. 2.4.10A, B). Notably, ISG responses upon cGAMP stimulation were robustly amplified in female compared to male keratinocytes with *HERC6* KD (Fig. 2.4.10C). To identify mechanisms involved

in this sex bias, we used cGAMP stimulated female SLE keratinocytes along with siRNAs against *HERC6* and *VGLL3*, a transcriptional co-factor previously implicated in sex-biased immune responses (71) and a regulator of Hippo signaling activity (105). We observed increased VGLL3 in *HERC6* KD female keratinocytes compared to male keratinocytes (Fig. 2.4.10E). Furthermore, there were increased DEGs in both unstimulated and cGAMP stimulated female compared to male keratinocytes, consistent with more robust ISG responses with *HERC6* KD (Fig. 2.4.10D).

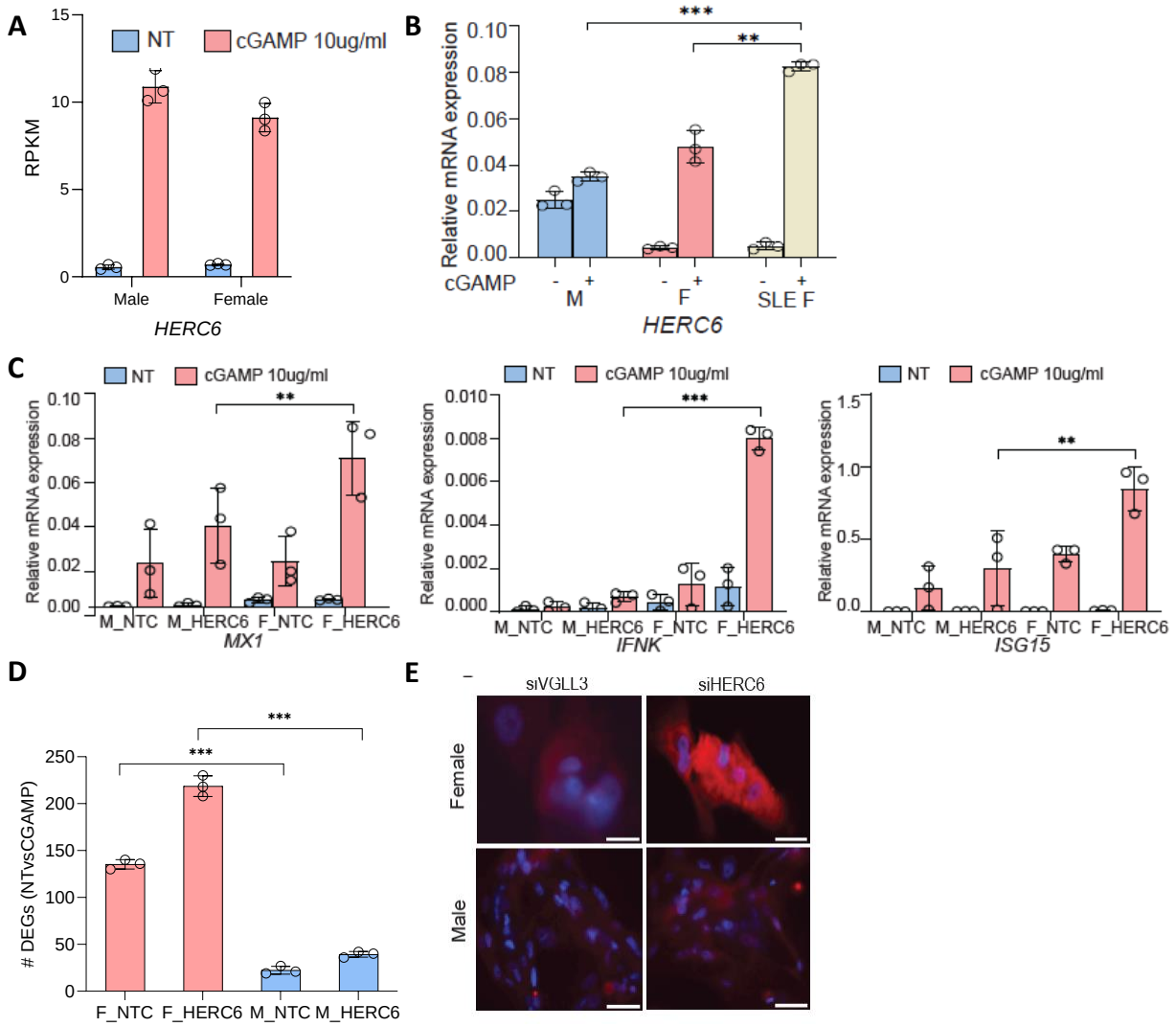

Figure 2.4.10: HERC6 knockout keratinocytes exhibit female biased IFN responses upon cGAMP stimulation.

A) *HERC6* expression in primary male (M) or female (F) keratinocytes stimulated with or without cGAMP. B) *HERC6* gene expression in normal male (M), normal female (F), or SLE female (SLE F) keratinocytes with or without cGAMP stimulation (Mean +/- SD, P<0.001 = ***, P<0.01 = **, P<0.05 = *, ns = not significant, Two-way ANOVA, n=3). C) Interferon-stimulated gene expression in normal male (M) or normal female (F) keratinocytes with control (NTC) or *HERC6* knockdown and with or without cGAMP stimulation (Mean +/- SD, P<0.001 = ***, P<0.01 = **, P<0.05 = *, ns = not significant, Two-way ANOVA, n=3). D) Total number of DEGs in female or male control knockdown (siNTC) or *HERC6* knockdown keratinocytes with cGAMP stimulation. E) Immunofluorescence staining of VGLL3 in primary human keratinocytes with *VGLL3* or *HERC6* knockdown (VGLL3 in red & DAPI nuclear staining in blue).

2.4.11 Sex-biased IFN responses in HERC6 deficient keratinocytes are VGLL3-dependent

To identify mechanisms involved in this sex bias, we used cGAMP-stimulated female SLE keratinocytes along with siRNAs against HERC6 and VGLL3, a transcriptional co-factor previously implicated in sex-biased immune responses (71) and a regulator of Hippo signaling activity (105). The knockdown efficiency for *HERC6* and *VGLL3* in lupus keratinocytes was 80% and 72.2% efficient, and KD of both *VGLL3* and *HERC6* together attenuated heightened ISG activity (Fig. 2.4.11A). Consistent with these findings, analysis of bulk RNA-seq data from cGAMP-stimulated primary human female and male keratinocytes demonstrated that *HERC6* KD was associated with greater enrichment for GO terms associated with IFN responses and cytosolic sensing of foreign DNA in female keratinocytes (Fig. 2.4.11B). Overall, these findings show that HERC6 suppresses ISG responses through modulation of VGLL3-dependent Hippo pathway signaling and may be responsible for dampening female-biased immune responses, through modulation of STING activity, during heightened interferon states (Fig. 2.4.11C).

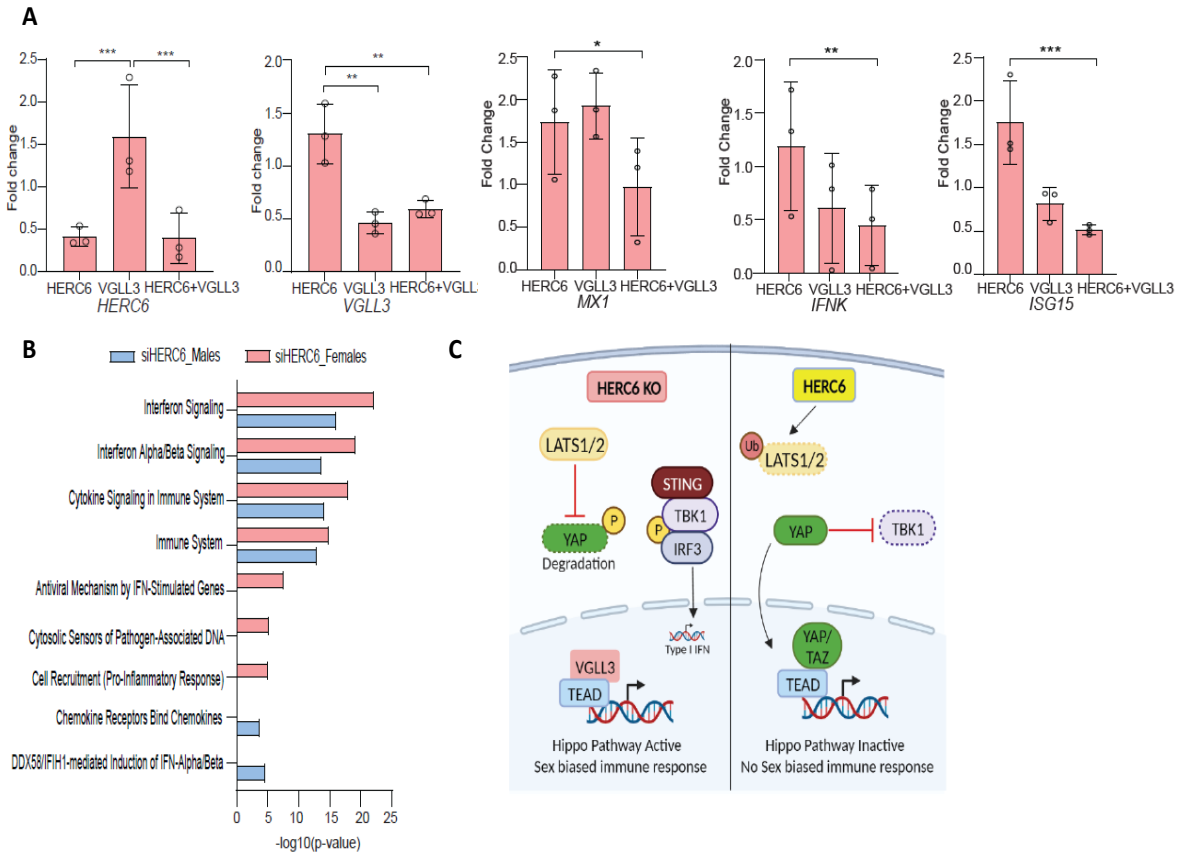

Figure 2.4.11: HERC6 suppresses cGAMP-dependent sex-biased IFN responses in lupus keratinocytes in a VGLL3-dependent manner.

A) Gene expression analysis representing fold change compared to knockdown of non-targeting control (NTC) of *HERC6*, *VGLL3*, or both *HERC6+VGLL3* in non-lesional female lupus keratinocytes (Mean +/- SD, P<0.001 = ***, P<0.01 = **, P<0.05 = *, ns = not significant, Ordinary one-way ANOVA fold-change relative to control knockdown, n=3). B) GO terms for HERC6 knockdown (siHERC6) male or female keratinocytes showing significance with cGAMP stimulation ((FDR-adjusted p-value of 0.05, n=3). C) Schematic illustrating the mechanism involving sex biased IFN responses in *HERC6* KO keratinocytes through modulation of VGLL3 Hippo pathway

2.5 Discussion

Our study showed that HERC6, an E3 ubiquitin ligase, is rapidly upregulated in epidermal keratinocytes following stimulation with IFNα or nucleotide sensing mechanisms triggered by dsDNA or dsRNA. This induction of HERC6 is dependent on both STING and autocrine IFN-κ

activity. Importantly, we observed that HERC6 specifically acts as a suppressor of cGAMP signaling in epidermal keratinocytes and not in fibroblasts. This suppression occurs through modulation of the LATS2/TBK1/VGLL3 Hippo-pathway, inhibiting female-biased immune responses.

Our findings strongly support the notion that HERC6 plays a significant role as a modulator of the STING pathway, particularly in diseases such as systemic lupus erythematosus (SLE), characterized by prominent type I IFN activity (89). The modulation of STING activation by HERC6 occurs through the ubiquitination of LATS2 kinase rather than directly affecting STING itself. This ubiquitination of LATS2 leads to a decrease in LATS2 activity, potentially promoting its proteasomal degradation. Consequently, there is an increase in YAP1 levels, which subsequently inhibits TBK1, resulting in the suppression of downstream IRF3-dependent signaling mediated by STING.

Conversely, reduced levels of HERC6 led to enhanced degradation of YAP1, leading to decreased cytoplasmic and nuclear levels of YAP1. This reduction in YAP1 levels reduces competition for binding to TEADs transcription factors with nuclear transcription co-factors, such as VGLL3 (113). This shift in binding preference towards increased VGLL3:TEAD activity amplifies VGLL3 responses. Importantly, as VGLL3 is primarily located in the nucleus of female keratinocytes, this shift in binding preference likely occurs exclusively in women, amplifying IFN responses. These findings align with our previous discoveries regarding VGLL3 as a key regulator of sex-biased immune responses (114). Previous studies have described a cross-talk between the Hippo-STING signaling pathways (115, 116), and the deletion of LATS1/2 has been shown to enhance type I IFN response in melanoma cells (117). However, the sex-specific regulation of immune responses through modulation of STING activation has not been previously reported.

SLE is a disease that primarily affects women and is characterized by heightened type I IFN responses [1, 2]. While there is a tendency for the peak of elevated type I IFN activity to occur earlier in female patients, there are no significant quantitative differences in type I IFN activity between male and female SLE patients once the disease state is fully established (118). Female-biased type I IFN responses have been reported in plasmacytoid dendritic cells (pDCs) from healthy individuals in response to TLR7 or TLR9 ligands (119). However, it is noteworthy that pDCs are markedly diminished in inflamed SLE skin (120), and have also been described to have lost their effector capacity (121). These findings suggest that while there may be sex-specific differences at baseline in type I IFN responses between men and women, these differences become balanced once the disease process is established.

In the absence of HERC6, these underlying female-biased responses are unmasked and amplified, indicating that HERC6 functions as a suppressor of female-specific immune responses by modulating STING responses. Consistent with this, we have observed that when HERC6 is active, there is minimal STING activity, as evidenced by negligible induction of ISGs in vitro and low levels of p-STING in the epidermis of SLE patients. This role of HERC6 may extend beyond the skin, as differential expression of HERC6 has been reported in SLE PBMCs, and glomeruli of lupus nephritis patients (122, 123).

While we did not find evidence for the involvement of HERC6 in TLR3 responses, which is a sensor of intracellular double-stranded RNA (dsRNA) (124), we did not address the potential role(s) of HERC6 on TLR7 or TLR9 pathways, both of which have been previously implicated in sex-biased immune responses (125, 126). Notably, though, TLR3 stimulation through Poly(I:C) was a stronger inducer of HERC6 expression than stimulation with the STING agonist cGAMP,

suggesting that HERC6 might have a role in cross-regulation between TLR3 and STING signaling, but this will need to be addressed in future studies.

Our findings have major implications regarding our understanding of STING signaling and sex-biased immune responses and emphasize the role of the Hippo pathway through modulation of HERC6-STING activity as a critical circuit in the modulation of autoimmune diseases such as SLE.

Chapter 3 STING-IFN-κ-APOBEC3G Axis Mediates Resistance to CRISPR DNA in Keratinocytes

This chapter has been published in the *Journal of Clinical Investigation*:

Mrinal K Sarkar, **Ranjitha Uppala**, Chang Zeng, Allison C Billi, Lam C Tsoi, Austin Kidder, Xianying Xing, Bethany E Perez White, Shuai Shao, Olesya Plazyo, Sirisha Sirobhushanam, Enze Xing, Yanyun Jiang, Katherine A Gallagher, John J Voorhees, J Michelle Kahlenberg, Johann E Gudjonsson. Keratinocytes sense and eliminate CRISPR DNA through STING/IFN-κ activation and APOBEC3G induction.

3.1 Chapter Summary

Basal keratinocytes (KCs) have poor DNA transfection efficiency, an approach crucial to generate CRISPR-Cas9-mediated genetic knockouts (KO). The mechanism that involves transfection resistance in KCs is not well characterized. We show that transfection with CRISPR plasmid activates the cytosolic DNA sensor, Stimulator of Interferon Genes (STING), resulting in the production of type I interferons (IFN) through induction of IFNκ, interferon-stimulated gene (ISG) expression, and the cytidine deaminase, APOBEC3G to decrease the plasmid stability. CRISPR-Cas9-based genetic KOs generated in KCs exhibit continued IFNκ suppression and hypermethylation mediated by the DNA methyltransferase, DNMT3B, in the promoter region of IFNK. Inhibiting type I IFN signaling using JAK1/JAK2 inhibitor, baricitinib before transfection resulted in increased transfection efficiency, normal IFNκ activity, and ISG expression without hypermethylation in the promoter region of the IFNK. Our data indicate that gene editing using CRISPR technology can alter the antiviral IFN responses, which can be prevented by blocking the IFN signaling using a JAK1/JAK2 inhibitor. This study has implications in gene therapy for

treating genetically inherited skin disorders using CRISPR technology. The contents of this chapter have been peer-reviewed and published in the Journal of Clinical Investigation.

3.2 Introduction

Keratinocytes have long been recognized as a highly refractory cell type for transfection, with the underlying mechanisms of this resistance remaining elusive (127, 128). Keratinocytes are the principal cellular components of the epidermis, which serves as the primary interface between the body and external pathogens such as bacteria and viruses. Beyond their crucial role as a physical barrier, keratinocytes exhibit robust immunological activity through a repertoire of pattern recognition receptors and the secretion of diverse cytokines (129).

The prokaryote-derived clustered regularly interspaced short palindromic repeats (CRISPR)/Cas9 technology has revolutionized our capacity to precisely manipulate specific DNA and RNA sequences within living cells (130). This system relies on guide RNAs (gRNAs) to achieve targeted specificity and operates by creating deliberate breaks in the DNA, which prompt repair mechanisms within the cell. CRISPR technology enables the insertion or deletion of small DNA segments through nonhomologous end-joining and single-base editing through homology-directed repair (130).

CRISPR/Cas9 has witnessed increasing applications in gene therapy for various human diseases, including retinitis pigmentosa (131), Duchennne muscular dystrophy (132), and monogenic dominant conditions such as epidermolysis bullosa (133-136) – a severe and often fatal disorder caused by mutations in structural genes essential for epidermal function. However, the inherent resistance of keratinocytes to CRISPR/Cas9 transfection and the potential involvement of keratinocytes' intrinsic antiviral defense mechanisms in mediating this resistance has not yet been

explored. Investigating these aspects in keratinocytes would significantly enhance future endeavors to achieve efficient gene correction in inherited epidermal disorders.

3.3 Materials and Methods

3.3.1 Keratinocytes culture and treatment.

An immortalized keratinocytes cell line, N/TERT (N/TERT-2G) (105), was used with permission from James G. Rheinwald (Brigham and Women's Hospital, Boston, Massachusetts, USA) for the generation of KO cell lines using nonhomologous end joining via CRISPR/Cas9. This cell line has been shown to have normal differentiation characteristics in both monolayer and organotypic skin models. N/TERTs were grown in Keratinocyte-SFM medium (Thermo Fisher Scientific, 17005-042) supplemented with 30 μg/mL bovine pituitary extract, 0.2 ng/mL epidermal growth factor, and 0.3 mM calcium chloride (106). Keratinocytes (WT and KO) were treated with a demethylating agent, 5-dAza-C (10 μM; MilliporeSigma, A3656-5MG) for the restoration IFNK expression following a previously described protocol.

3.3.2 Generation of CRISPR KO lines in N/TERT keratinocytes.

CRISPR KO keratinocytes were generated as previously described (26). In brief, the sgRNA target sequences were developed (Supplemental Table 1) using a web interface for CRISPR design (https://portals.broadinstitute.org/gpp/public/analysis-tools/sgrna-design). Synthetic sgRNA target sequences were inserted into a cloning backbone, pSpCas9 (BB)-2A-GFP (PX458) (Addgene, 48138), and then cloned into competent E. coli (Thermo Fisher Scientific, C737303). Proper insertion was validated by Sanger sequencing. The plasmid with proper insertion was then transfected into an immortalized KERATINOCYTES line (N/TERTs) using the TransfeX transfection kit (ATCC, ACS4005) in the presence or absence of the JAK1/JAK2 inhibitor

baricitinib (10 μg/mL; Advanced Chemblocks, G-5743). GFP-positive single cells were plated and then expanded. Cells were then genotyped and analyzed by Sanger sequencing.

3.3.3 Generation of DNMT overexpressing keratinocytes lines.

DNMT1-, DNMT3A-, and DNMT3B-overexpressing keratinocytes were generated by lentiviral transduction of mammalian vectors containing Myc-DDK–tagged human DNMT1 (Origene, NM_001130823), DNMT3A (Origene, NM_175629), and DNMT3B (Origene, NM_006892). HEK293T cells were used for viral packaging. Briefly, 10 μg of expression vector was mixed with an equal amount of packaging plasmid (Origene, TR30037) in 1 mL Opti-MEM medium (Invitrogen, 31985062) and 30 μL Turbofectin (Origene, TF8100), and incubated at room temperature for 5 minutes. The obtained mixture was added to the HEK293T cells without dislodging the cells. Supernatants from infected HEK293T cells were harvested after 24 hours, filtered using 0.45 μm syringe filters, aliquoted, and stored at –80°C or used immediately. N/TERT keratinocytes were plated 1 day before transduction in serum- and antibiotic-free medium. The next day, the cells were transduced at a multiplicity of infection of 0.5 along with 8 μg/mL polybrene (Sigma-Aldrich, TR-1003-G). Twenty-four hours after transfection, media were replaced with complete growth media. Cells were passaged the following day, and the puromycin medium was used. Puromycin concentration for keratinocytes was determined by performing a drug-kill curve. An empty mammalian expression vector containing the Myc-DDK tag (Origene, PS100001) was used as a negative control for transduction experiments. Nontransduced cells were also treated with puromycin to observe complete cell death. Once all the cells in control wells were killed, limited dilution was performed to obtain expanded single cells, and the clones were verified for overexpression by Western blotting.

3.3.4 RNA extraction and qRT-PCR.

RNA extraction, qRT-PCR, and RNA-seq were performed following manufacturer's protocol. RNAs were isolated from cell cultures using a Qiagen RNeasy plus kit (catalog 74136). qRT-PCR was performed on a 7900HT Fast Real-time PCR system (Applied Biosystems) with TaqMan Universal PCR Master Mix (Thermo Fisher Scientific) and TaqMan probes (*IFNK*, Hs00737883_m1; *MX1*, Hs00895608_m1; *TMEM173*, Hs00736955_g1; *APOBEC3A*, Hs02572821_s1; *APOBEC3B*, Hs00358981_m1; *APOBEC3C*, Hs00819353_m1; *APOBEC3D*, Hs00537163_m1; *APOBEC3F*, Hs01665324_m1; *APOBEC3G*, Hs00222415_m1; *APOBEC3H*, Hs00419665_m1; *FLG*, Hs00856927_g1: *CCL5*, Hs00982282_m1; *CXCL10*, Hs00171042_m1; *IFIT2*, Hs01584837_s1; *IFNL1*, Hs00601677_g1; *IRF7*, Hs01014809_g1; *DNMT3B*, Hs00171876_m1; *IFNB1*, Hs01077958_s1; *TREX1*, Hs03989617_s1; *DNASEI*, hs00173736_m1; *DNASEII*, Hs00172391_m1).

3.3.5 scRNA-seq from human skin.

Single-cell suspensions were generated for scRNA-seq as follows from the normal human epidermis. Samples were incubated overnight in 0.4% Dispase (Life Technologies) in Hank's balanced saline solution (Gibco) at 4°C. Epidermis and dermis were separated. The epidermis was digested in 0.25% Trypsin-EDTA (Gibco) with 10 U/mL DNase I (Thermo Fisher Scientific) for 1 hour at 37°C, quenched with FBS (Atlanta Biologicals), and strained through a 70 μm mesh. The dermis was minced, digested in 0.2% collagenase II (Life Technologies) and 0.2% collagenase V (Sigma-Aldrich) in plain medium for 1.5 hours at 37°C, and strained through a 70 μm mesh. Epidermal and dermal cells were recombined, and libraries were constructed by the University of Michigan Advanced Genomics Core on the 10× Genomics Chromium system. Libraries were then sequenced on the Illumina NovaSeq 6000 sequencer to generate 151-bp paired-end reads. Data processing, including quality control, read alignment, and gene quantification, was conducted

using the 10X Genomics Cell Ranger software. Seurat was used for normalization, data integration, and clustering analysis. Clustered cells were mapped to corresponding cell types by matching cell cluster gene signatures with putative cell-type-specific markers. The scRNA-seq data can be found in the NCBI Gene Expression Omnibus (GEO GSE179162).

3.3.6 scATAC-seq from human skin.

Skin biopsies (4 mm) were obtained from the palm/hip of a healthy individual. Biopsies were then incubated in 0.4% Dispase overnight to separate the epidermis and dermis. After the separation, the epidermis was transferred to 0.25% Trypsin-EDTA with 10 U/mL DNase mixture and incubated at 37°C for 1 hour. The epidermis mixture was then quenched with FBS and precipitated by centrifugation. Cell pellets were then resuspended in PBS with 0.04% BSA. Cell numbers were counted at this step for future dilution calculation. The nuclei isolation protocol was carried out as described by 10× Genomics. Of note, cells obtained from the epidermis were incubated in lysis buffer on ice for 7 minutes to achieve the optimal lysis efficiency. The cell lysis efficiency was determined by Countess II FL Automated Cell Counter. The scATAC-seq library was prepared by the Advanced Genomics Core at the University of Michigan. Ten thousand nuclei per sample and 25,000 reads per nuclei were targeted, and the libraries were sequenced using a NovaSeq SP 100 cycle flow cell. The raw data were first processed by the Chromium Single Cell ATAC Software Suite (10× Genomics), and then analyzed using the Signac package in R. Briefly, the scATAC-seq data underwent a serial of analyses, including quality control, dimension reduction, clustering, and integration with previously annotated scRNA-seq data. The DNA accessibility profile was then visualized in different cell types and samples. The scATAC-seq data can be found in the NCBI Gene Expression Omnibus (GEO GSE226926).

3.3.7 Accell siRNA knockdown.

N/TERT keratinocytes were plated in 96-well plates (30,000 cells/well) and incubated at 37°C with 5% CO2 overnight. Accell siRNA (100 μM; Dharmacon: *APOBEC3A*, E-017432-00-0005; *APOBEC3B*, E-017322-01-0005; *APOBEC3G*, E-013072-00-0005; *APOBEC3H*, E-019144-00-0005; *DNASE1*, E-016280-00-0005) was prepared in 1× siRNA buffer (Dharmacon, B-002000-UB-100). One microliter of 100 μM siRNA was diluted with 100 μL Accell delivery medium (Dharmacon, B-005000) for each well of 96-well plates. The growth medium was removed from the cells, and 100 μL of the appropriate delivery mix with siRNA was added to each well, and the plate was incubated at 37°C with 5% CO2. Accell Non-targeting Control siRNA (Dharmacon, D-001910-01-05) was used as a negative control. After 72 hours, cells were harvested for RNA preparation. RNA isolation and qRT-PCR were as described above.

3.3.8 3D human epidermal tissue cultures.

Normal human epidermal keratinocytes were isolated from a pool of neonatal foreskins (n = 3) and grown using J2-3T3 mouse fibroblasts as a feeder layer, as originally described by Rheinwald and Green (137). 3D human epidermal raft cultures seeded in collagen hydrogels were prepared using 3 distinct donor pools as described previously (45) and grown at an air-liquid interface for 12 days in E-Medium (DMEM/DMEM-F12 [1:1], 5% FBS, 180 μM adenine, 5 μg/mL bovine pancreatic insulin, 5 μg/mL human apo-transferrin, 5 μg/mL triiodothyronine, 4 mM L-glutamine, 10 ng/mL cholera toxin, 10 μg/mL gentamicin, and 0.25 μg/mL amphotericin B). After 9 days at an air-liquid-interface to allow for epidermal maturation, the reconstructed human epidermises were treated with 0.1% BSA/PBS (Sigma-Aldrich) as vehicle control or 10 ng/mL TNF-α, IL-17A, and IL-22 (R&D Systems) alone or in combination for 72 hours, harvested, and analyzed for changes in gene expression as described previously (46). Epidermal tissues were separated from

the collagen scaffold and lysed in QIAzol (Qiagen) for RNA isolation. RNA-seq and analyses were performed according to the methods described above.

3.3.9 Measurement of CRISPR plasmid stability in keratinocytes.

CRISPR plasmid (PX458, Addgene, 48138) was transfected into keratinocytes using a Transfex transfection kit (ATCC, ACS-4005). Cells were then harvested at different time points (0, 6, 12, 24, and 48 hours) and washed with PBS 3 times to remove extracellular plasmid from the cells. The DNA was then purified using the QIAamp DNA Blood Mini kit (Qiagen, 51106). CRISPR plasmid–specific primers (GFP-F1, GGAGAGGGCAGAGGAAGTCT and GFP-R1, GAACTTCAGGGTCAGCTTGC) were used to perform qPCR with the DNAs isolated from the transfected KERATINOCYTESs using SYBR Green PCR Master Mix (Thermo Fisher Scientific, 4309155) on the 7300 Real-Time PCR System (Applied Biosystems).

3.3.10 Transfection efficiency measurement.

Different cell types such as keratinocytes, fibroblasts, and HEK293T cells were grown in their respective culture medium, and the cells were then transfected with either GFP-linked CRISPR plasmid (PX458 from Addgene) or non-CRISPR plasmid (pCMV-GFP from Addgene) using a Transfex kit (ATCC) or FuGene6 (Promega). Cells were then kept in a CO2 incubator for 24 hours. Cells were then harvested using 0.25% Trypsin-EDTA and then resuspended in PBS. GFP-positive cells were then analyzed at the University of Michigan Flow Cytometry core. We consider the percentage of GFP-positive cells as the transfection efficiency of the respective cell types.

3.3.11 Bisulfite sequencing analysis of the IFNK promoter.

Based on the vendor's recommendations, bisulfite treatment was performed on DNA isolated from WT and CRISPR KO keratinocytes using the EZ DNA Methylation-Gold kit (Zymo Research, D5005). Bisulfite-converted DNA was amplified with the following primers: IFNK-BS-F9

(TGTTGGGATGGATTATTTAGGTATT) and IFNK-BS-R9 (TTCAACAAAAAAAATTTTCTCATTC). PCR products were cloned in pCR2.1-TOPO vector (Thermo Fisher Scientific, K204040) and those clones were then subjected to Sanger sequencing using M13Rev and T7 primers.

3.3.12 Western blotting.

Total protein was isolated from cells using Pierce RIPA buffer (Thermo Fisher Scientific, 89900) with PMSF protease inhibitor (Sigma-Aldrich, 36978) and run in precast gels (Bio-Rad, 456-1094S). The membrane was blocked with 3% BSA and then probed with primary antibodies against the proteins p-IRF3 (Thermo Fisher Scientific, PA536775), IRF3 (Abcam, ab68481), p-STING (Cell Signaling Technology, 19781S), p-STAT1 (Thermo Fisher Scientific, 33-3400), DNMT3B (Cell Signaling Technology, 67259S), and β-actin (Sigma-Aldrich, A5441), followed by secondary antibodies (anti-mouse or -rabbit IgG, AP-linked, Cell Signaling Technology), washed 3 times, and substrate added (Thermo Fisher Scientific, 45-000-947). They were then developed with a chemiluminescence kit and imaged on an iBright imager (Thermo Fisher Scientific).

3.3.13 Immunostaining.

Formalin-fixed, paraffin-embedded tissue slides obtained from healthy individuals were heated for 30 minutes at 60°C, rehydrated, and epitope retrieved with Tris-EDTA (pH 6). Slides were blocked and incubated with primary antibodies against IFN-κ (Abnova, H00056832-M01), APOBEC3G (Abcam, Ab223704), and DNMT3B (Cell Signaling Technology, 67259S) overnight at 4°C. Slides were incubated with biotinylated secondary antibodies (biotinylated goat anti-rabbit IgG antibody, Vector Laboratories, BA1000; biotinylated horse anti-mouse IgG antibody, Vector Laboratories, BA2000) and then incubated with fluorochrome-conjugated streptavidin. Slides were prepared in

mounting medium with 4′,6-diamidino-2-phenylindole (DAPI) (VECTASHIELD Antifade Mounting Medium with DAPI, H-1200, VECTOR). Images were acquired using an inverted Zeiss microscope. Images presented are representative of at least 3 biologic replicates.

3.4 Results

3.4.1 Keratinocytes display a remarkable level of resistance to CRISPR/Cas9 transfection.

Keratinocytes exhibit a high level of resistance to CRISPR/Cas9 transfection. We compared transfection efficiency among human embryonic kidney 239T (HEK293T) cells, dermal fibroblasts, and keratinocytes to investigate this transfection resistance. Using a liposome-based transfection system, we achieved an efficiency of over 60% in HEK293T cells, 7% in fibroblasts, and merely 1% in keratinocytes (Figure 3.4.1A). To gain insights into the underlying factors contributing to these differences in transfection efficiency, we observed that keratinocytes exhibit constitutive expression of the IFN-stimulated gene (ISG) MX1. At the same time, fibroblasts and HEK293T cells did not show this expression. Additionally, keratinocytes exclusively displayed elevated type I IFN (IFN-κ) expression, which was not detected in fibroblasts or HEK293T cells (Figure 3.4.1B). Importantly, following CRISPR plasmid transfection, we observed a significant increase in both IFN-κ and MX1 mRNA expression in keratinocytes (Figure 3.4.1C), indicating that the CRISPR plasmid is recognized by intracellular nucleic acid sensors in keratinocytes. While IFNB1 also exhibited induction in keratinocytes after CRISPR transfection, the extent of induction was comparatively lower (Data not shown here).

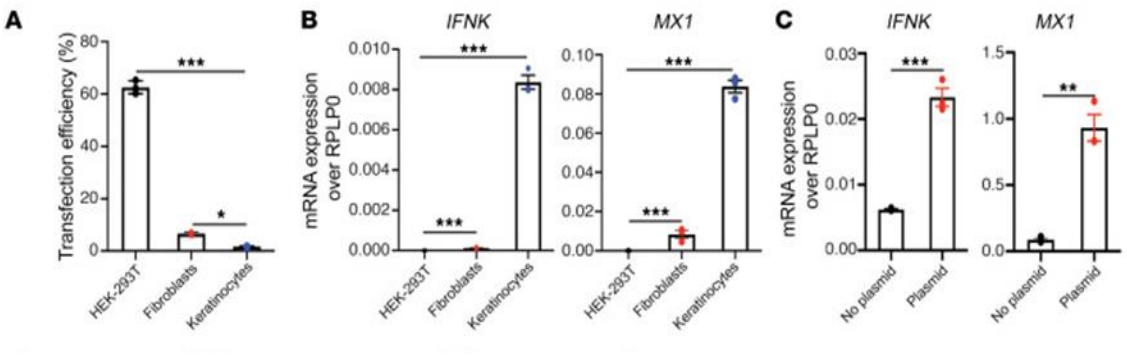

Figure 3.4.1: Keratinocytes activate type I IFN responses to foreign DNA.

A) Comparison of transfection efficiency in keratinocytes (KCs), fibroblasts (FBs), and HEK293T cells (n = 3). B) *IFNK* and *MX1* mRNA expression in KCs, FBs, and HEK293T cells (n = 3). *RPLPO*, large ribosomal protein mRNA (loading control). C) Induction of *IFNK* and IFN-stimulated gene (ISG) *MX1* by CRISPR plasmid transfection (n = 3).

3.4.2 Upon sensing CRISPR DNA, keratinocytes exhibit an inherent STING-dependent IFN response

The stimulator of IFN genes (STING) is a known regulator of innate immune gene induction in response to double-stranded DNA (dsDNA) recognition (138). To investigate the role of STING in the response of keratinocytes to CRISPR transfection, we generated keratinocytes with TMEM173 (STING protein) knockout (KO) (Figure 3.4.2A). In contrast to wild type (WT), TMEM173 KO keratinocytes completely abolished the expression of both *IFNK* and *MX1* and the IFN response following CRISPR transfection (Figure 3.4.2B). STING activation leads to the transcription factor IFN regulatory factor 3 (IRF3) recruitment and facilitates IRF3 phosphorylation (139), which activates type I IFNs and ISGs. We evaluated the phosphorylation of IRF3 (p-IRF3) through western blotting in WT and KO keratinocytes, including *TMEM173* and *IFNK* KOs. While robust p-IRF3 was observed in WT, control KO, and *IFNK* KO keratinocytes, p-IRF3 levels were significantly reduced in *TMEM173* KO keratinocytes following CRISPR/Cas9 transfection (Figure 3.4.2C). These findings suggest that CRISPR/Cas9 transfection induces IFNK

and ISGs in keratinocytes by activating the STING pathway. Importantly, the activation of the STING pathway was not reliant on the constitutive activity of IFNK, as evidenced by the robust phosphorylation of IRF-3 in *IFNK* KO keratinocytes.

We then investigated whether the upregulation of IFNK varied depending on the differentiation state of keratinocytes. IFNK plays a well-established role in host defense against viral pathogens, such as human papillomaviruses (HPVs) (14, 42). Non-oncogenic HPV infections typically do not involve the basal layer of the epidermis (140) but are localized in the upper spinous layers (141). Consistent with a stronger IFNK response in basal keratinocytes, both *TMEM173* and *IFNK* mRNA expression were highest in undifferentiated KRT5+ basal epithelium, contrasting with more differentiated keratinocytes (FLG+), and corresponded to open chromatin regions around the IFNK promoter, as revealed by single-cell ATAC-seq (scATAC-seq) analysis (Figure 3.4.2D). Furthermore, scRNA-seq of epidermal cells demonstrated that both *IFNK* and most ISGs were predominantly expressed in the basal layer of the epidermis (Figure 3.4.2E). These observations suggest that keratinocytes in the basal layer of the epidermis are likely to exhibit greater resistance to CRISPR/Cas9 transfection.

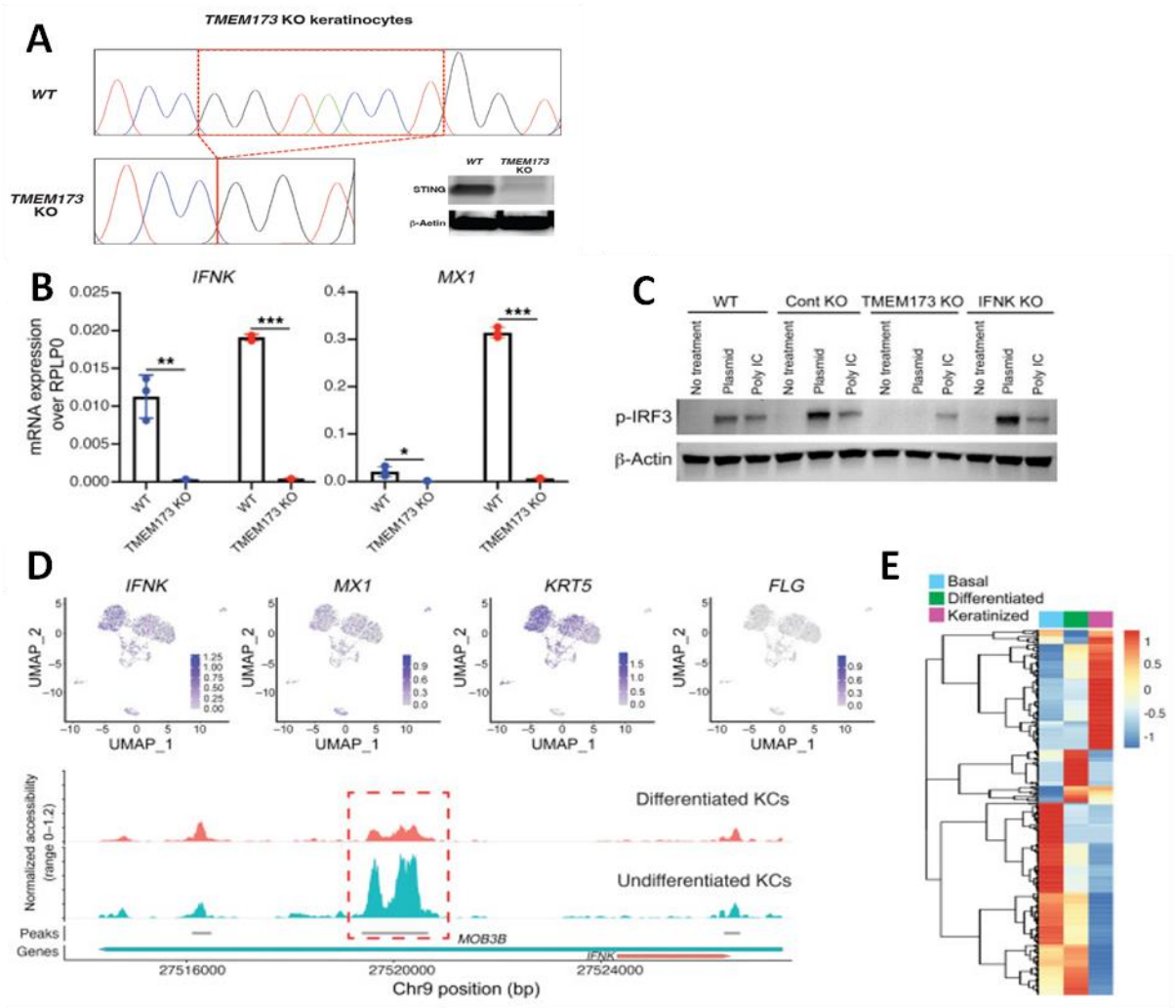

Figure 3.4.2: Keratinocytes activate type I IFN responses, sense foreign DNA through the STING pathway, and resist CRISPR/Cas9 transfection.

A) CRISPR-Cas9 generated *TMEM173* (STING protein) KO in keratinocytes. Chromatogram shows homozygous mutation with 7 nucleotides deletion. STING western blot in TMEM173 KO KCs. E) *IFNK* and *MX1* expression in WT and *TMEM173-KO* (STING-KO) KCs treated with CRISPR plasmid (n = 3). Bars with blue dots indicate no treatment; red dots indicate CRISPR plasmid treatment. B) p-IRF3 Western blot of plasmid-treated KO KCs. C) scATAC-seq from healthy human epidermis shows the overlap between IFNK, MX1, and KRT5 open chromatin regions (upper panels). Chromatin accessibility in the IFNK promoter region is greater in undifferentiated KCs compared with differentiated KCs (indicated by the dotted red box, lower panel). D) Heatmap of type I ISGs from scRNA-seq data of healthy human epidermis shows localization of majority of ISGs in the basal epidermal compartment (n = 3). In the heatmap, red indicates a higher expression, and blue denotes the lower expression of type I ISGs. Data in A–E are represented as mean ± SEM. *P < 0.05; **P < 0.01; ***P < 0.001 by 1-way ANOVA with Tukey's test (A and B) or 2-tailed Student's t test (C and D).

3.4.3 The induction of the cytidine deaminase APOBEC3G, which is dependent on STING, limits the efficiency of CRISPR/Cas9 transfection in keratinocytes

To investigate the uptake and stability of CRISPR/Cas9 plasmids in keratinocytes, we assess the presence of CRISPR/Cas9 GFP-tagged plasmids in keratinocytes at various time points after transfection. Approximately 6-8% of keratinocytes initially exhibited CRISPR/Cas9 GFP+ expression, but this proportion rapidly declined to 1-2% within 48 hours (Figure 3.4.3A). This rapid uptake, followed by a subsequent decrease, suggests an active degradation process of the CRISPR plasmid by keratinocytes, occurring before the interaction of CRISPR/Cas9 with its DNA target. Previous studies have indicated the involvement of DNase I, DNase II, and the APOBEC3 family of cytidine deaminases in the clearance of foreign DNA from human cells (142-144). To examine the role of these factors in the clearance of CRISPR/Cas9 plasmids in keratinocytes, we performed RNA-seq analysis comparing the expression profiles of type I IFN-treated keratinocytes with *IFNK* KO keratinocytes. While most members of the APOBEC3 family showed increased mRNA expression, minor shifts were observed for *DNASE1*, and no changes were detected in *DNASE2* mRNA expression. Additionally, *IFNK* KO keratinocytes exhibited decreased mRNA expression of *APOBEC3A*, *APOBEC3F*, and *APOBEC3G*, with only *APOBEC3H* showing increased expression (Figure 3.4.3B). To investigate the potential involvement of these APOBEC3 members and DNase1 in CRISPR/Cass9 plasmid stability, we employed siRNA knockdown of each of the four APOBEC3 genes and DNase1 in keratinocytes. Only treatments with *siAPOBEC3B* and *siAPOBEC3G* resulted in increased plasmid stability (Figure 3.4.3C).

To explore the relationship between APOBEC3G, epidermal differentiation, and IFNK mRNA expression, we analyzed RNA-seq data from monolayer keratinocytes and epidermal raft systems. This analysis revealed an inverse correlation between the differentiation stage of

keratinocytes and the expression levels of both *IFNK* and *APOBEC3G* (Figure 3.4.3D). Immunostaining further supported this finding, as APOBEC3G expression was strongest in the basal layer of the epidermis, coinciding with IFN-κ (Figure 3.4.3E). Consistent with the role of TMEM173 in regulating IFN responses to CRISPR/Cas9 transfection, significant suppression of APOBEC3G mRNA expression was observed in *TMEM173* KO keratinocytes (Figure 3.4.3F). These findings suggest that STING/ IFN-κ dependent induction of APOBEC3G cytidine deaminase is responsible for the degradation of CRISPR plasmids in keratinocytes.

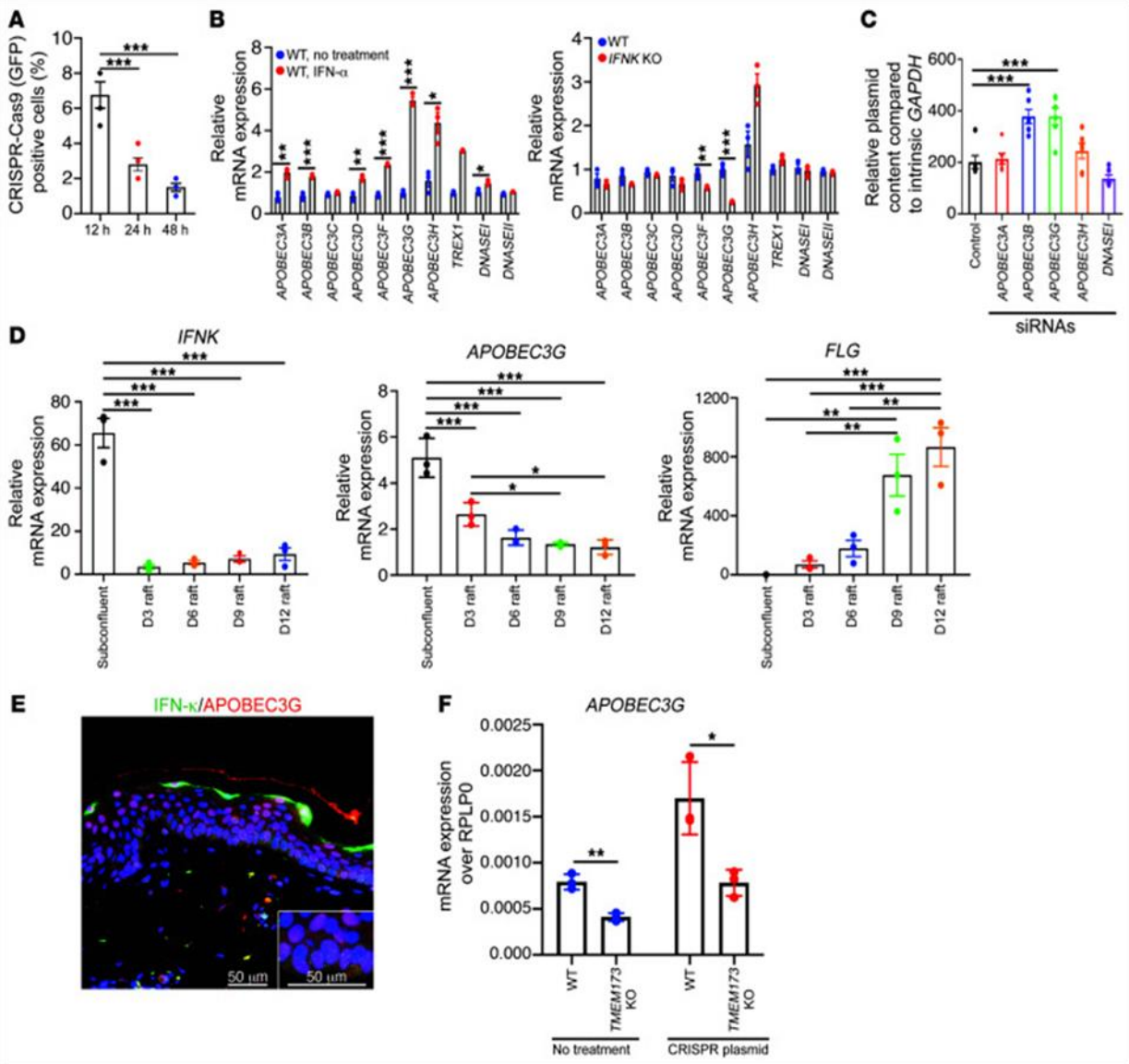

Figure 3.4.3: STING-dependent cytidine deaminase APOBEC3G induction restricts CRISPR/Cas9 transfection efficiency in keratinocytes.

A) Percentage of GFP-positive cells at different time points after CRISPR transfection (n = 3). B) *APOBEC3* mRNA expression in IFN-α–treated keratinocytes (KCs) and *IFNK* KO KCs (n = 3). C) CRISPR plasmid stability in KCs treated with *APOBEC3* siRNAs (n = 5). D) Expression of *IFNK*, *APOBEC3G*, and *FLG* mRNA in subconfluent monolayer cultures and 3D epithelial raft cultures at different stages of differentiation (day 3 [D3] through D12) (n = 3). E) APOBEC3G (red) and IFN-κ (green) immunostaining in healthy skin (n = 3). Scale bars: 50 μm. F) *APOBEC3G* mRNA expression in *TMEM173*-KO KCs (n = 3). Data in A–D and F are represented as mean ± SEM. *P < 0.05; **P < 0.01; ***P < 0.001 by 1-way ANOVA with Tukey's test (A, C, and D) or 2-tailed Student's t-test (B and F).

3.4.4 Downregulation of IFNK and ISG expression in KO keratinocytes generated through CRISPR/Cas9

Subsequently, we investigated whether the successful transfection of keratinocytes relied on the repression of IFNK expression. Our findings supported this hypothesis, as we observed a consistent suppression of both *IFNK* and ISG transcripts in CRISPR/Cas9-generated KO keratinocytes, regardless of the targeted gene (Figure 3.4.4A). Transcriptional regulation often involves CpG methylation, an epigenetic modification (145), and it is known to play a role in controlling *IFNK* expression (41). Thus, we examined whether CpG methylation could explain the observed IFNK and ISG suppression in transfected cells. Treatment of KO keratinocytes with a demethylating agent called 5′-aza-2′-deoxycytidine (5-dAza-C) resulted in a significant increase in *IFNK* expression (Figure 3.4.4B) across all KO keratinocytes treated. Furthermore, bisulfite sequencing of the IFNK promoter region showed a substantial rise in CpG methylation levels in CRISPR KO keratinocytes compared to WT keratinocytes (Figure 3.4.4C). DNA methyltransferases (DNMTs) are enzymes involved in CpG methylation (146) and are expressed in the skin (147). To elucidate the role of DNMTs in regulating IFN-κ, we generated keratinocytes overexpressing *DNMT1*, *DNMT3A*, or *DNMT3B*. Notably, only *DNMT3B* overexpression led to significant suppression of *IFNK* mRNA expression (Figure 3.4.4D), accompanied by CpG hypermethylation of the *IFNK* promoter region (Figure 3.4.4E).

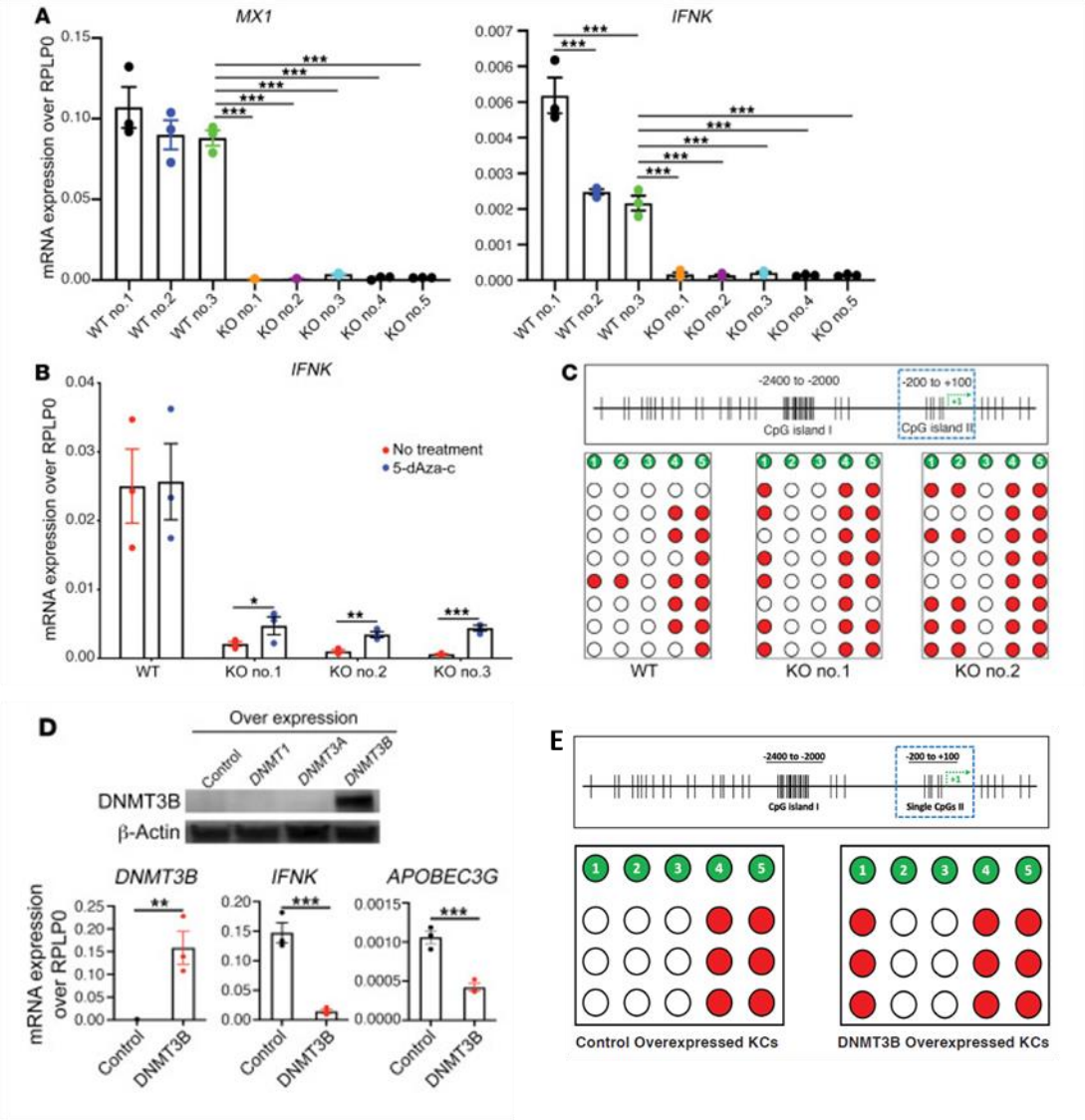

Figure 3.4.4: CRISPR/Cas9-generated keratinocyte knockouts have suppressed type I IFN responses and IFNK expression.

A) Decreased *IFNK* expression and type I IFN response (*MX1* expression) in CRISPR/Cas9-generated KO keratinocytes (KCs) (n = 3). B) Reversal of IFNK expression in CRISPR/Cas9-generated KO KCs after treatment with the demethylating agent 5-dAza-c (n = 3). C) CpG hypermethylation in the IFNK promoter region in KO KCs (KO 1 and KO 2) compared with nontransfected WT control (n = 8). D) Western blot of the DNA methyltransferase DNMT3B in transgenic DNMT1-, DNMT3A-, and DNMT3B-overexpressing KCs (each lane is representative of n = 3 independently transfected KCs [upper panel]). Suppression of *IFNK* and *APOBEC3G* mRNA expression in DNMT3B-transgenic KCs (lower panel). E) CpG hypermethylation in the IFNK promoter region in the DNMT3B overexpressed compared to control overexpressed keratinocytes (n=3).

3.4.5 DNMT methyltransferase plays a crucial role in regulating IFNK expression

To validate the involvement of DNMT in regulating IFNK in vivo, we conducted further experiments. Interestingly, we observed a positive correlation between DNMT3B expression and epidermal differentiation, with the highest expression levels detected in fully differentiated epidermal rafts (Figure 3.4.5A). DNMT3B expression was consistently elevated in CRISPR-generated KO KCs compared to WT KCs (Figure 3.4.5B). Immunostaining analysis of healthy epidermis confirmed the nuclear localization of DNMT3B protein in the upper layers of the epidermis, while its expression was minimal in the lower layers (Figure 3.4.5C). Notably, IFN-κ and APOBEC3G were typically co-localized in the basal layer of the epidermis (Figure 3.4.3E), where minimal DNMT3B staining was observed. These findings suggest that DNMT3B acts as a negative regulator of IFN-κ expression through hypermethylation of the IFNK promoter. Consequently, our study provides valuable insights into the mechanisms underlying the regulation of IFN-κ activity during epidermal differentiation.

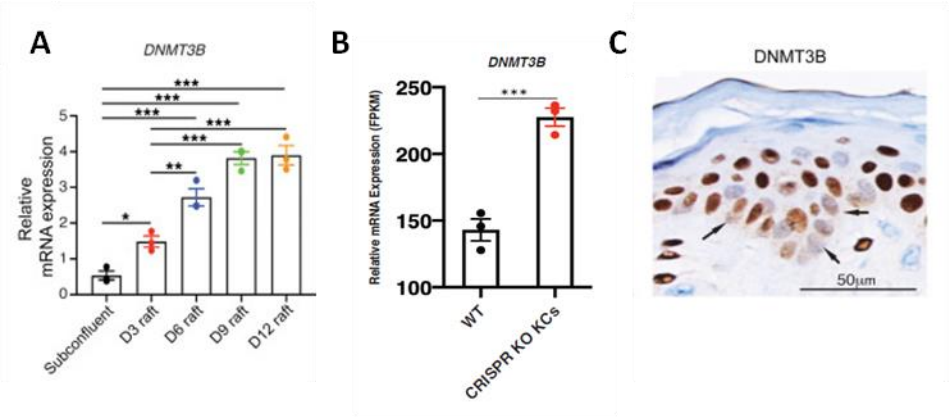

Figure 3.4.5: CRISPR/Cas9-generated keratinocyte knockouts have suppressed IFNK expression due to DNMT3B.

A) *DNMT3B* mRNA expression in 3D epithelial rafts at different stages of differentiation (n = 3). B) *DNMT3B* expression in CRISPR KO keratinocytes. C) DNMT3B protein expression is low in the basal layer (arrows) but increases progressively in the more differentiated layers of the epidermis (n = 3). Scale bar: 50 μm. Data are represented as mean ± SEM. *P < 0.05; **P < 0.01;

***P < 0.001 by 1-way ANOVA with Tukey's test (A and E) or 2-tailed Student's t-test (B and D).

3.4.6. Pharmacologic JAK inhibition enhances transfection efficiency and prevents the generation of low-*IFNK*-expressing KO keratinocytes by inhibiting type I IFN autocrine responses

The expression of IFN-κ, induced by CRISPR/Cas9 transfection, directly influences the expression of APOBEC3 cytidine deaminases, which, in turn, facilitate the degradation of intracellular CRISPR/Cas9 plasmids. To investigate the impact of inhibiting type I IFN signaling on CRISPR/Cas9 transfection efficiency, we utilized *IFNK*- and *TYK2*-KO keratinocytes to disrupt this IFN autocrine loop. Surprisingly, we observed a significant increase in transfection efficiency, indicated by enhanced GFP positivity, in both *IFNK* and *TYK2* KO keratinocytes. Moreover, the control KO keratinocytes exhibited approximately three times higher transfection efficiency than WT keratinocytes, likely due to suppressed IFN-κ autocrine responses. These results were consistent with our observations of improved stability of CRISPR plasmids over time in *IFNK* KO keratinocytes.

To validate these findings and determine if pharmacological inhibition of Janus kinase (JAK)/IFN signaling could reproduce the results, we employed the JAK1/JAK2 inhibitor baricitinib. Baricitinib effectively reduced the mRNA expression of both *IFNK* and the ISG-*MX1* in a dose-dependent manner while increasing transfection efficiency to the same level observed in *IFNK* and *TYK2* KO keratinocytes. To assess whether IFN-κ influences and promotes the selection of keratinocytes with low *IFNK* and ISG expression, we performed CRISPR/Cas9 transfection in the presence or absence of baricitinib. Indeed, *IFNK* and *MX1* expression remained unaffected in KO keratinocytes generated in the presence of baricitinib.

As anticipated, keratinocytes with KO generated in the presence of baricitinib exhibited a notable difference compared to KO keratinocytes generated without baricitinib. Specifically, no hypermethylation was observed in the promoter region of IFNK in the KO keratinocytes generated in the presence of baricitinib. In contrast, hypermethylation was evident in the KO keratinocytes generated without baricitinib.

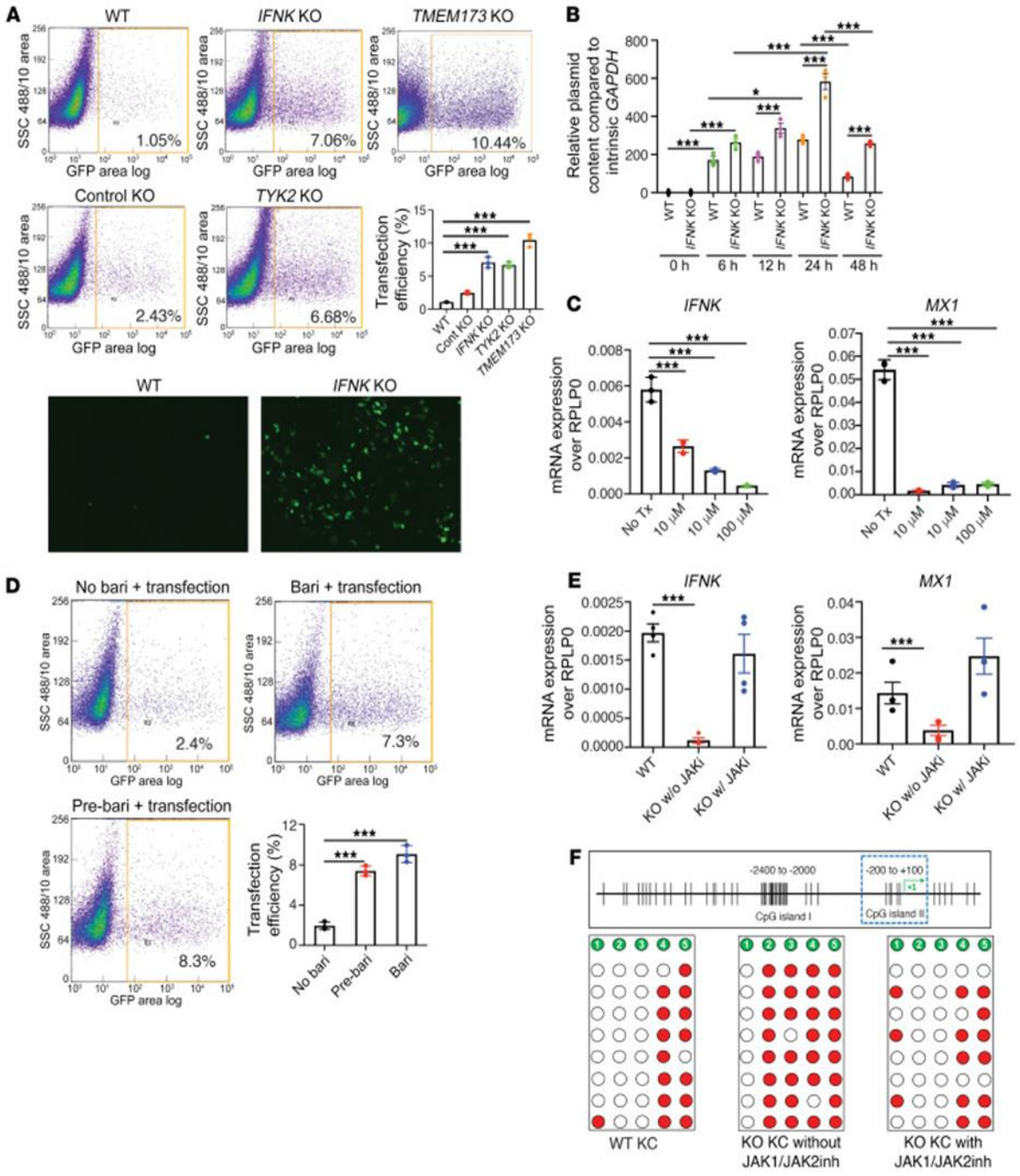

Figure 3.4.6: JAK1/JAK2 inhibition prevents suppression of type I IFN response in CRISPR/Cas9-generated knockout keratinocytes.

A) Increased transfection efficiency in CRISPR/Cas9-generated KO keratinocytes (KCs) (control), and KCs with KO of I*FNK*, *TYK2*, or *TMEM173*, all of which were KOs generated without baricitinib pretreatment (n = 3). (B) CRISPR/Cas9-generated *IFNK*-KO KCs have increased CRISPR/Cas9 plasmid stability (n = 3). (C) Suppression of *IFNK* and *MX1* mRNA expression in baricitinib-treated (JAK1/JAK2 inhibitor) KCs (n = 3). (D) CRISPR/Cas9 transfection efficiency

in baricitinib-treated KCs (n = 3). (E) *IFNK* and M*X1* mRNA expression in the CRISPR/Cas9-generated KO KCs with (w/) or without (w/o) JAK1/JAK2 inhibitor (JAKi). KO KCs with JAK inhibitor (right bar of each panel) were selected after JAK inhibitor treatment (n = 3). (F) CpG methylation in the IFNK promoter region in JAK1/JAK2 inhibitor–treated CRISPR KO KCs. KO KCs with JAK inhibitor (right panel) were selected after JAK inhibitor treatment (n = 8). Data in A–E are represented as mean ± SEM. *P < 0.05; **P < 0.01; ***P < 0.001 by 1-way ANOVA with Tukey's test (A–D) or 2-tailed Student's t-test (E).

3.5 Discussion

Keratinocytes comprise approximately 90% of the cells in the epidermis and play a crucial role in detecting and defending against external agents and pathogens such as bacteria and viruses (148, 149). Keratinocytes express IFN-κ, a type I interferon, predominantly in the basal layer of the epidermis. In the context of human papillomavirus (HPV) infections, which primarily affect the mid to upper layers of the epidermis, the cGAS/STING DNA-sensing pathway is antagonized by HPVs to facilitate infection (150, 151). The study demonstrates that CRISPR plasmids trigger a similar antiviral response through STING in keratinocytes and identifies cytidine deaminase APOBEC3G as a key regulator in limiting CRISPR transfection in keratinocytes.

Interestingly, we observed that keratinocyte KOs lacked IFN-κ due to CRISPR/Cas9 gene editing and displayed permanent suppression of IFN-κ mRNA expression and interferon-stimulated gene (ISG) responses. This suppression was attributed to hypermethylation of the IFN-κ promoter. Normally, IFN-κ expression is limited to the basal layer of the epidermis and decreases as the cells differentiate, coinciding with increased expression of the DNA methyltransferase DNMT3B. Our study demonstrates that DNMT3B is responsible for IFN-κ promoter hypermethylation in CRISPR-edited keratinocytes, subsequently suppressing *IFNK* mRNA expression.

These findings suggest that CRISPR transfection is more efficient in cells where IFN-κ expression has been turned off through promoter methylation. This is further supported by the observation that baricitinib-treated keratinocytes with low *IFNK* expression can easily uptake the CRISPR plasmid (Figure 3.5.1). This parallels the selective effect of HPV infection on keratinocytes that do not express IFN-κ and explains why HPV infections primarily involve the mid to upper layers of the epidermis (152), where IFN-κ is not expressed. Notably, the expression of DNMT3B has been linked to HPV infection, and APOBEC3 proteins have been shown to restrict HPV infection (153-155). HPV can suppress IFN-κ expression through its oncogenic proteins, enabling the virus to enter the lower layers of the epidermis where epidermal stem cells reside (156, 157).

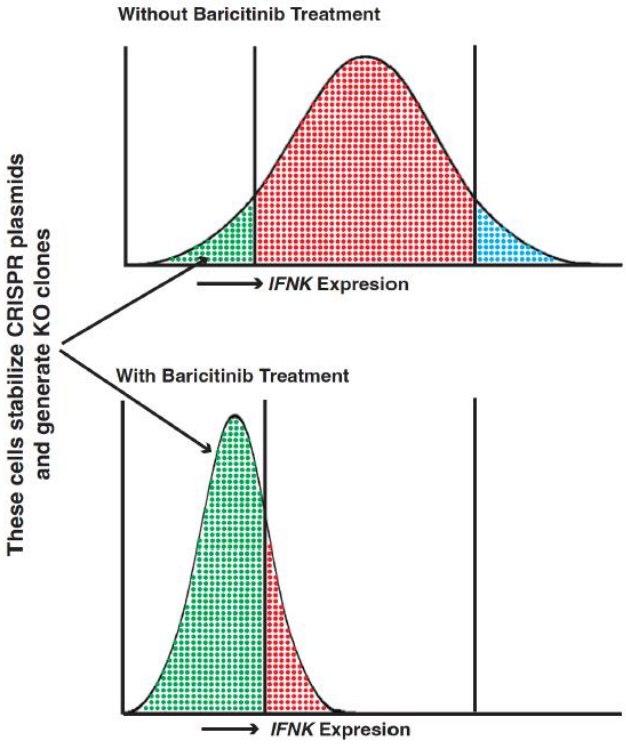

Figure 3.4.7: Schematic illustrating the feasibility of generating CRISPR/Cas9 based genetic knockout keratinocytes following baricitinib treatment.

Previous studies investigating the immunological aspects of CRISPR transfection have mainly focused on the immunogenicity of Cas proteins and the role of the tumor suppressor p53 (158, 159). The interaction between CRISPR/Cas9 and intracellular viral sensing pathways, as revealed in this study, has not been addressed before. The identified IFN-κ/APOBEC3G pathway is likely to apply to other transfection systems that rely on DNA-based plasmids, although its applicability to RNA-based transfections remains to be determined.

The potential use of CRISPR for correcting inherited skin disorders holds great promise. The presented data offers insights into the molecular mechanisms underlying keratinocytes transfection resistance, including the suppression of IFN responses in genetically corrected keratinocytes. The study also suggests that JAK inhibition could be a simple way to overcome these challenges.

Chapter 4 – Conclusions and Future Directions

4.1 Chapter Summary

In my thesis work, I initially aimed to investigate the mechanistic role of the E3 ubiquitin ligase, HERC6, in regulating type I IFN signaling in keratinocytes. However, this seemingly straightforward question became much more complex than anticipated. Throughout my dissertation, I delved into the functions of HERC6 in response to STING activation and established a functional connection between HERC6 and the Hippo pathway. Additionally, I embarked on a side project that focused on unraveling the mechanisms underlying keratinocyte resistance to exogenous CRISPR DNA transfection.

In this concluding chapter, I will summarize the key findings from each of these studies presented in my research chapters and emphasize their significance for the field of keratinocyte biology and innate immune signaling. By shedding light on the intricate roles of HERC6 in down-modulating ISG activity by regulating STING activation and cross-talking with the Hippo pathway, my work contributes to a deeper understanding of the complex regulatory networks governing these processes in a sex-biased fashion. Furthermore, my investigation into keratinocyte resistance to DNA transfection provides insights into the mechanisms, which include type I IFN signaling and post-translational modifications that impact the efficiency of exogenous DNA delivery into these cells. This research opens new avenues for exploring the development of innovative strategies for treating skin diseases and harnessing the immune response of keratinocytes against pathogens.

4.2 Major findings and implications from Chapter 2

Genes that are induced upon IFN activation are referred to as ISGs. An aspect of some of the ISGs is that not all of them are IFN inducible but are also basally expressed. Such a characteristic can be seen in resting keratinocytes which express basal level of *IFNK*, conferring host defense responses to several pathogens the skin often encounters (Figure 1.1). This baseline IFNK expression by keratinocytes is STING-dependent. Studies in human keratinocytes demonstrate STING as an upstream regulator of IFNK expression and down-modulation of STING and IFNK is a mechanism that foreign DNA or viruses use to evade immune mechanisms (21). Here, we report *HERC6* as another such ISG that keratinocytes express at basal level, and is induced upon IFNα, dsDNA or dsRNA agonist treatment (Figure 2.4.2A). HERC6 expression is further dependent on STING and IFNK expression in keratinocytes, suggesting an evolutionarily conserved role for HERC6 in the IFN signaling pathway in keratinocytes (Figure 2.4.2E). We did not find the same response in human fibroblasts, which do not express *IFNK* (Figures 1.1 & 2.4.2B).

HERC6 expression highly correlates with *MX1*, a classic type I IFN inducible gene, and several other ISGs in keratinocytes (Figures 2.4.1A, B & C). An interesting observation was that *HERC6* KO keratinocytes have increased ISG expression and sustained activation of STING/IFN signaling only when treated with cGAMP, a STING agonist elucidating the regulatory role of HERC6 in STING/IFN signaling (Figure 2.4.2A). Our study reveals a novel molecular mechanism of HERC6 regulatory function at the interplay of Hippo-STING-IFN signaling. HERC6 regulates LATS2 activity through ubiquitination mechanism (Figure 2.4.8A). In line with this, *HERC6* KO keratinocytes have increased LATS2 that undergoes phosphorylation, resulting in YAP1 cytoplasmic retention and degradation (Figures 2.4.6A & B). Previous studies have elucidated

YAP/TAZ to restrain, whereas the MST1/2 and LATS1/2 core kinases reciprocate innate immune responses. Our study identifies HERC6 as an upstream regulator of the crosstalk of STING activation-induced Hippo/IFN axis regulation in keratinocytes (Figure 4.1), where the role of YAP1 in TBK1 suppression in this context has not previously been reported.

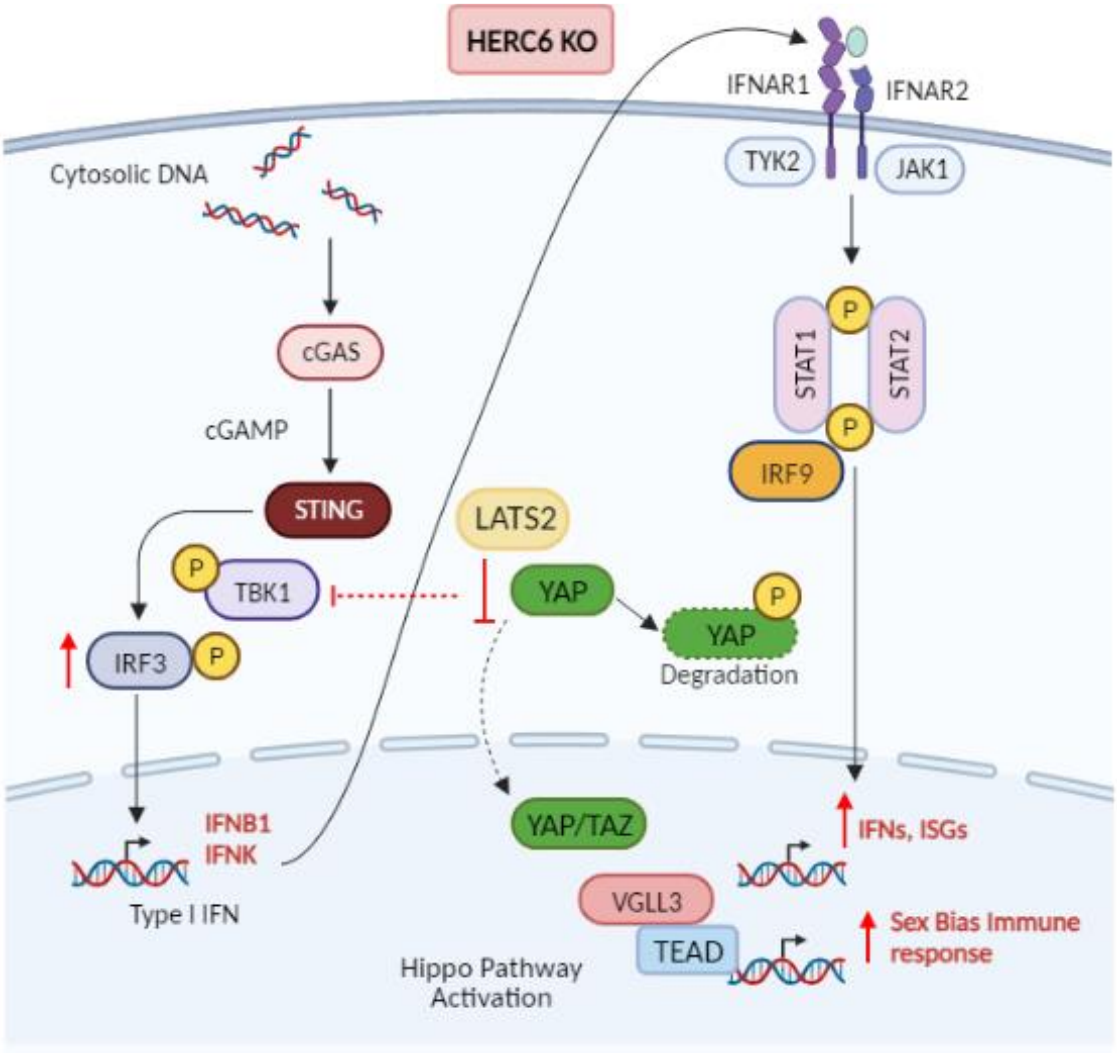

Figure 4.1: Graphical Abstract. *HERC6 negatively regulates type I IFN response in keratinocytes through LAST2 ubiquitination to modulate STING-TBK1 signaling and suppress sex-biased IFN response.*

HERC6 functions are distinct in humans compared to mice. Mouse HERC6 was reported to be functionally similar to human HERC5. Moreover, murine HERC6 can undergo ISGylation whereas human HERC6 cannot, and thus *HERC6* knockout mice were reported to be a suitable model to study human HERC5 and its role in antiviral responses (98). Hence, all our experiments were performed in human primary and immortalized keratinocytes.

More recently, some groups have reported differential expression of HERC6 from the PBMCs of SLE patients and glomeruli of lupus nephritis patients. Other bioinformatic studies have revealed HERC6 as a potential diagnostic biomarker for SLE. Moreover, through network analysis, studies have demonstrated HERC6 to be closely associated with the IFN family of proteins, although its role in promoting disease has not been addressed. We show upregulated HERC6 expression in lupus skin, particularly by the basal and suprabasal keratinocytes (Figures 2.4.9A & B). But the IFN signaling negative regulatory functions of HERC6 is masked in lupus KCs where we observe more IFN-rich inflammatory responses (Figure 2.4.10A). Thus, more studies on strategies to increase HERC6 activity in lupus skin might be beneficial to resolve IFN-induced skin inflammation, as over-expressing HERC6 in keratinocytes was able to attenuate the ISG activity to basal levels (Figure 2.4.5B). More studies are needed to better understand the mechanisms behind the impaired inhibitory function of HERC6-expressing keratinocytes in lupus skin, which would offer valuable insights into any potential inhibitory factors affecting HERC6 activity within the inflammatory environment.

Lupus is a female-biased disease with increased IFN responses in females compared to males (17). The molecular mechanisms for this bias are largely unexplained. We show that HERC6 is involved in sex biased IFN responses upon STING signaling activation. *HERC6* KD keratinocytes exhibited significantly higher ISG responses in primary female Keratinocytes

compared to males (Figure 2.4.10D). This response was even higher in SLE female keratinocytes. We have previously reported a role for the transcription cofactor, VGLL3, in driving cutaneous and systemic disease that is associated with increased IFNK. Interestingly, by inhibiting *VGLL3* activity through the knockdown approach, we were able to suppress amplified ISGs in the HERC6-deficient female SLE keratinocytes suggesting the involvement of VGLL3 in the female-biased IFN responses in lupus keratinocytes (Fig. 2.4.11A). This bias in VGLL3 activity is further supported by increased cytoplasmic VGLL3 in *HERC6* deficient female keratinocytes but not males (Fig. 2.4.10E). Finally, the involvement of VGLL3 in STING/IFN signaling is further strengthened by the RNA-sequencing analysis of *HERC6* knockdown keratinocytes. As shown by the p-values, *HERC6* KD female keratinocytes have higher number of DEGs and GO terms for biological processes with than the *HERC6* KD male keratinocytes (Fig. 2.4.11B).

In summary, this study identifies HERC6 as a negative regulator of STING activation induced IFN responses in keratinocytes that are amplified in lupus skin and are female-biased. Mechanistically, HERC6 acts on LATS2, increasing TBK1 activity due to suppressed YAP1. These findings will affect targeting of HERC6 as a potential therapeutic candidate for lupus and boosting antiviral host immune response.

4.3 Major findings and implications from Chapter 3

This study shows that keratinocytes, the major cells in the epidermis, are highly resistant to CRISPR/Cas9 transfection compared to other cell types, such as fibroblasts and HEK293T cells. Keratinocytes confer this resistance to exogenous DNA by constitutive expression of the IFN-stimulated gene *MX1* and the type I interferon IFN-κ, which is absent in fibroblasts or HEK293T cells. Furthermore, keratinocytes activate the STING pathway, involved in the induction of innate immune genes in response to the recognition of double-stranded DNA (dsDNA) CRISPR plasmid.

Keratinocytes rapidly degrade the CRISPR/Cas9 plasmid shortly after transfection, potentially limiting its effectiveness. DNases and the APOBEC3 family of cytidine deaminases mediate this degradation. *APOBEC3G*, one of the cytidine deaminases, is specifically induced by STING/IFN-κ signaling and plays a role in the degradation of CRISPR/Cas9 plasmids in keratinocytes.

Regardless of the targeted gene, we observed consistent suppression of IFNK and ISG transcripts in CRISPR/Cas9-geneated KO keratinocytes suggesting that transfection of keratinocytes depended on inhibiting *IFNK* expression. To investigate IFNK transcriptional regulation in KO keratinocytes, we investigated CpG methylation, an epigenetic modification that alters gene expression. On a CpG site, where a cytosine nucleotide is followed by a guanine nucleotide, is methylated, a methyl group is added to the cytosine residue. This methylation can lead to gene silencing or reduced gene expression by affecting the binding of transcription factors to DNA or by recruiting proteins that inhibit gene transcription. Essentially, CpG methylation can act as a regulatory mechanism to control gene expression by influencing the accessibility of DNA to the transcriptional machinery. Methylation patterns can be heritable and can also be influenced by various environmental factors. We observed that KOs generated through CRISPR/Cas9 has increased CpG methylation sites due to increased expression of a DNA methyltransferase, DNMT3B.

Suppression of IFNK in CRISPR/Cas9-generated keratinocyte knockouts is associated with increased CpG methylation in the IFNK promoter region. Overexpression of the DNA methyltransferase DNMT3B leads to the suppression of *IFNK* expression and CpG hypermethylation of the IFNK promoter region. Knockout of *IFNK* using CRISPR/Cas9 in

keratinocytes results in suppressed IFN-κ and ISG expression, sufficient to increase the KO efficiency to a limited extent.

Overall, these findings suggest that intrinsic resistance of keratinocytes to CRISPR/Cas9 transfection is mediated by the activation of the STING pathway, induction of IFN-κ, and subsequent degradation of CRISPR/Cas9 plasmids by APOBEC3 cytidine deaminases. Suppression of IFN-κ expression and CpG methylation in the IFNK promoter region contribute to the increased efficiency of CRISPR/Cas9-mediated gene knockout in keratinocytes (Figure 4.2). These insights are crucial for developing strategies to enhance gene correction in inherited epidermal diseases using CRISPR technology.

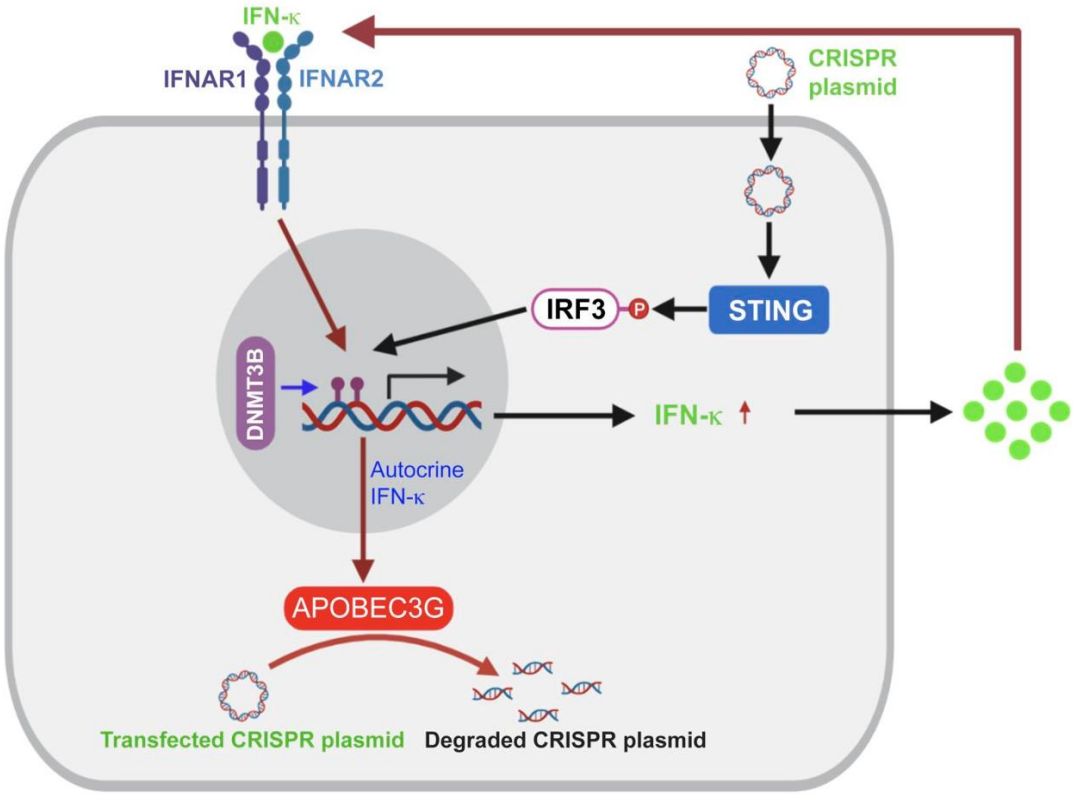

Figure 4.2: Graphical Abstract. *Schematics illustrating the mechanism of CRISPR plasmid transfection resistance in keratinocytes.*

4.4 Future Directions

Does HERC6 play a role in promoting viral replication?

Given the supporting evidence for the involvement of HERC6 in the regulation of ISG expression, further research is required to investigate its potential role in the context of viral infections. For example, it would be interesting to investigate IFN activity in keratinocytes during HPV infection or how viruses may manipulate or evade HERC6-dependent mechanisms. HPV infections are responsible for a spectrum of diseases, ranging from harmless warts to invasive cancers (160). These viruses target epithelial cells, and their replication cycle is intricately linked to the differentiation process of the infected keratinocytes (161). Notably, robust viral gene expression leading to the production of viral proteins and subsequent virus assembly occurs exclusively in the upper layers of the stratum spinosum and granulosum of squamous epithelial tissues (161). In these layers, where *IFNK* expression is limited, it can be inferred that HPV infects the keratinocytes which have compromised IFN-mediated immune responses (13). Notably, these are also the layers where *HERC6* expression is elevated (Fig 4.3). This implies a connection between heightened HERC6 expression, suppressed IFN activity, and increased viral replication.

Given these observations, it becomes intriguing to propose a potential role for HERC6 in enhancing viral replication through suppression of type I IFN activity. However, substantiating this hypothesis would require further comprehensive investigation. This could be addressed by examining cell viability, relative infectivity, and ISG activity in control or HERC6 *KO* keratinocytes infected with luciferase-containing HPV (hpv16-LucF) or an empty lentivirus expressing luciferase (162). Since HPV is a double-stranded DNA virus (163), it is expected that the *HERC6* KO keratinocytes will have reduced viral infectivity and cell death due to increased ISG activity compared to control keratinocytes.

What is the mechanism behind increased VGLL3 activity in HERC6 deficient keratinocytes?

We show evidence that HERC6 mediates LATS2 ubiquitination to suppress STING activation in response to cGAMP stimulation. But how does this relate to VGLL3 and what is inducing VGLL3 expression in *HERC6* deficient female keratinocytes?

VGLL3 is triggered by TGF-β in a manner reliant on the activity of SMAD2/3 and is facilitated by epigenetic modifications (164). Considering the complex regulation of ISGs involving Hippo signaling in *HERC6* KO keratinocytes, we did not examine TGFβ-Smad signaling in our current system, renowned for its ability to activate NF-κB and subsequent pro-inflammatory cytokines (165, 166). Postulating the involvement of TGFβ in VGLL3 induction aligns with our observation of heightened IL-6 in *HERC6* KO keratinocytes. This hypothesis could be addressed in future investigations, involving the assessment of TGFβ levels, NF-κB subunits, total and phosphorylated Smad2/3 in control or *HERC6* KO keratinocytes, both with and without VGLL3 knockdown, and under cGAMP stimulation across male and female keratinocytes.

We have observed an increase in both nuclear and cytoplasmic localization of VGLL3 in HERC6 knockdown female keratinocytes. Nuclear localization of VGLL3, coupled with TEAD transcription factors holds significance in driving sex specific IFN responses (81, 167). The impact of HERC6 deficiency, whether it solely affects localization or is related to overall VGLL3 stability, remains a question. This can be addressed by conducting Western blots to distinguish nuclear and cytoplasmic VGLL3 and by employing pulse-chase assays to assess stability. Control or HERC6 KO keratinocytes can be pulsed with L-azidohomoalanine (AHA) and then subjected to a chase with methionine for various time intervals. Subsequently, lysates will be collected and VGLL3 will be immunoprecipitated. The immunopurified AHA-labeled proteins will be reacted with cyclooctyne modified with a biotin probe. SDS-PAGE gels will resolve AHA-cyclooctyne

conjugates, which will then be detected using the HRP-Streptavidin system. AHA selectively incorporates newly synthesized protein, it is non-toxic, doesn't hinder protein synthesis, and does not affect global protein ubiquitination or degradation (168, 169).

What constitutes the catalytically active component of HERC6 that imparts ubiquitination activity?

HERC6 belongs to the HECT-family E3 ligases which play a pivotal role in ubiquitinating protein substrates, exerting control over a wide range of cellular processes including differentiation, signaling regulation and DNA damage response (170). Their dysregulation is implicated in various diseases (96, 122). The distinguishing characteristic of HECT from other E3 ligases is their C-terminal HECT domain, which comprises two flexible N- and C- lobes. The N-terminal domain plays a role in dynamic regulation by mediating autoinhibition and influencing subcellular localization. Whereas the C-terminal lobe is the catalytic domain known to interact with the acceptor ubiquitin to be transferred onto a target protein (171, 172). Notably, the structural and functional characteristics of HECT E3 ligases are revealed through biochemical studies of a best-characterized class of HECT E3s, the NEDD4-family (171, 173). Furthermore, HERC6 contains an RCC1-like domain (RLD), predicted to function as a guanine nucleotide exchange factor for small G proteins.

However, there exists limited knowledge regarding the structural and functional arrangement of these domains within HERC6. Further investigations that focus on elucidating the catalytic domain responsible for its ubiquitination capabilities are poised to facilitate the therapeutic manipulation of this domain to modify the functions of HERC6. While our current grasp of the biochemical characteristics remains limited, we can approach identification of the

catalytic subunit of HERC6 through truncation of the N-terminal, C-terminal, or the RLD domains and investigate LATS2 ubiquitination in keratinocytes.

What roles does HERC6 play in response to different stimulations?

Our research primarily focusses on the role of HERC6 upon STING activation, but we know from our preliminary data that HERC6 is rapidly induced in keratinocytes with TLR3 activation (Figure 2.4.2). More studies are needed to address the role of HERC6 upon activation of diverse pattern recognition receptors including TLR7 and TLR9 which are implicated in sex biased IFN responses (125, 126). Finally, we have not investigated the functions of HERC6 in response to UV radiation, which triggers flares and keratinocyte apoptosis in CLE skin (48). A better understanding of the role of HERC6 and its mechanism to regulating IFN responses in UV treated keratinocytes and the precise mechanism by which HERC6 fails to inhibit IFN responses in lupus keratinocytes will further shed light on the opportunities in developing HERC6-based interventions or modulators for clinical use.

What function does HERC6 serve in immune cells?

Given the negative regulatory role of HERC6 in keratinocytes this brings into question its function in immune cells where there is room for more research. HERC6 has been demonstrated to be a marker of pro-inflammatory neutrophils in the context of liver fibrosis. Inhibition of the chemokine, CCR2, has resulted in a decrease in hepatic HERC6 positive (HERC6+) neutrophils via inhibition of the STAT1/NFκB pathway (174). This indicates a possible interplay between HERC6 and other G protein-coupled receptors such as CCR2 within neutrophils. This also suggests a potential pro-inflammatory role for HERC6 that could become active during inflammatory conditions. Supporting this notion, we have observed an elevated HERC6 expression in basal as well as spinous keratinocytes of lupus patients compared to normal healthy patients

(Figure 4.3). A distinctive elevation in STING and type I IFN activity is observed in lupus skin. Our findings from Chapter 2 have revealed the ability of HERC6 to dampen STING-induced IFN responses which prompts many questions: Why is HERC6 not mitigating IFN activity in lupus skin? Could the heightened IFN activity be a result of the shifting immune landscape within lupus skin? Alternatively, might the role of HERC6 be altered in IFN rich conditions? Could the functions of HERC6 vary between immune cells and keratinocytes due to their distinct roles and contexts within the immune response and overall physiological processes? Does HERC6 play a role in the cellular stress response pathway, assisting keratinocytes in adapting to various stressors and maintaining homeostasis? Is it possible that other factors are activated which inhibit the functions of HERC6 within lupus skin? To elucidate these intricacies, further investigation is needed to ascertain whether the suppressive role of HERC6 remains intact or becomes skewed in lupus skin.

Should the negative regulatory function of HERC6 be somehow subdued in the context of autoimmune skin diseases like lupus, a significant avenue for future research lies in identifying therapeutic strategies aimed at restoring HERC6 levels. This would serve to mitigate the aberrant IFN signaling that has gone awry. While this dissertation may not have completely unraveled the function of HERC6 in lupus skin, it nevertheless succeeds in generating thought-provoking hypotheses for other researchers to delve into comprehensively.

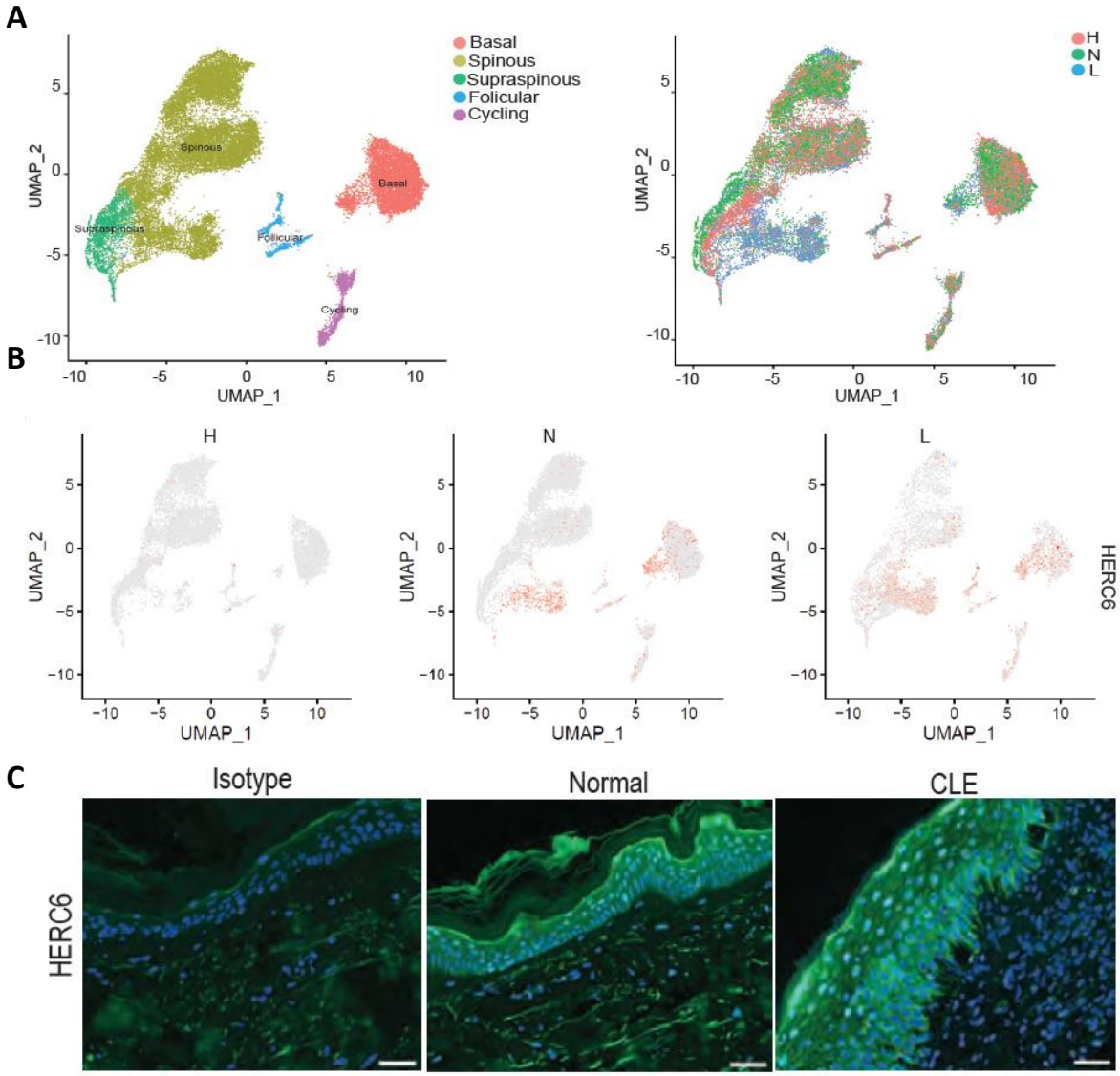

Figure 4.3: Increased HERC6 expression in lupus skin.

A. UMAP plot on the left showing various keratinocyte cell states in different colors across the epidermis, & on the right various cell states colored by sample type as Healthy (H) in coral, non-lesional (N) in green or lesional (L) lupus keratinocytes in blue. B. UMAP plots representing HERC6 MRNA expression across different keratinocyte cell states in healthy (H), non-lesional (N), or lesional (L) lupus skin. C. Immunofluorescence staining of HERC6 in normal healthy or CLE human skin (HERC6 in green & DAPI nuclear staining in blue).

Use of other delivery technologies to enhance transfection efficiency in keratinocytes

In chapter 3 of this thesis, we show that constitutive expression of IFNK in keratinocytes is responsible for poor transfection efficiency. Hence, it would be valuable to explore approaches to improve the delivery of CRISPR components into keratinocytes, including the use of viral vectors, or utilizing new delivery technologies like nano particles (175, 176). We have exhibited the ability of the epigenetic landscape to control the expression of *IFNK*. However, the use of demethylating agents to manipulate these epigenetic modifications has yielded only partial improvements in transfection efficiency. Consequently, alternative strategies are required to effectively regulate the expression of *IFNK*. Further investigation is needed to understand the molecular mechanisms responsible for the constitutive IFNK expression in keratinocytes. Identifying the upstream regulators involved could provide insights into the unique immune properties of keratinocytes and their role in maintaining skin homeostasis.

Upcoming genome editing technologies

While CRISPR/Cas9 is a widely used gene-editing tool, its limitations in keratinocytes highlight the need to explore alternative gene editing technologies. Investigating other genome editing systems, such as base editors, prime editors, or CRISPR-Cas variants, could offer potential solutions to overcome the challenges encountered with CRISPR/Cas9 in keratinocytes (177, 178). Exploring whether other genome editing systems involve the same mechanism of STING activation, induction of APOBEC3G, and other epigenetic modifications would add an intriguing dimension.

Off-target effects to be considered when utilizing CRISPR for gene editing

CRISPR technology holds promise for treating genetic disorders such as cystic fibrosis, sickle cell anemia, Huntington's disease, and Duchenne muscular dystrophy (179). CRISPR is

being investigated as a potential cure for blood disorders like beta-thalassemia and retinitis pigmentosa. However, it is important to note that while CRISPR shows promise, many of these applications are still in the experimental stage or undergoing clinical trials (180). Investigating the specificity and potential off-target effects of CRISPR/Cas9 editing is important. Conducting comprehensive off-target analysis using high-throughput sequencing methods and assessing the impact on the phenotype will help ensure the safety, accuracy, and long-term consequences of CRISPR/Cas9-mediated gene editing in keratinocyte-based therapies.

Is it possible to increase transfection efficiency through HERC6 inhibition in keratinocytes?

We have observed attenuated ISG responses in CGAMP stimulated HERC6 over expressing keratinocytes (Figure 2.4.6). Given our findings from chapter 3 which indicate reduced ISG activity in the successfully generated KOs, it becomes captivating to explore the potential for enhanced transfection efficiency by modulating HERC6 activity. This could be investigated by transfecting control or HERC6 over expressing keratinocytes with GFP expressing CRISPR plasmid and subsequently evaluating the percentage of GFP positive keratinocytes.

Only a few studies have investigated the exogenous DNA sensing mechanisms in human keratinocytes. Upon activation of DNA sensors, keratinocytes exhibit a proficient capacity for undergoing apoptosis, effectively eliminating cells harboring deleterious DNA alterations. Moreover, keratinocytes can synthesize antimicrobial peptides and elicit innate immune responses specifically targeted against foreign DNA elements. Future research endeavors must elucidate the intricate mechanisms underlying apoptosis and antimicrobial peptide production, as they hold substantial importance in comprehending skin diseases and unraveling the interplay between environmental factors and skin health.

This dissertation emphasizes significant mechanisms related to the regulation of type I IFN upon DNA sensing in keratinocytes. Both chapters of the thesis underscore the activation of the STING pathway as a critical factor in keratinocytes for controlling gene expression at both the transcriptional and post-translational levels. Further exploration of the activation of alternative nucleic acid sensing pathways and the regulation of IFN signaling will contribute to a better understanding of the fundamental biology and the relevance of these processes to skin-related diseases.

Appendix

Author Contributions and Acknowledgements

Chapter 2

The E3 ubiquitin ligase HERC6 regulates STING-TBK1 activity in a sex-biased manner through modulation of LATS2/VGLL3 Hippo signaling.

Portions of this chapter have been submitted for publication:

Ranjitha Uppala, Mrinal K. Sarkar, Kelly Z. Young, Feiyang Ma, Pritika Vemulapalli, Rachael Wasikowski, Olesya Plazyo, William R. Swindell, Emanual Maverakis, Mehrnaz Gharaee-Kermani, Allison C. Billi, Lam C. Tsoi, Michelle J. Kahlenberg, Johann E. Gudjonsson.

Author contributions:

RU and JEG conceptualized the current study. RU, MKS, KZY, PV, OP, and MGK performed experiments and analyzed data. RU generated the HERC6 knockout and over-expressing keratinocytes. FM, RW, WRS, EM, RU, ACB, and LCT analyzed the bulk RNA-seq and scRNA-seq data. RU and JEG wrote the original manuscript. JMK and JEG contributed by providing supervision. All the authors contributed by reviewing the manuscript.

Acknowledgements:

This work was supported by the National Institute of Arthritis and Musculoskeletal and Skin 779 Disease of the NIH under award numbers R21-AR077741 (JEG), P30-AR075043 (JEG), R01-780

AI130025 (JEG), the A. Alfred Taubman Medical Research Institute (JEG), R01-AR071384 (JMK), R01-AR081640 (JMK), and K24-AR076975 (JMK).

Chapter 3

Keratinocytes sense and eliminate CRISPR DNA through STING/IFN-κ activation and APOBEC3G induction.

This chapter has been published in the Journal of Clinical Investigation:

Mrinal K Sarkar, **Ranjitha Uppala**, Chang Zeng, Allison C Billi, Lam C Tsoi, Austin Kidder, Xianying Xing, Bethany E Perez White, Shuai Shao, Olesya Plazyo, Sirisha Sirobhushanam, Enze Xing, Yanyun Jiang, Katherine A Gallagher, John J Voorhees, J Michelle Kahlenberg, Johann E Gudjonsson.

Author contributions:

MKS and JEG conceptualized the study. MKS, RU, AK, XX, S Shao, OP, S Sirobhushanam, EX, and YJ performed experiments and analyzed data. MKS developed the CRISPR/Cas9 method in keratinocytes. RU generated lentiviral particles in-house, specifically targeting various DNA methyl transferases (DNMT's including a control, DNMT3A, DNMT3B & DNMT3C) for over-expression in keratinocytes. RU performed the lentiviral packaging, transductions and drafted the methodology for the manuscript. RU performed stimulations in various knockout keratinocytes (including generation of control CRISPR knockout line) and western blotting to investigate STING pathway activation upon CRISPR plasmid transfection (Figures 3.4.2B, 3.4.2C, 3.4.3C, 3.4.4D, 3.4.4E, 3.4.6A). CZ, ACB, and LCT analyzed scATAC-seq and scRNA-seq data. BEPW provided RNAs from 3D raft keratinocytes. MKS, JEG, LCT, and JMK acquired funding for this research.

MKS and JEG wrote the original draft of the manuscript. MKS, RU, CZ, ACB, LCT, AK, XX, BEPW, S Shao, OP, S Sirobhushanam, EX, YJ, KAG, JJV, JMK, and JEG reviewed and edited the manuscript.

Acknowledgements:

We thank Kathleen J. Green and Lisa M. Godsel (Department of Dermatology, Northwestern University, Chicago, Illinois, USA) for providing the primary human keratinocytes to study transfection efficiency. This work was supported by the National Institute of Arthritis and Musculoskeletal and Skin Diseases of the NIH under award numbers R01-AR060802 (to JEG), P30-AR075043 (to JEG, LCT, MKS, and JMK), R01-AR069071 (to JEG), R01-AR071384 (to JMK), K24-AR076975 (to JMK), R21-AR077741 (to JEG), and K01-AR072129 (to LCT), National Psoriasis Foundation Translational Research Grant 852098 (to MKS), the A. Alfred Taubman Medical Research Institute (to JEG and JMK), and the Parfet Emerging Scholar Award (to JMK). This work was also supported by the National Psoriasis Foundation Psoriasis Prevention Initiative and the Dermatology Foundation (to JEG).

Bibliography

1. Isaacs A, Lindenmann J. Virus interference. I. The interferon. Proc R Soc Lond B Biol Sci. 1957;147(927):258-67. doi: 10.1098/rspb.1957.0048. PubMed PMID: 13465720.

2. Ronco LV, Karpova AY, Vidal M, Howley PM. Human papillomavirus 16 E6 oncoprotein binds to interferon regulatory factor-3 and inhibits its transcriptional activity. Genes Dev. 1998;12(13):2061-72. doi: 10.1101/gad.12.13.2061. PubMed PMID: 9649509; PubMed Central PMCID: PMC316980.

3. Ludwig S, Wang X, Ehrhardt C, Zheng H, Donelan N, Planz O, et al. The influenza A virus NS1 protein inhibits activation of Jun N-terminal kinase and AP-1 transcription factors. J Virol. 2002;76(21):11166-71. doi: 10.1128/jvi.76.21.11166-11171.2002. PubMed PMID: 12368362; PubMed Central PMCID: PMC136597.

4. Ivashkiv LB, Donlin LT. Regulation of type I interferon responses. Nat Rev Immunol. 2014;14(1):36-49. doi: 10.1038/nri3581. PubMed PMID: 24362405; PubMed Central PMCID: PMC4084561.

5. Song J, Guan M, Zhao Z, Zhang J. Type I Interferons Function as Autocrine and Paracrine Factors to Induce Autotaxin in Response to TLR Activation. PLoS One. 2015;10(8):e0136629. Epub 20150827. doi: 10.1371/journal.pone.0136629. PubMed PMID: 26313906; PubMed Central PMCID: PMC4552386.

6. Vidalain PO, Laine D, Zaffran Y, Azocar O, Servet-Delprat C, Wild TF, et al. Interferons mediate terminal differentiation of human cortical thymic epithelial cells. J Virol.

2002;76(13):6415-24. doi: 10.1128/jvi.76.13.6415-6424.2002. PubMed PMID: 12050353; PubMed Central PMCID: PMC136281.

7. Kuka M, De Giovanni M, Iannacone M. The role of type I interferons in CD4(+) T cell differentiation. Immunol Lett. 2019;215:19-23. Epub 20190213. doi: 10.1016/j.imlet.2019.01.013. PubMed PMID: 30771379; PubMed Central PMCID: PMC7234836.

8. Eggenberger J, Blanco-Melo D, Panis M, Brennand KJ, tenOever BR. Type I interferon response impairs differentiation potential of pluripotent stem cells. Proc Natl Acad Sci U S A. 2019;116(4):1384-93. Epub 20190103. doi: 10.1073/pnas.1812449116. PubMed PMID: 30606801; PubMed Central PMCID: PMC6347712.

9. Shao S, Tsoi LC, Sarkar MK, Xing X, Xue K, Uppala R, et al. IFN-gamma enhances cell-mediated cytotoxicity against keratinocytes via JAK2/STAT1 in lichen planus. Sci Transl Med. 2019;11(511). doi: 10.1126/scitranslmed.aav7561. PubMed PMID: 31554739; PubMed Central PMCID: PMC7285657.

10. Haller O, Arnheiter H, Gresser I, Lindenmann J. Virus-specific interferon action. Protection of newborn Mx carriers against lethal infection with influenza virus. J Exp Med. 1981;154(1):199-203. doi: 10.1084/jem.154.1.199. PubMed PMID: 6166723; PubMed Central PMCID: PMC2186399.

11. Pandey AK, Yang Y, Jiang Z, Fortune SM, Coulombe F, Behr MA, et al. NOD2, RIP2 and IRF5 play a critical role in the type I interferon response to Mycobacterium tuberculosis. PLoS Pathog. 2009;5(7):e1000500. Epub 20090703. doi: 10.1371/journal.ppat.1000500. PubMed PMID: 19578435; PubMed Central PMCID: PMC2698121.

12. Watanabe T, Asano N, Fichtner-Feigl S, Gorelick PL, Tsuji Y, Matsumoto Y, et al. NOD1 contributes to mouse host defense against Helicobacter pylori via induction of type I IFN and activation of the ISGF3 signaling pathway. J Clin Invest. 2010;120(5):1645-62. Epub 20100412. doi: 10.1172/JCI39481. PubMed PMID: 20389019; PubMed Central PMCID: PMC2860924.

13. Sarkar MK, Hile GA, Tsoi LC, Xing X, Liu J, Liang Y, et al. Photosensitivity and type I IFN responses in cutaneous lupus are driven by epidermal-derived interferon kappa. Ann Rheum Dis. 2018;77(11):1653-64. Epub 20180718. doi: 10.1136/annrheumdis-2018-213197. PubMed PMID: 30021804; PubMed Central PMCID: PMC6185784.

14. LaFleur DW, Nardelli B, Tsareva T, Mather D, Feng P, Semenuk M, et al. Interferon-kappa, a novel type I interferon expressed in human keratinocytes. J Biol Chem. 2001;276(43):39765-71. Epub 20010820. doi: 10.1074/jbc.M102502200. PubMed PMID: 11514542.

15. Bin Xu YST, Jon Musai, William R Swindell, Mrinal Sakar, Johann Gudjonsson, J. Michelle Kahlenberg and Grace Hile. A Novel Requirement for IFNβ1 Signaling for IFNκ Induction in Keratinocytes (Abstract). 2021.

16. Li Y, Song Y, Zhu L, Wang X, Yang B, Lu P, et al. Interferon Kappa Is Up-Regulated in Psoriasis and It Up-Regulates Psoriasis-Associated Cytokines in vivo. Clin Cosmet Investig Dermatol. 2019;12:865-73. Epub 20191129. doi: 10.2147/CCID.S218243. PubMed PMID: 31819584; PubMed Central PMCID: PMC6890215.

17. Xing E, Billi AC, Gudjonsson JE. Sex Bias and Autoimmune Diseases. J Invest Dermatol. 2022;142(3 Pt B):857-66. Epub 20210803. doi: 10.1016/j.jid.2021.06.008. PubMed PMID: 34362556.

18. Capobianchi MR, Uleri E, Caglioti C, Dolei A. Type I IFN family members: similarity, differences and interaction. Cytokine Growth Factor Rev. 2015;26(2):103-11. Epub 20141031. doi: 10.1016/j.cytogfr.2014.10.011. PubMed PMID: 25466633; PubMed Central PMCID: PMC7108279.

19. Ali S, Mann-Nuttel R, Schulze A, Richter L, Alferink J, Scheu S. Sources of Type I Interferons in Infectious Immunity: Plasmacytoid Dendritic Cells Not Always in the Driver's Seat. Front Immunol. 2019;10:778. Epub 20190412. doi: 10.3389/fimmu.2019.00778. PubMed PMID: 31031767; PubMed Central PMCID: PMC6473462.

20. Hile GA, Gudjonsson JE, Kahlenberg JM. The influence of interferon on healthy and diseased skin. Cytokine. 2020;132:154605. Epub 20181206. doi: 10.1016/j.cyto.2018.11.022. PubMed PMID: 30527631; PubMed Central PMCID: PMC6551332.

21. Almine JF, O'Hare CA, Dunphy G, Haga IR, Naik RJ, Atrih A, et al. IFI16 and cGAS cooperate in the activation of STING during DNA sensing in human keratinocytes. Nat Commun. 2017;8:14392. Epub 20170213. doi: 10.1038/ncomms14392. PubMed PMID: 28194029; PubMed Central PMCID: PMC5316833.

22. Miller LS. Toll-like receptors in skin. Adv Dermatol. 2008;24:71-87. doi: 10.1016/j.yadr.2008.09.004. PubMed PMID: 19256306; PubMed Central PMCID: PMC2633625.

23. Kim JA, Seong RK, Son SW, Shin OS. Insights into ZIKV-Mediated Innate Immune Responses in Human Dermal Fibroblasts and Epidermal Keratinocytes. J Invest Dermatol. 2019;139(2):391-9. Epub 20180912. doi: 10.1016/j.jid.2018.07.038. PubMed PMID: 30218650.

24. Li S, Kang P, Zhang W, Jian Z, Zhang Q, Yi X, et al. Activated NLR family pyrin domain containing 3 (NLRP3) inflammasome in keratinocytes promotes cutaneous T-cell

response in patients with vitiligo. J Allergy Clin Immunol. 2020;145(2):632-45. Epub 20191119. doi: 10.1016/j.jaci.2019.10.036. PubMed PMID: 31756352.

25. Spreu J, Kuttruff S, Stejfova V, Dennehy KM, Schittek B, Steinle A. Interaction of C-type lectin-like receptors NKp65 and KACL facilitates dedicated immune recognition of human keratinocytes. Proc Natl Acad Sci U S A. 2010;107(11):5100-5. Epub 20100301. doi: 10.1073/pnas.0913108107. PubMed PMID: 20194751; PubMed Central PMCID: PMC2841919.

26. Arase H, Arase N, Saito T. Interferon gamma production by natural killer (NK) cells and NK1.1+ T cells upon NKR-P1 cross-linking. J Exp Med. 1996;183(5):2391-6. doi: 10.1084/jem.183.5.2391. PubMed PMID: 8642351; PubMed Central PMCID: PMC2192568.

27. Bhat P, Leggatt G, Waterhouse N, Frazer IH. Interferon-gamma derived from cytotoxic lymphocytes directly enhances their motility and cytotoxicity. Cell Death Dis. 2017;8(6):e2836. Epub 20170601. doi: 10.1038/cddis.2017.67. PubMed PMID: 28569770; PubMed Central PMCID: PMC5520949.

28. Kajita AI, Morizane S, Takiguchi T, Yamamoto T, Yamada M, Iwatsuki K. Interferon-Gamma Enhances TLR3 Expression and Anti-Viral Activity in Keratinocytes. J Invest Dermatol. 2015;135(8):2005-11. Epub 20150330. doi: 10.1038/jid.2015.125. PubMed PMID: 25822580.

29. Pastore S, Corinti S, La Placa M, Didona B, Girolomoni G. Interferon-gamma promotes exaggerated cytokine production in keratinocytes cultured from patients with atopic dermatitis. J Allergy Clin Immunol. 1998;101(4 Pt 1):538-44. doi: 10.1016/S0091-6749(98)70361-6. PubMed PMID: 9564808.

30. Fallahi P, Ruffilli I. Contact dermatitis and interferon-gamma dependent chemokines. Clin Ter. 2016;167(5):e112-e6. doi: 10.7417/CT.2016.1953. PubMed PMID: 27845488.

31. Wack A, Terczynska-Dyla E, Hartmann R. Guarding the frontiers: the biology of type III interferons. Nat Immunol. 2015;16(8):802-9. doi: 10.1038/ni.3212. PubMed PMID: 26194286; PubMed Central PMCID: PMC7096991.

32. Sommereyns C, Paul S, Staeheli P, Michiels T. IFN-lambda (IFN-lambda) is expressed in a tissue-dependent fashion and primarily acts on epithelial cells in vivo. PLoS Pathog. 2008;4(3):e1000017. Epub 20080314. doi: 10.1371/journal.ppat.1000017. PubMed PMID: 18369468; PubMed Central PMCID: PMC2265414.

33. Finotti G, Tamassia N, Cassatella MA. Interferon-λs and Plasmacytoid Dendritic Cells: A Close Relationship. Front Immunol. 2017;8:1015. Epub 20170823. doi: 10.3389/fimmu.2017.01015. PubMed PMID: 28878776; PubMed Central PMCID: PMC5572322.

34. Misumi I, Whitmire JK. IFN-λ exerts opposing effects on T cell responses depending on the chronicity of the virus infection. J Immunol. 2014;192(8):3596-606. Epub 20140319. doi: 10.4049/jimmunol.1301705. PubMed PMID: 24646741; PubMed Central PMCID: PMC4157331.

35. Weir SA, Kc K, Shoaib S, Yusuf N. The Immunotherapeutic Role of Type I and III Interferons in Melanoma and Non-Melanoma Skin Cancers. Life (Basel). 2023;13(6). Epub 20230601. doi: 10.3390/life13061310. PubMed PMID: 37374093; PubMed Central PMCID: PMC10303590.

36. Darnell JE, Jr., Kerr IM, Stark GR. Jak-STAT pathways and transcriptional activation in response to IFNs and other extracellular signaling proteins. Science. 1994;264(5164):1415-21. doi: 10.1126/science.8197455. PubMed PMID: 8197455.

37. Platanias LC. Mechanisms of type-I- and type-II-interferon-mediated signalling. Nat Rev Immunol. 2005;5(5):375-86. doi: 10.1038/nri1604. PubMed PMID: 15864272.

38. Schwab LSU, Villalon-Letelier F, Tessema MB, Londrigan SL, Brooks AG, Hurt A, et al. Expression of a Functional Mx1 Protein Is Essential for the Ability of RIG-I Agonist Prophylaxis to Provide Potent and Long-Lasting Protection in a Mouse Model of Influenza A Virus Infection. Viruses. 2022;14(7). Epub 20220715. doi: 10.3390/v14071547. PubMed PMID: 35891527; PubMed Central PMCID: PMC9319350.

39. Aaronson DS, Horvath CM. A road map for those who don't know JAK-STAT. Science. 2002;296(5573):1653-5. doi: 10.1126/science.1071545. PubMed PMID: 12040185.

40. Kotenko SV, Gallagher G, Baurin VV, Lewis-Antes A, Shen M, Shah NK, et al. IFN-lambdas mediate antiviral protection through a distinct class II cytokine receptor complex. Nat Immunol. 2003;4(1):69-77. Epub 20021216. doi: 10.1038/ni875. PubMed PMID: 12483210.

41. Scott ML, Woodby BL, Ulicny J, Raikhy G, Orr AW, Songock WK, et al. Human Papillomavirus 16 E5 Inhibits Interferon Signaling and Supports Episomal Viral Maintenance. J Virol. 2020;94(2). Epub 20200106. doi: 10.1128/JVI.01582-19. PubMed PMID: 31666385; PubMed Central PMCID: PMC6955282.

42. Li Y, Song Y, Zhu L, Wang X, Richers B, Leung DYM, et al. Interferon Kappa Is Important for Keratinocyte Host Defense against Herpes Simplex Virus-1. J Immunol Res. 2020;2020:5084682. Epub 20200103. doi: 10.1155/2020/5084682. PubMed PMID: 32352019; PubMed Central PMCID: PMC7178474.

43. Wolf SJ, Audu CO, Joshi A, denDekker A, Melvin WJ, Davis FM, et al. IFN-kappa is critical for normal wound repair and is decreased in diabetic wounds. JCI Insight. 2022;7(9).

Epub 20220509. doi: 10.1172/jci.insight.152765. PubMed PMID: 35358091; PubMed Central PMCID: PMC9090246.

44. Ikic D, Padovan I, Pipic N, Knezevic M, Djakovic N, Rode B, et al. Interferon therapy for basal cell carcinoma and squamous cell carcinoma. Int J Clin Pharmacol Ther Toxicol. 1991;29(9):342-6. PubMed PMID: 1937994.

45. Ismail A, Yusuf N. Type I interferons: key players in normal skin and select cutaneous malignancies. Dermatol Res Pract. 2014;2014:847545. Epub 20140105. doi: 10.1155/2014/847545. PubMed PMID: 24516470; PubMed Central PMCID: PMC3913103.

46. Cooper EE, Pisano CE, Shapiro SC. Cutaneous Manifestations of "Lupus": Systemic Lupus Erythematosus and Beyond. Int J Rheumatol. 2021;2021:6610509. Epub 20210518. doi: 10.1155/2021/6610509. PubMed PMID: 34113383; PubMed Central PMCID: PMC8154312.

47. Robinson ES, Werth VP. The role of cytokines in the pathogenesis of cutaneous lupus erythematosus. Cytokine. 2015;73(2):326-34. Epub 20150309. doi: 10.1016/j.cyto.2015.01.031. PubMed PMID: 25767072.

48. Stannard JN, Reed TJ, Myers E, Lowe L, Sarkar MK, Xing X, et al. Lupus Skin Is Primed for IL-6 Inflammatory Responses through a Keratinocyte-Mediated Autocrine Type I Interferon Loop. J Invest Dermatol. 2017;137(1):115-22. Epub 20160916. doi: 10.1016/j.jid.2016.09.008. PubMed PMID: 27646883; PubMed Central PMCID: PMC5183476.

49. Garelli CJ, Refat MA, Nanaware PP, Ramirez-Ortiz ZG, Rashighi M, Richmond JM. Current Insights in Cutaneous Lupus Erythematosus Immunopathogenesis. Front Immunol. 2020;11:1353. Epub 20200702. doi: 10.3389/fimmu.2020.01353. PubMed PMID: 32714331; PubMed Central PMCID: PMC7343764.

50. Skonieczna K, Czajkowski R, Kaszewski S, Gawrych M, Jakubowska A, Grzybowski T. Genetic similarities and differences between discoid and systemic lupus erythematosus patients within the Polish population. Postepy Dermatol Alergol. 2017;34(3):228-32. Epub 20170529. doi: 10.5114/pdia.2017.67479. PubMed PMID: 28670251; PubMed Central PMCID: PMC5471372.

51. Jarvinen TM, Hellquist A, Koskenmies S, Einarsdottir E, Koskinen LL, Jeskanen L, et al. Tyrosine kinase 2 and interferon regulatory factor 5 polymorphisms are associated with discoid and subacute cutaneous lupus erythematosus. Exp Dermatol. 2010;19(2):123-31. Epub 20090916. doi: 10.1111/j.1600-0625.2009.00982.x. PubMed PMID: 19758313.

52. Peschke K, Friebe F, Zimmermann N, Wahlicht T, Schumann T, Achleitner M, et al. Deregulated type I IFN response in TREX1-associated familial chilblain lupus. J Invest Dermatol. 2014;134(5):1456-9. Epub 20131122. doi: 10.1038/jid.2013.496. PubMed PMID: 24270665.

53. Harley IT, Niewold TB, Stormont RM, Kaufman KM, Glenn SB, Franek BS, et al. The role of genetic variation near interferon-kappa in systemic lupus erythematosus. J Biomed Biotechnol. 2010;2010. Epub 20100715. doi: 10.1155/2010/706825. PubMed PMID: 20706608; PubMed Central PMCID: PMC2914299.

54. Lowes MA, Suarez-Farinas M, Krueger JG. Immunology of psoriasis. Annu Rev Immunol. 2014;32:227-55. doi: 10.1146/annurev-immunol-032713-120225. PubMed PMID: 24655295; PubMed Central PMCID: PMC4229247.

55. El Malki K, Karbach SH, Huppert J, Zayoud M, Reissig S, Schuler R, et al. An alternative pathway of imiquimod-induced psoriasis-like skin inflammation in the absence of

interleukin-17 receptor a signaling. J Invest Dermatol. 2013;133(2):441-51. Epub 20120906. doi: 10.1038/jid.2012.318. PubMed PMID: 22951726.

56. Gharaee-Kermani M, Estadt SN, Tsoi LC, Wolf-Fortune SJ, Liu J, Xing X, et al. IFN-kappa Is a Rheostat for Development of Psoriasiform Inflammation. J Invest Dermatol. 2022;142(1):155-65 e3. Epub 20210805. doi: 10.1016/j.jid.2021.05.029. PubMed PMID: 34364883; PubMed Central PMCID: PMC8688309.

57. Bissonnette R, Papp K, Maari C, Yao Y, Robbie G, White WI, et al. A randomized, double-blind, placebo-controlled, phase I study of MEDI-545, an anti-interferon-alfa monoclonal antibody, in subjects with chronic psoriasis. J Am Acad Dermatol. 2010;62(3):427-36. doi: 10.1016/j.jaad.2009.05.042. PubMed PMID: 20159310.

58. Both T, Dalm VA, van Hagen PM, van Daele PL. Reviewing primary Sjogren's syndrome: beyond the dryness - From pathophysiology to diagnosis and treatment. Int J Med Sci. 2017;14(3):191-200. Epub 20170223. doi: 10.7150/ijms.17718. PubMed PMID: 28367079; PubMed Central PMCID: PMC5370281.

59. Hile GA, Lowe L, Kahlenberg JM. Cutaneous purpura of Sjogren syndrome successfully treated with hydroxychloroquine. JAAD Case Rep. 2017;3(4):326-8. Epub 20170718. doi: 10.1016/j.jdcr.2017.04.011. PubMed PMID: 28752122; PubMed Central PMCID: PMC5517835.

60. Nguyen CQ, Peck AB. The Interferon-Signature of Sjogren's Syndrome: How Unique Biomarkers Can Identify Underlying Inflammatory and Immunopathological Mechanisms of Specific Diseases. Front Immunol. 2013;4:142. Epub 20130705. doi: 10.3389/fimmu.2013.00142. PubMed PMID: 23847613; PubMed Central PMCID: PMC3701867.

61. An J, Woodward JJ, Sasaki T, Minie M, Elkon KB. Cutting edge: Antimalarial drugs inhibit IFN-beta production through blockade of cyclic GMP-AMP synthase-DNA interaction. J Immunol. 2015;194(9):4089-93. Epub 20150327. doi: 10.4049/jimmunol.1402793. PubMed PMID: 25821216.

62. Wang X, Zhang T, Guo Z, Pu J, Riaz F, Feng R, et al. The Efficiency of Hydroxychloroquine for the Treatment of Primary Sjogren's Syndrome: A Systematic Review and Meta-Analysis. Front Pharmacol. 2021;12:693796. Epub 20210907. doi: 10.3389/fphar.2021.693796. PubMed PMID: 34588979; PubMed Central PMCID: PMC8475756.

63. Sarkar MK, Uppala R, Zeng C, Billi AC, Tsoi LC, Kidder A, et al. Keratinocytes sense and eliminate CRISPR DNA through STING/IFN-kappa activation and APOBEC3G induction. J Clin Invest. 2023;133(9). Epub 20230501. doi: 10.1172/JCI159393. PubMed PMID: 36928117; PubMed Central PMCID: PMC10145927.

64. Sun L, Wu J, Du F, Chen X, Chen ZJ. Cyclic GMP-AMP synthase is a cytosolic DNA sensor that activates the type I interferon pathway. Science. 2013;339(6121):786-91. Epub 20121220. doi: 10.1126/science.1232458. PubMed PMID: 23258413; PubMed Central PMCID: PMC3863629.

65. Dobbs N, Burnaevskiy N, Chen D, Gonugunta VK, Alto NM, Yan N. STING Activation by Translocation from the ER Is Associated with Infection and Autoinflammatory Disease. Cell Host Microbe. 2015;18(2):157-68. Epub 20150730. doi: 10.1016/j.chom.2015.07.001. PubMed PMID: 26235147; PubMed Central PMCID: PMC4537353.

66. Ma F, Li B, Yu Y, Iyer SS, Sun M, Cheng G. Positive feedback regulation of type I interferon by the interferon-stimulated gene STING. EMBO Rep. 2015;16(2):202-12. Epub

20150108. doi: 10.15252/embr.201439366. PubMed PMID: 25572843; PubMed Central PMCID: PMC4328747.

67. Kong L, Sui C, Chen T, Zhang L, Zhao W, Zheng Y, et al. The ubiquitin E3 ligase TRIM10 promotes STING aggregation and activation in the Golgi apparatus. Cell Rep. 2023;42(4):112306. Epub 20230326. doi: 10.1016/j.celrep.2023.112306. PubMed PMID: 36972172.

68. Cui Y, Yu H, Zheng X, Peng R, Wang Q, Zhou Y, et al. SENP7 Potentiates cGAS Activation by Relieving SUMO-Mediated Inhibition of Cytosolic DNA Sensing. PLoS Pathog. 2017;13(1):e1006156. Epub 20170117. doi: 10.1371/journal.ppat.1006156. PubMed PMID: 28095500; PubMed Central PMCID: PMC5271409.

69. Liu S, Cai X, Wu J, Cong Q, Chen X, Li T, et al. Phosphorylation of innate immune adaptor proteins MAVS, STING, and TRIF induces IRF3 activation. Science. 2015;347(6227):aaa2630. Epub 20150129. doi: 10.1126/science.aaa2630. PubMed PMID: 25636800.

70. Chen G, Yan Q, Liu L, Wen X, Zeng H, Yin S. Histone Deacetylase 3 Governs beta-Estradiol-ERalpha-Involved Endometrial Tumorigenesis via Inhibition of STING Transcription. Cancers (Basel). 2022;14(19). Epub 20220928. doi: 10.3390/cancers14194718. PubMed PMID: 36230643; PubMed Central PMCID: PMC9563443.

71. Zhao D, Gao Y, Su Y, Zhou Y, Yang T, Li Y, et al. Oroxylin A regulates cGAS DNA hypermethylation induced by methionine metabolism to promote HSC senescence. Pharmacol Res. 2023;187:106590. Epub 20221202. doi: 10.1016/j.phrs.2022.106590. PubMed PMID: 36464146.

72. Panchanathan R, Choubey D. Murine BAFF expression is up-regulated by estrogen and interferons: implications for sex bias in the development of autoimmunity. Mol Immunol. 2013;53(1-2):15-23. Epub 20120710. doi: 10.1016/j.molimm.2012.06.013. PubMed PMID: 22784990; PubMed Central PMCID: PMC3439561.

73. Ruggieri A, Anticoli S, D'Ambrosio A, Giordani L, Viora M. The influence of sex and gender on immunity, infection and vaccination. Ann Ist Super Sanita. 2016;52(2):198-204. doi: 10.4415/ANN_16_02_11. PubMed PMID: 27364394.

74. Singh RP, Hahn BH, Bischoff DS. Interferon Genes Are Influenced by 17beta-Estradiol in SLE. Front Immunol. 2021;12:725325. Epub 20211018. doi: 10.3389/fimmu.2021.725325. PubMed PMID: 34733276; PubMed Central PMCID: PMC8558410.

75. Rider V, Abdou NI, Kimler BF, Lu N, Brown S, Fridley BL. Gender Bias in Human Systemic Lupus Erythematosus: A Problem of Steroid Receptor Action? Front Immunol. 2018;9:611. Epub 20180328. doi: 10.3389/fimmu.2018.00611. PubMed PMID: 29643853; PubMed Central PMCID: PMC5882779.

76. Brandt JE, Priori R, Valesini G, Fairweather D. Sex differences in Sjögren's syndrome: a comprehensive review of immune mechanisms. Biol Sex Differ. 2015;6:19. Epub 20151103. doi: 10.1186/s13293-015-0037-7. PubMed PMID: 26535108; PubMed Central PMCID: PMC4630965.

77. Bruno KA, Morales-Lara AC, Bittencourt EB, Siddiqui H, Bommarito G, Patel J, et al. Sex differences in comorbidities associated with Sjögren's disease. Front Med (Lausanne). 2022;9:958670. Epub 20220804. doi: 10.3389/fmed.2022.958670. PubMed PMID: 35991633; PubMed Central PMCID: PMC9387724.

78. Brito-Zerón P, Acar-Denizli N, Ng WF, Horváth IF, Rasmussen A, Seror R, et al. Epidemiological profile and north-south gradient driving baseline systemic involvement of primary Sjögren's syndrome. Rheumatology (Oxford). 2020;59(9):2350-9. doi: 10.1093/rheumatology/kez578. PubMed PMID: 31873754.

79. Passia E, Vis M, Coates LC, Soni A, Tchetverikov I, Gerards AH, et al. Sex-specific differences and how to handle them in early psoriatic arthritis. Arthritis Res Ther. 2022;24(1):22. Epub 20220111. doi: 10.1186/s13075-021-02680-y. PubMed PMID: 35016726; PubMed Central PMCID: PMC8751248.

80. Crow MK, Olferiev M, Kirou KA. Type I Interferons in Autoimmune Disease. Annu Rev Pathol. 2019;14:369-93. Epub 20181017. doi: 10.1146/annurev-pathol-020117-043952. PubMed PMID: 30332560.

81. Billi AC, Gharaee-Kermani M, Fullmer J, Tsoi LC, Hill BD, Gruszka D, et al. The female-biased factor VGLL3 drives cutaneous and systemic autoimmunity. JCI Insight. 2019;4(8). Epub 20190418. doi: 10.1172/jci.insight.127291. PubMed PMID: 30996136; PubMed Central PMCID: PMC6538382.

82. Du Y, Cui R, Tian N, Chen M, Zhang XL, Dai SM. Regulation of type I interferon signature by VGLL3 in the fibroblast-like synoviocytes of rheumatoid arthritis patients via targeting the Hippo pathway. Arthritis Res Ther. 2022;24(1):188. Epub 20220808. doi: 10.1186/s13075-022-02880-0. PubMed PMID: 35941675; PubMed Central PMCID: PMC9358906.

83. Fu M, Hu Y, Lan T, Guan KL, Luo T, Luo M. The Hippo signalling pathway and its implications in human health and diseases. Signal Transduct Target Ther. 2022;7(1):376. Epub

20221108. doi: 10.1038/s41392-022-01191-9. PubMed PMID: 36347846; PubMed Central PMCID: PMC9643504.

84. Qi S, Zhu Y, Liu X, Li P, Wang Y, Zeng Y, et al. WWC proteins mediate LATS1/2 activation by Hippo kinases and imply a tumor suppression strategy. Mol Cell. 2022;82(10):1850-64 e7. Epub 20220415. doi: 10.1016/j.molcel.2022.03.027. PubMed PMID: 35429439.

85. Oka T, Mazack V, Sudol M. Mst2 and Lats kinases regulate apoptotic function of Yes kinase-associated protein (YAP). J Biol Chem. 2008;283(41):27534-46. Epub 20080717. doi: 10.1074/jbc.M804380200. PubMed PMID: 18640976.

86. Ma S, Tang T, Probst G, Konradi A, Jin C, Li F, et al. Transcriptional repression of estrogen receptor alpha by YAP reveals the Hippo pathway as therapeutic target for ER(+) breast cancer. Nat Commun. 2022;13(1):1061. Epub 20220225. doi: 10.1038/s41467-022-28691-0. PubMed PMID: 35217640; PubMed Central PMCID: PMC8881512.

87. Zhang Q, Meng F, Chen S, Plouffe SW, Wu S, Liu S, et al. Hippo signalling governs cytosolic nucleic acid sensing through YAP/TAZ-mediated TBK1 blockade. Nat Cell Biol. 2017;19(4):362-74. Epub 20170327. doi: 10.1038/ncb3496. PubMed PMID: 28346439; PubMed Central PMCID: PMC5398908.

88. Aravamudhan A, Haak AJ, Choi KM, Meridew JA, Caporarello N, Jones DL, et al. TBK1 regulates YAP/TAZ and fibrogenic fibroblast activation. Am J Physiol Lung Cell Mol Physiol. 2020;318(5):L852-L63. Epub 20200311. doi: 10.1152/ajplung.00324.2019. PubMed PMID: 32159970; PubMed Central PMCID: PMC7272740.

89. Sirobhushanam S, Lazar S, Kahlenberg JM. Interferons in Systemic Lupus Erythematosus. Rheum Dis Clin North Am. 2021;47(3):297-315. Epub 20210610. doi: 10.1016/j.rdc.2021.04.001. PubMed PMID: 34215365; PubMed Central PMCID: PMC8254852.

90. Sontheimer RD. The lexicon of cutaneous lupus erythematosus--a review and personal perspective on the nomenclature and classification of the cutaneous manifestations of lupus erythematosus. Lupus. 1997;6(2):84-95. doi: 10.1177/096120339700600203. PubMed PMID: 9061656.

91. Decout A, Katz JD, Venkatraman S, Ablasser A. The cGAS-STING pathway as a therapeutic target in inflammatory diseases. Nat Rev Immunol. 2021;21(9):548-69. Epub 20210408. doi: 10.1038/s41577-021-00524-z. PubMed PMID: 33833439; PubMed Central PMCID: PMC8029610.

92. Kemp MG, Lindsey-Boltz LA, Sancar A. UV Light Potentiates STING (Stimulator of Interferon Genes)-dependent Innate Immune Signaling through Deregulation of ULK1 (Unc51-like Kinase 1). J Biol Chem. 2015;290(19):12184-94. Epub 20150319. doi: 10.1074/jbc.M115.649301. PubMed PMID: 25792739; PubMed Central PMCID: PMC4424351.

93. Tsoi LC, Hile GA, Berthier CC, Sarkar MK, Reed TJ, Liu J, et al. Hypersensitive IFN Responses in Lupus Keratinocytes Reveal Key Mechanistic Determinants in Cutaneous Lupus. J Immunol. 2019;202(7):2121-30. Epub 20190211. doi: 10.4049/jimmunol.1800650. PubMed PMID: 30745462; PubMed Central PMCID: PMC6424612.

94. Wang W, Xu L, Su J, Peppelenbosch MP, Pan Q. Transcriptional Regulation of Antiviral Interferon-Stimulated Genes. Trends Microbiol. 2017;25(7):573-84. Epub 20170127. doi: 10.1016/j.tim.2017.01.001. PubMed PMID: 28139375; PubMed Central PMCID: PMC7127685.

95. Jacquet S, Pontier D, Etienne L. Rapid Evolution of HERC6 and Duplication of a Chimeric HERC5/6 Gene in Rodents and Bats Suggest an Overlooked Role of HERCs in Mammalian Immunity. Front Immunol. 2020;11:605270. Epub 20201218. doi: 10.3389/fimmu.2020.605270. PubMed PMID: 33391270; PubMed Central PMCID: PMC7775381.

96. Dong Z, Yan Q, Cao W, Liu Z, Wang X. Identification of key molecules in COVID-19 patients significantly correlated with clinical outcomes by analyzing transcriptomic data. Front Immunol. 2022;13:930866. Epub 20220822. doi: 10.3389/fimmu.2022.930866. PubMed PMID: 36072597; PubMed Central PMCID: PMC9441550.

97. Zhong Y, Zhang W, Hong X, Zeng Z, Chen Y, Liao S, et al. Screening Biomarkers for Systemic Lupus Erythematosus Based on Machine Learning and Exploring Their Expression Correlations With the Ratios of Various Immune Cells. Front Immunol. 2022;13:873787. Epub 20220610. doi: 10.3389/fimmu.2022.873787. PubMed PMID: 35757721; PubMed Central PMCID: PMC9226453.

98. Oudshoorn D, van Boheemen S, Sanchez-Aparicio MT, Rajsbaum R, Garcia-Sastre A, Versteeg GA. HERC6 is the main E3 ligase for global ISG15 conjugation in mouse cells. PLoS One. 2012;7(1):e29870. Epub 20120117. doi: 10.1371/journal.pone.0029870. PubMed PMID: 22272257; PubMed Central PMCID: PMC3260183.

99. Karnell JL, Wu Y, Mittereder N, Smith MA, Gunsior M, Yan L, et al. Depleting plasmacytoid dendritic cells reduces local type I interferon responses and disease activity in patients with cutaneous lupus. Sci Transl Med. 2021;13(595). doi: 10.1126/scitranslmed.abf8442. PubMed PMID: 34039741.

100. Berghofer B, Frommer T, Haley G, Fink L, Bein G, Hackstein H. TLR7 ligands induce higher IFN-alpha production in females. J Immunol. 2006;177(4):2088-96. doi: 10.4049/jimmunol.177.4.2088. PubMed PMID: 16887967.

101. Meier A, Chang JJ, Chan ES, Pollard RB, Sidhu HK, Kulkarni S, et al. Sex differences in the Toll-like receptor-mediated response of plasmacytoid dendritic cells to HIV-1. Nat Med. 2009;15(8):955-9. Epub 20090713. doi: 10.1038/nm.2004. PubMed PMID: 19597505; PubMed Central PMCID: PMC2821111.

102. Hile GA, Coit P, Xu B, Victory AM, Gharaee-Kermani M, Estadt SN, et al. Regulation of Photosensitivity by the Hippo Pathway in Lupus Skin. Arthritis Rheumatol. 2023;75(7):1216-28. Epub 20230418. doi: 10.1002/art.42460. PubMed PMID: 36704840.

103. Swindell WR, Sarkar MK, Liang Y, Xing X, Baliwag J, Elder JT, et al. RNA-seq identifies a diminished differentiation gene signature in primary monolayer keratinocytes grown from lesional and uninvolved psoriatic skin. Sci Rep. 2017;7(1):18045. Epub 20171222. doi: 10.1038/s41598-017-18404-9. PubMed PMID: 29273799; PubMed Central PMCID: PMC5741737.

104. Rittie L, Fisher GJ. Isolation and culture of skin fibroblasts. Methods Mol Med. 2005;117:83-98. doi: 10.1385/1-59259-940-0:083. PubMed PMID: 16118447.

105. Dickson MA, Hahn WC, Ino Y, Ronfard V, Wu JY, Weinberg RA, et al. Human keratinocytes that express hTERT and also bypass a p16(INK4a)-enforced mechanism that limits life span become immortal yet retain normal growth and differentiation characteristics. Mol Cell Biol. 2000;20(4):1436-47. doi: 10.1128/MCB.20.4.1436-1447.2000. PubMed PMID: 10648628; PubMed Central PMCID: PMC85304.

106. Swindell WR, Beamer MA, Sarkar MK, Loftus S, Fullmer J, Xing X, et al. RNA-Seq Analysis of IL-1B and IL-36 Responses in Epidermal Keratinocytes Identifies a Shared MyD88-Dependent Gene Signature. Front Immunol. 2018;9:80. Epub 20180129. doi: 10.3389/fimmu.2018.00080. PubMed PMID: 29434599; PubMed Central PMCID: PMC5796909.

107. Staeheli P, Haller O, Boll W, Lindenmann J, Weissmann C. Mx protein: constitutive expression in 3T3 cells transformed with cloned Mx cDNA confers selective resistance to influenza virus. Cell. 1986;44(1):147-58. doi: 10.1016/0092-8674(86)90493-9. PubMed PMID: 3000619.

108. Buljan M, Ciuffa R, van Drogen A, Vichalkovski A, Mehnert M, Rosenberger G, et al. Kinase Interaction Network Expands Functional and Disease Roles of Human Kinases. Mol Cell. 2020;79(3):504-20 e9. Epub 20200723. doi: 10.1016/j.molcel.2020.07.001. PubMed PMID: 32707033; PubMed Central PMCID: PMC7427327.

109. Zou R, Xu Y, Feng Y, Shen M, Yuan F, Yuan Y. YAP nuclear-cytoplasmic translocation is regulated by mechanical signaling, protein modification, and metabolism. Cell Biol Int. 2020;44(7):1416-25. Epub 20200327. doi: 10.1002/cbin.11345. PubMed PMID: 32190949.

110. Stein C, Bardet AF, Roma G, Bergling S, Clay I, Ruchti A, et al. YAP1 Exerts Its Transcriptional Control via TEAD-Mediated Activation of Enhancers. PLoS Genet. 2015;11(8):e1005465. Epub 20150821. doi: 10.1371/journal.pgen.1005465. PubMed PMID: 26295846; PubMed Central PMCID: PMC4546604.

111. Livneh I, Cohen-Kaplan V, Cohen-Rosenzweig C, Avni N, Ciechanover A. The life cycle of the 26S proteasome: from birth, through regulation and function, and onto its death. Cell Res.

2016;26(8):869-85. Epub 20160722. doi: 10.1038/cr.2016.86. PubMed PMID: 27444871; PubMed Central PMCID: PMC4973335.

112. Kastan N, Gnedeva K, Alisch T, Petelski AA, Huggins DJ, Chiaravalli J, et al. Small-molecule inhibition of Lats kinases may promote Yap-dependent proliferation in postmitotic mammalian tissues. Nat Commun. 2021;12(1):3100. Epub 20210525. doi: 10.1038/s41467-021-23395-3. PubMed PMID: 34035288; PubMed Central PMCID: PMC8149661.

113. Figeac N, Mohamed AD, Sun C, Schonfelder M, Matallanas D, Garcia-Munoz A, et al. VGLL3 operates via TEAD1, TEAD3 and TEAD4 to influence myogenesis in skeletal muscle. J Cell Sci. 2019;132(13). Epub 20190705. doi: 10.1242/jcs.225946. PubMed PMID: 31138678; PubMed Central PMCID: PMC6633393.

114. Liang Y, Tsoi LC, Xing X, Beamer MA, Swindell WR, Sarkar MK, et al. A gene network regulated by the transcription factor VGLL3 as a promoter of sex-biased autoimmune diseases. Nat Immunol. 2017;18(2):152-60. Epub 20161219. doi: 10.1038/ni.3643. PubMed PMID: 27992404; PubMed Central PMCID: PMC5289297.

115. Yuan L, Mao Y, Luo W, Wu W, Xu H, Wang XL, et al. Palmitic acid dysregulates the Hippo-YAP pathway and inhibits angiogenesis by inducing mitochondrial damage and activating the cytosolic DNA sensor cGAS-STING-IRF3 signaling mechanism. J Biol Chem. 2017;292(36):15002-15. Epub 20170711. doi: 10.1074/jbc.M117.804005. PubMed PMID: 28698384; PubMed Central PMCID: PMC5592676.

116. Sladitschek-Martens HL, Guarnieri A, Brumana G, Zanconato F, Battilana G, Xiccato RL, et al. YAP/TAZ activity in stromal cells prevents ageing by controlling cGAS-STING. Nature. 2022;607(7920):790-8. Epub 20220629. doi: 10.1038/s41586-022-04924-6. PubMed PMID: 35768505; PubMed Central PMCID: PMC7613988.

117. Moroishi T, Hayashi T, Pan WW, Fujita Y, Holt MV, Qin J, et al. The Hippo Pathway Kinases LATS1/2 Suppress Cancer Immunity. Cell. 2016;167(6):1525-39 e17. doi: 10.1016/j.cell.2016.11.005. PubMed PMID: 27912060; PubMed Central PMCID: PMC5512418.

118. Niewold TB, Adler JE, Glenn SB, Lehman TJ, Harley JB, Crow MK. Age- and sex-related patterns of serum interferon-alpha activity in lupus families. Arthritis Rheum. 2008;58(7):2113-9. doi: 10.1002/art.23619. PubMed PMID: 18576315; PubMed Central PMCID: PMC2729701.

119. Congy-Jolivet N, Cenac C, Dellacasagrande J, Puissant-Lubrano B, Apoil PA, Guedj K, et al. Monocytes are the main source of STING-mediated IFN-alpha production. EBioMedicine. 2022;80:104047. Epub 20220510. doi: 10.1016/j.ebiom.2022.104047. PubMed PMID: 35561451; PubMed Central PMCID: PMC9108881.

120. Billi AC, Ma F, Plazyo O, Gharaee-Kermani M, Wasikowski R, Hile GA, et al. Nonlesional lupus skin contributes to inflammatory education of myeloid cells and primes for cutaneous inflammation. Sci Transl Med. 2022;14(642):eabn2263. Epub 20220427. doi: 10.1126/scitranslmed.abn2263. PubMed PMID: 35476593; PubMed Central PMCID: PMC9169615.

121. Psarras A, Alase A, Antanaviciute A, Carr IM, Md Yusof MY, Wittmann M, et al. Functionally impaired plasmacytoid dendritic cells and non-haematopoietic sources of type I interferon characterize human autoimmunity. Nat Commun. 2020;11(1):6149. Epub 20201201. doi: 10.1038/s41467-020-19918-z. PubMed PMID: 33262343; PubMed Central PMCID: PMC7708979.

122. Cao L, Zhang H, Bai J, Wu T, Wang Y, Wang N, et al. HERC6 is upregulated in peripheral blood mononuclear cells of patients with systemic lupus erythematosus and promotes

the disease progression. Autoimmunity. 2022;55(8):506-14. Epub 20220726. doi: 10.1080/08916934.2022.2103800. PubMed PMID: 35880641.

123. Qing J, Song W, Tian L, Samuel SB, Li Y. Potential Small Molecules for Therapy of Lupus Nephritis Based on Genetic Effect and Immune Infiltration. Biomed Res Int. 2022;2022:2259164. Epub 20220423. doi: 10.1155/2022/2259164. PubMed PMID: 35502341; PubMed Central PMCID: PMC9056222.

124. Alexopoulou L, Holt AC, Medzhitov R, Flavell RA. Recognition of double-stranded RNA and activation of NF-kappaB by Toll-like receptor 3. Nature. 2001;413(6857):732-8. doi: 10.1038/35099560. PubMed PMID: 11607032.

125. Souyris M, Cenac C, Azar P, Daviaud D, Canivet A, Grunenwald S, et al. TLR7 escapes X chromosome inactivation in immune cells. Sci Immunol. 2018;3(19). doi: 10.1126/sciimmunol.aap8855. PubMed PMID: 29374079.

126. Torcia MG, Nencioni L, Clemente AM, Civitelli L, Celestino I, Limongi D, et al. Sex differences in the response to viral infections: TLR8 and TLR9 ligand stimulation induce higher IL10 production in males. PLoS One. 2012;7(6):e39853. Epub 20120629. doi: 10.1371/journal.pone.0039853. PubMed PMID: 22768144; PubMed Central PMCID: PMC3387221.

127. Gresch O, Altrogge L. Transfection of difficult-to-transfect primary mammalian cells. Methods Mol Biol. 2012;801:65-74. doi: 10.1007/978-1-61779-352-3_5. PubMed PMID: 21987247.

128. Zare S, Zarei MA, Ghadimi T, Fathi F, Jalili A, Hakhamaneshi MS. Isolation, cultivation and transfection of human keratinocytes. Cell Biol Int. 2014;38(4):444-51. Epub 20140106. doi: 10.1002/cbin.10218. PubMed PMID: 24323435.

129. Jiang R, Fichtner ML, Hoehn KB, Pham MC, Stathopoulos P, Nowak RJ, et al. Single-cell repertoire tracing identifies rituximab-resistant B cells during myasthenia gravis relapses. JCI Insight. 2020;5(14). Epub 20200723. doi: 10.1172/jci.insight.136471. PubMed PMID: 32573488; PubMed Central PMCID: PMC7453893.

130. Pickar-Oliver A, Gersbach CA. The next generation of CRISPR-Cas technologies and applications. Nat Rev Mol Cell Biol. 2019;20(8):490-507. doi: 10.1038/s41580-019-0131-5. PubMed PMID: 31147612; PubMed Central PMCID: PMC7079207.

131. Suzuki K, Tsunekawa Y, Hernandez-Benitez R, Wu J, Zhu J, Kim EJ, et al. In vivo genome editing via CRISPR/Cas9 mediated homology-independent targeted integration. Nature. 2016;540(7631):144-9. Epub 20161116. doi: 10.1038/nature20565. PubMed PMID: 27851729; PubMed Central PMCID: PMC5331785.

132. Young CS, Hicks MR, Ermolova NV, Nakano H, Jan M, Younesi S, et al. A Single CRISPR-Cas9 Deletion Strategy that Targets the Majority of DMD Patients Restores Dystrophin Function in hiPSC-Derived Muscle Cells. Cell Stem Cell. 2016;18(4):533-40. Epub 20160211. doi: 10.1016/j.stem.2016.01.021. PubMed PMID: 26877224; PubMed Central PMCID: PMC4826286.

133. Bilousova G. Gene Therapy for Skin Fragility Diseases: The New Generation. J Invest Dermatol. 2019;139(8):1634-7. doi: 10.1016/j.jid.2019.04.001. PubMed PMID: 31331444.

134. Kocher T, Peking P, Klausegger A, Murauer EM, Hofbauer JP, Wally V, et al. Cut and Paste: Efficient Homology-Directed Repair of a Dominant Negative KRT14 Mutation via CRISPR/Cas9 Nickases. Mol Ther. 2017;25(11):2585-98. Epub 20170824. doi: 10.1016/j.ymthe.2017.08.015. PubMed PMID: 28888469; PubMed Central PMCID: PMC5675592.

135. Benati D, Miselli F, Cocchiarella F, Patrizi C, Carretero M, Baldassarri S, et al. CRISPR/Cas9-Mediated In Situ Correction of LAMB3 Gene in Keratinocytes Derived from a Junctional Epidermolysis Bullosa Patient. Mol Ther. 2018;26(11):2592-603. Epub 20180804. doi: 10.1016/j.ymthe.2018.07.024. PubMed PMID: 30122422; PubMed Central PMCID: PMC6224783.

136. Wu W, Lu Z, Li F, Wang W, Qian N, Duan J, et al. Efficient in vivo gene editing using ribonucleoproteins in skin stem cells of recessive dystrophic epidermolysis bullosa mouse model. Proc Natl Acad Sci U S A. 2017;114(7):1660-5. Epub 20170130. doi: 10.1073/pnas.1614775114. PubMed PMID: 28137859; PubMed Central PMCID: PMC5321012.

137. Rheinwald JG, Green H. Epidermal growth factor and the multiplication of cultured human epidermal keratinocytes. Nature. 1977;265(5593):421-4. doi: 10.1038/265421a0. PubMed PMID: 299924.

138. Abe T, Barber GN. Cytosolic-DNA-mediated, STING-dependent proinflammatory gene induction necessitates canonical NF-kappaB activation through TBK1. J Virol. 2014;88(10):5328-41. Epub 20140305. doi: 10.1128/JVI.00037-14. PubMed PMID: 24600004; PubMed Central PMCID: PMC4019140.

139. Tsuchiya Y, Jounai N, Takeshita F, Ishii KJ, Mizuguchi K. Ligand-induced Ordering of the C-terminal Tail Primes STING for Phosphorylation by TBK1. EBioMedicine. 2016;9:87-96. Epub 20160601. doi: 10.1016/j.ebiom.2016.05.039. PubMed PMID: 27333035; PubMed Central PMCID: PMC4972534.

140. Steenbergen RD, Parker JN, Isern S, Snijders PJ, Walboomers JM, Meijer CJ, et al. Viral E6-E7 transcription in the basal layer of organotypic cultures without apparent p21cip1 protein precedes immortalization of human papillomavirus type 16- and 18-transfected human

keratinocytes. J Virol. 1998;72(1):749-57. doi: 10.1128/JVI.72.1.749-757.1998. PubMed PMID: 9420282; PubMed Central PMCID: PMC109431.

141. Doorbar J, Egawa N, Griffin H, Kranjec C, Murakami I. Human papillomavirus molecular biology and disease association. Rev Med Virol. 2015;25 Suppl 1(Suppl Suppl 1):2-23. doi: 10.1002/rmv.1822. PubMed PMID: 25752814; PubMed Central PMCID: PMC5024016.

142. Stenglein MD, Burns MB, Li M, Lengyel J, Harris RS. APOBEC3 proteins mediate the clearance of foreign DNA from human cells. Nat Struct Mol Biol. 2010;17(2):222-9. Epub 20100110. doi: 10.1038/nsmb.1744. PubMed PMID: 20062055; PubMed Central PMCID: PMC2921484.

143. Kawane K, Motani K, Nagata S. DNA degradation and its defects. Cold Spring Harb Perspect Biol. 2014;6(6). Epub 20140602. doi: 10.1101/cshperspect.a016394. PubMed PMID: 24890510; PubMed Central PMCID: PMC4031964.

144. Oliveri M, Daga A, Cantoni C, Lunardi C, Millo R, Puccetti A. DNase I mediates internucleosomal DNA degradation in human cells undergoing drug-induced apoptosis. Eur J Immunol. 2001;31(3):743-51. doi: 10.1002/1521-4141(200103)31:3<743::aid-immu743>3.0.co;2-9. PubMed PMID: 11241278.

145. Jang HS, Shin WJ, Lee JE, Do JT. CpG and Non-CpG Methylation in Epigenetic Gene Regulation and Brain Function. Genes (Basel). 2017;8(6). Epub 20170523. doi: 10.3390/genes8060148. PubMed PMID: 28545252; PubMed Central PMCID: PMC5485512.

146. Edwards JR, Yarychkivska O, Boulard M, Bestor TH. DNA methylation and DNA methyltransferases. Epigenetics Chromatin. 2017;10:23. Epub 20170508. doi: 10.1186/s13072-017-0130-8. PubMed PMID: 28503201; PubMed Central PMCID: PMC5422929.

147. Moulin L, Cenizo V, Antu AN, Andre V, Pain S, Sommer P, et al. Methylation of LOXL1 Promoter by DNMT3A in Aged Human Skin Fibroblasts. Rejuvenation Res. 2017;20(2):103-10. Epub 20160811. doi: 10.1089/rej.2016.1832. PubMed PMID: 27396912.

148. Wikramanayake TC, Stojadinovic O, Tomic-Canic M. Epidermal Differentiation in Barrier Maintenance and Wound Healing. Adv Wound Care (New Rochelle). 2014;3(3):272-80. doi: 10.1089/wound.2013.0503. PubMed PMID: 24669361; PubMed Central PMCID: PMC3955965.

149. Jiang Y, Tsoi LC, Billi AC, Ward NL, Harms PW, Zeng C, et al. Cytokinocytes: the diverse contribution of keratinocytes to immune responses in skin. JCI Insight. 2020;5(20). Epub 20201015. doi: 10.1172/jci.insight.142067. PubMed PMID: 33055429; PubMed Central PMCID: PMC7605526.

150. Egawa N, Egawa K, Griffin H, Doorbar J. Human Papillomaviruses; Epithelial Tropisms, and the Development of Neoplasia. Viruses. 2015;7(7):3863-90. Epub 20150716. doi: 10.3390/v7072802. PubMed PMID: 26193301; PubMed Central PMCID: PMC4517131.

151. Lau L, Gray EE, Brunette RL, Stetson DB. DNA tumor virus oncogenes antagonize the cGAS-STING DNA-sensing pathway. Science. 2015;350(6260):568-71. Epub 20150924. doi: 10.1126/science.aab3291. PubMed PMID: 26405230.

152. DeCarlo CA, Severini A, Edler L, Escott NG, Lambert PF, Ulanova M, et al. IFN-kappa, a novel type I IFN, is undetectable in HPV-positive human cervical keratinocytes. Lab Invest. 2010;90(10):1482-91. Epub 20100517. doi: 10.1038/labinvest.2010.95. PubMed PMID: 20479716.

153. Leonard SM, Wei W, Collins SI, Pereira M, Diyaf A, Constandinou-Williams C, et al. Oncogenic human papillomavirus imposes an instructive pattern of DNA methylation changes

which parallel the natural history of cervical HPV infection in young women. Carcinogenesis. 2012;33(7):1286-93. Epub 20120502. doi: 10.1093/carcin/bgs157. PubMed PMID: 22552403.

154. Lin TS, Lee H, Chen RA, Ho ML, Lin CY, Chen YH, et al. An association of DNMT3b protein expression with P16INK4a promoter hypermethylation in non-smoking female lung cancer with human papillomavirus infection. Cancer Lett. 2005;226(1):77-84. doi: 10.1016/j.canlet.2004.12.031. PubMed PMID: 16004934.

155. Warren CJ, Xu T, Guo K, Griffin LM, Westrich JA, Lee D, et al. APOBEC3A functions as a restriction factor of human papillomavirus. J Virol. 2015;89(1):688-702. Epub 20141029. doi: 10.1128/JVI.02383-14. PubMed PMID: 25355878; PubMed Central PMCID: PMC4301161.

156. Rincon-Orozco B, Halec G, Rosenberger S, Muschik D, Nindl I, Bachmann A, et al. Epigenetic silencing of interferon-kappa in human papillomavirus type 16-positive cells. Cancer Res. 2009;69(22):8718-25. Epub 20091103. doi: 10.1158/0008-5472.CAN-09-0550. PubMed PMID: 19887612.

157. Reiser J, Hurst J, Voges M, Krauss P, Munch P, Iftner T, et al. High-risk human papillomaviruses repress constitutive kappa interferon transcription via E6 to prevent pathogen recognition receptor and antiviral-gene expression. J Virol. 2011;85(21):11372-80. Epub 20110817. doi: 10.1128/JVI.05279-11. PubMed PMID: 21849431; PubMed Central PMCID: PMC3194958.

158. Haapaniemi E, Botla S, Persson J, Schmierer B, Taipale J. CRISPR-Cas9 genome editing induces a p53-mediated DNA damage response. Nat Med. 2018;24(7):927-30. Epub 20180611. doi: 10.1038/s41591-018-0049-z. PubMed PMID: 29892067.

159. Ihry RJ, Worringer KA, Salick MR, Frias E, Ho D, Theriault K, et al. p53 inhibits CRISPR-Cas9 engineering in human pluripotent stem cells. Nat Med. 2018;24(7):939-46. Epub 20180611. doi: 10.1038/s41591-018-0050-6. PubMed PMID: 29892062.

160. Cubie HA. Diseases associated with human papillomavirus infection. Virology. 2013;445(1-2):21-34. Epub 20130809. doi: 10.1016/j.virol.2013.06.007. PubMed PMID: 23932731.

161. Graham SV. Keratinocyte Differentiation-Dependent Human Papillomavirus Gene Regulation. Viruses. 2017;9(9). Epub 20170830. doi: 10.3390/v9090245. PubMed PMID: 28867768; PubMed Central PMCID: PMC5618011.

162. Griffin LM, Cicchini L, Xu T, Pyeon D. Human keratinocyte cultures in the investigation of early steps of human papillomavirus infection. Methods Mol Biol. 2014;1195:219-38. doi: 10.1007/7651_2013_49. PubMed PMID: 24281871; PubMed Central PMCID: PMC4076347.

163. McMurray HR, Nguyen D, Westbrook TF, McAnce DJ. Biology of human papillomaviruses. Int J Exp Pathol. 2001;82(1):15-33. doi: 10.1046/j.1365-2613.2001.00177.x. PubMed PMID: 11422538; PubMed Central PMCID: PMC2517699.

164. Tufegdzic Vidakovic A, Rueda OM, Vervoort SJ, Sati Batra A, Goldgraben MA, Uribe-Lewis S, et al. Context-Specific Effects of TGF-β/SMAD3 in Cancer Are Modulated by the Epigenome. Cell Rep. 2015;13(11):2480-90. Epub 20151210. doi: 10.1016/j.celrep.2015.11.040. PubMed PMID: 26686634; PubMed Central PMCID: PMC4695334.

165. Baba AB, Rah B, Bhat GR, Mushtaq I, Parveen S, Hassan R, et al. Transforming Growth Factor-Beta (TGF-β) Signaling in Cancer-A Betrayal Within. Front Pharmacol. 2022;13:791272. Epub 20220228. doi: 10.3389/fphar.2022.791272. PubMed PMID: 35295334; PubMed Central PMCID: PMC8918694.

166. Torrealba N, Vera R, Fraile B, Martínez-Onsurbe P, Paniagua R, Royuela M. TGF-β/PI3K/AKT/mTOR/NF-kB pathway. Clinicopathological features in prostate cancer. Aging Male. 2020;23(5):801-11. Epub 20190411. doi: 10.1080/13685538.2019.1597840. PubMed PMID: 30973040.

167. Hori N, Okada K, Takakura Y, Takano H, Yamaguchi N. Vestigial-like family member 3 (VGLL3), a cofactor for TEAD transcription factors, promotes cancer cell proliferation by activating the Hippo pathway. J Biol Chem. 2020;295(26):8798-807. Epub 20200508. doi: 10.1074/jbc.RA120.012781. PubMed PMID: 32385107; PubMed Central PMCID: PMC7324512.

168. Kiick KL, Saxon E, Tirrell DA, Bertozzi CR. Incorporation of azides into recombinant proteins for chemoselective modification by the Staudinger ligation. Proc Natl Acad Sci U S A. 2002;99(1):19-24. Epub 20011218. doi: 10.1073/pnas.012583299. PubMed PMID: 11752401; PubMed Central PMCID: PMC117506.

169. Dieterich DC, Link AJ, Graumann J, Tirrell DA, Schuman EM. Selective identification of newly synthesized proteins in mammalian cells using bioorthogonal noncanonical amino acid tagging (BONCAT). Proc Natl Acad Sci U S A. 2006;103(25):9482-7. Epub 20060612. doi: 10.1073/pnas.0601637103. PubMed PMID: 16769897; PubMed Central PMCID: PMC1480433.

170. Hochrainer K, Mayer H, Baranyi U, Binder B, Lipp J, Kroismayr R. The human HERC family of ubiquitin ligases: novel members, genomic organization, expression profiling, and evolutionary aspects. Genomics. 2005;85(2):153-64. doi: 10.1016/j.ygeno.2004.10.006. PubMed PMID: 15676274.

171. Zhang W, Wu KP, Sartori MA, Kamadurai HB, Ordureau A, Jiang C, et al. System-Wide Modulation of HECT E3 Ligases with Selective Ubiquitin Variant Probes. Mol Cell.

2016;62(1):121-36. Epub 20160303. doi: 10.1016/j.molcel.2016.02.005. PubMed PMID: 26949039; PubMed Central PMCID: PMC4988125.

172. Rotin D, Kumar S. Physiological functions of the HECT family of ubiquitin ligases. Nat Rev Mol Cell Biol. 2009;10(6):398-409. Epub 20090513. doi: 10.1038/nrm2690. PubMed PMID: 19436320.

173. Scheffner M, Kumar S. Mammalian HECT ubiquitin-protein ligases: biological and pathophysiological aspects. Biochim Biophys Acta. 2014;1843(1):61-74. Epub 20130329. doi: 10.1016/j.bbamcr.2013.03.024. PubMed PMID: 23545411.

174. Guo Y, Zhao C, Dai W, Wang B, Lai E, Xiao Y, et al. C-C motif chemokine receptor 2 inhibition reduces liver fibrosis by restoring the immune cell landscape. Int J Biol Sci. 2023;19(8):2572-87. Epub 20230508. doi: 10.7150/ijbs.83530. PubMed PMID: 37215993; PubMed Central PMCID: PMC10197881.

175. Xu CL, Ruan MZC, Mahajan VB, Tsang SH. Viral Delivery Systems for CRISPR. Viruses. 2019;11(1). Epub 20190104. doi: 10.3390/v11010028. PubMed PMID: 30621179; PubMed Central PMCID: PMC6356701.

176. Duan L, Ouyang K, Xu X, Xu L, Wen C, Zhou X, et al. Nanoparticle Delivery of CRISPR/Cas9 for Genome Editing. Front Genet. 2021;12:673286. Epub 20210512. doi: 10.3389/fgene.2021.673286. PubMed PMID: 34054927; PubMed Central PMCID: PMC8149999.

177. Ali A, Zafar MM, Farooq Z, Ahmed SR, Ijaz A, Anwar Z, et al. Breakthrough in CRISPR/Cas system: Current and future directions and challenges. Biotechnol J. 2023:e2200642. Epub 20230511. doi: 10.1002/biot.202200642. PubMed PMID: 37166088.

178. Scholefield J, Harrison PT. Prime editing - an update on the field. Gene Ther. 2021;28(7-8):396-401. Epub 20210524. doi: 10.1038/s41434-021-00263-9. PubMed PMID: 34031549; PubMed Central PMCID: PMC8376635.

179. Mani I. CRISPR-Cas9 for treating hereditary diseases. Prog Mol Biol Transl Sci. 2021;181:165-83. Epub 20210224. doi: 10.1016/bs.pmbts.2021.01.017. PubMed PMID: 34127193.

180. Ledford H. Landmark CRISPR trial shows promise against deadly disease. Nature. 2021. Epub 20210629. doi: 10.1038/d41586-021-01776-4. PubMed PMID: 34188245.